137

Diagnostic Methods to Detect Ageing in MOSA Valve Elements

by

Xiangxiao Qiu （邱 向 肖）

A Thesis

Submitted to the Faculty of Graduate Studies

in partial fulfilment of the requirements

for the degree of

Master of Science

Department of Electrical and Computer Engineering

University of Manitoba

Winnipeg, Manitoba

ISBN 0-612-13460-1

Name

Dissertation Abstracts International is arranged by broad, general subject categories. Please select the one subject which most nearly describes the content of your dissertation. Enter the corresponding four-digit code in the spaces provided.

Electrical Engineering

SUBJECT TERM

0544

SUBJECT CODE

U·M·I

Subject Categories

THE HUMANITIES AND SOCIAL SCIENCES

COMMUNICATIONS AND THE ARTS

Architecture 0729
Art History 0377
Cinema 0900
Dance 0378
Fine Arts 0357
Information Science 0723
Journalism 0391
Library Science 0399
Mass Communications 0708
Music 0413
Speech Communication 0459
Theater 0465

EDUCATION

General 0515
Administration 0514
Adult and Continuing 0516
Agricultural 0517
Art 0273
Bilingual and Multicultural 0282
Business 0688
Community College 0275
Curriculum and Instruction 0727
Early Childhood 0518
Elementary 0524
Finance 0277
Guidance and Counseling 0519
Health 0680
Higher 0745
History of 0520
Home Economics 0278
Industrial 0521
Language and Literature 0279
Mathematics 0280
Music 0522
Philosophy of 0998
Physical 0523
Psychology 0525
Reading 0535
Religious 0527
Sciences 0714
Secondary 0533
Social Sciences 0534
Sociology of 0340
Special 0529
Teacher Training 0530
Technology 0710
Tests and Measurements 0288
Vocational 0747

LANGUAGE, LITERATURE AND LINGUISTICS

Language
- General 0679
- Ancient 0289
- Linguistics 0290
- Modern 0291

Literature
- General 0401
- Classical 0294
- Comparative 0295
- Medieval 0297
- Modern 0298
- African 0316
- American 0591
- Asian 0305
- Canadian (English) 0352
- Canadian (French) 0355
- English 0593
- Germanic 0311
- Latin American 0312
- Middle Eastern 0315
- Romance 0313
- Slavic and East European 0314

PHILOSOPHY, RELIGION AND THEOLOGY

Philosophy 0422
Religion
- General 0318
- Biblical Studies 0321
- Clergy 0319
- History of 0320
- Philosophy of 0322

Theology 0469

SOCIAL SCIENCES

American Studies 0323
Anthropology
- Archaeology 0324
- Cultural 0326
- Physical 0327

Business Administration
- General 0310
- Accounting 0272
- Banking 0770
- Management 0454
- Marketing 0338

Canadian Studies 0385
Economics
- General 0501
- Agricultural 0503
- Commerce-Business 0505
- Finance 0508
- History 0509
- Labor 0510
- Theory 0511

Folklore 0358
Geography 0366
Gerontology 0351
History
- General 0578
- Ancient 0579
- Medieval 0581
- Modern 0582
- Black 0328
- African 0331
- Asia, Australia and Oceania 0332
- Canadian 0334
- European 0335
- Latin American 0336
- Middle Eastern 0333
- United States 0337

History of Science 0585
Law 0398
Political Science
- General 0615
- International Law and Relations 0616
- Public Administration 0617

Recreation 0814
Social Work 0452
Sociology
- General 0626
- Criminology and Penology 0627
- Demography 0938
- Ethnic and Racial Studies 0631
- Individual and Family Studies 0628
- Industrial and Labor Relations 0629
- Public and Social Welfare 0630
- Social Structure and Development 0700
- Theory and Methods 0344

Transportation 0709
Urban and Regional Planning 0999
Women's Studies 0453

THE SCIENCES AND ENGINEERING

BIOLOGICAL SCIENCES

Agriculture
- General 0473
- Agronomy 0285
- Animal Culture and Nutrition 0475
- Animal Pathology 0476
- Food Science and Technology 0359
- Forestry and Wildlife 0478
- Plant Culture 0479
- Plant Pathology 0480
- Plant Physiology 0817
- Range Management 0777
- Wood Technology 0746

Biology
- General 0306
- Anatomy 0287
- Biostatistics 0308
- Botany 0309
- Cell 0379
- Ecology 0329
- Entomology 0353
- Genetics 0369
- Limnology 0793
- Microbiology 0410
- Molecular 0307
- Neuroscience 0317
- Oceanography 0416
- Physiology 0433
- Radiation 0821
- Veterinary Science 0778
- Zoology 0472

Biophysics
- General 0786
- Medical 0760

EARTH SCIENCES

Biogeochemistry 0425
Geochemistry 0996
Geodesy 0370
Geology 0372
Geophysics 0373
Hydrology 0388
Mineralogy 0411
Paleobotany 0345
Paleoecology 0426
Paleontology 0418
Paleozoology 0985
Palynology 0427
Physical Geography 0368
Physical Oceanography 0415

HEALTH AND ENVIRONMENTAL SCIENCES

Environmental Sciences 0768
Health Sciences
- General 0566
- Audiology 0300
- Chemotherapy 0992
- Dentistry 0567
- Education 0350
- Hospital Management 0769
- Human Development 0758
- Immunology 0982
- Medicine and Surgery 0564
- Mental Health 0347
- Nursing 0569
- Nutrition 0570
- Obstetrics and Gynecology 0380
- Occupational Health and Therapy 0354
- Ophthalmology 0381
- Pathology 0571
- Pharmacology 0419
- Pharmacy 0572
- Physical Therapy 0382
- Public Health 0573
- Radiology 0574
- Recreation 0575
- Speech Pathology 0460
- Toxicology 0383

Home Economics 0386

PHYSICAL SCIENCES

Pure Sciences

Chemistry
- General 0485
- Agricultural 0749
- Analytical 0486
- Biochemistry 0487
- Inorganic 0488
- Nuclear 0738
- Organic 0490
- Pharmaceutical 0491
- Physical 0494
- Polymer 0495
- Radiation 0754

Mathematics 0405
Physics
- General 0605
- Acoustics 0986
- Astronomy and Astrophysics 0606
- Atmospheric Science 0608
- Atomic 0748
- Electronics and Electricity 0607
- Elementary Particles and High Energy 0798
- Fluid and Plasma 0759
- Molecular 0609
- Nuclear 0610
- Optics 0752
- Radiation 0756
- Solid State 0611

Statistics 0463

Applied Sciences

Applied Mechanics 0346
Computer Science 0984
Engineering
- General 0537
- Aerospace 0538
- Agricultural 0539
- Automotive 0540
- Biomedical 0541
- Chemical 0542
- Civil 0543
- Electronics and Electrical 0544
- Heat and Thermodynamics 0348
- Hydraulic 0545
- Industrial 0546
- Marine 0547
- Materials Science 0794
- Mechanical 0548
- Metallurgy 0743
- Mining 0551
- Nuclear 0552
- Packaging 0549
- Petroleum 0765
- Sanitary and Municipal 0554
- System Science 0790

Geotechnology 0428
Operations Research 0796
Plastics Technology 0795
Textile Technology 0994

PSYCHOLOGY

General 0621
Behavioral 0384
Clinical 0622
Developmental 0620
Experimental 0623
Industrial 0624
Personality 0625
Physiological 0989
Psychobiology 0349
Psychometrics 0632
Social 0451

Nom ______________________________

Dissertation Abstracts International est organisé en catégories de sujets. Veuillez s.v.p. choisir le sujet qui décrit le mieux votre thèse et inscrivez le code numérique approprié dans l'espace réservé ci-dessous.

______________________________ SUJET

☐☐☐☐ CODE DE SUJET

U·M·I

Catégories par sujets

HUMANITÉS ET SCIENCES SOCIALES

COMMUNICATIONS ET LES ARTS
Architecture 0729
Beaux-arts 0357
Bibliothéconomie 0399
Cinéma 0900
Communication verbale 0459
Communications 0708
Danse 0378
Histoire de l'art 0377
Journalisme 0391
Musique 0413
Sciences de l'information 0723
Théâtre 0465

ÉDUCATION
Généralités 515
Administration 0514
Art 0273
Collèges communautaires 0275
Commerce 0688
Économie domestique 0278
Éducation permanente 0516
Éducation préscolaire 0518
Éducation sanitaire 0680
Enseignement agricole 0517
Enseignement bilingue et multiculturel 0282
Enseignement industriel 0521
Enseignement primaire. 0524
Enseignement professionnel 0747
Enseignement religieux 0527
Enseignement secondaire 0533
Enseignement spécial 0529
Enseignement supérieur 0745
Évaluation 0288
Finances 0277
Formation des enseignants 0530
Histoire de l'éducation 0520
Langues et littérature 0279
Lecture 0535
Mathématiques 0280
Musique 0522
Orientation et consultation 0519
Philosophie de l'éducation 0998
Physique 0523
Programmes d'études et enseignement 0727
Psychologie 0525
Sciences 0714
Sciences sociales 0534
Sociologie de l'éducation 0340
Technologie 0710

LANGUE, LITTÉRATURE ET LINGUISTIQUE
Langues
- Généralités 0679
- Anciennes 0289
- Linguistique 0290
- Modernes 0291

Littérature
- Généralités 0401
- Anciennes 0294
- Comparée 0295
- Mediévale 0297
- Moderne 0298
- Africaine 0316
- Américaine 0591
- Anglaise 0593
- Asiatique 0305
- Canadienne (Anglaise) 0352
- Canadienne (Française) 0355
- Germanique 0311
- Latino-américaine 0312
- Moyen-orientale 0315
- Romane 0313
- Slave et est-européenne 0314

PHILOSOPHIE, RELIGION ET THÉOLOGIE
Philosophie 0422
Religion
- Généralités 0318
- Clergé 0319
- Études bibliques 0321
- Histoire des religions 0320
- Philosophie de la religion 0322

Théologie 0469

SCIENCES SOCIALES
Anthropologie
- Archéologie 0324
- Culturelle 0326
- Physique 0327

Droit 0398
Économie
- Généralités 0501
- Commerce-Affaires 0505
- Économie agricole 0503
- Économie du travail 0510
- Finances 0508
- Histoire 0509
- Théorie 0511

Études américaines 0323
Études canadiennes 0385
Études féministes 0453
Folklore 0358
Géographie 0366
Gérontologie 0351
Gestion des affaires
- Généralités 0310
- Administration 0454
- Banques 0770
- Comptabilité 0272
- Marketing 0338

Histoire
- Histoire générale 0578
- Ancienne 0579
- Médiévale 0581
- Moderne 0582
- Histoire des noirs 0328
- Africaine 0331
- Canadienne 0334
- États-Unis 0337
- Européenne 0335
- Moyen-orientale 0333
- Latino-américaine 0336
- Asie, Australie et Océanie 0332

Histoire des sciences 0585
Loisirs 0814
Planification urbaine et régionale 0999
Science politique
- Généralités 0615
- Administration publique 0617
- Droit et relations internationales 0616

Sociologie
- Généralités 0626
- Aide et bien-àtre social 0630
- Criminologie et établissements pénitentiaires 0627
- Démographie 0938
- Études de l' individu et de la famille 0628
- Études des relations interethniques et des relations raciales 0631
- Structure et développement social 0700
- Théorie et méthodes 0344
- Travail et relations industrielles 0629

Transports 0709
Travail social 0452

SCIENCES ET INGÉNIERIE

SCIENCES BIOLOGIQUES
Agriculture
- Généralités 0473
- Agronomie. 0285
- Alimentation et technologie alimentaire 0359
- Culture 0479
- Élevage et alimentation 0475
- Exploitation des péturages 0777
- Pathologie animale 0476
- Pathologie végétale 0480
- Physiologie végétale 0817
- Sylviculture et faune 0478
- Technologie du bois 0746

Biologie
- Généralités 0306
- Anatomie 0287
- Biologie (Statistiques) 0308
- Biologie moléculaire 0307
- Botanique 0309
- Cellule 0379
- Écologie 0329
- Entomologie 0353
- Génétique 0369
- Limnologie 0793
- Microbiologie 0410
- Neurologie 0317
- Océanographie 0416
- Physiologie 0433
- Radiation 0821
- Science vétérinaire 0778
- Zoologie 0472

Biophysique
- Généralités 0786
- Medicale 0760

SCIENCES DE LA TERRE
Biogéochimie 0425
Géochimie 0996
Géodésie 0370
Géographie physique 0368
Géologie 0372
Géophysique 0373
Hydrologie 0388
Minéralogie 0411
Océanographie physique 0415
Paléobotanique 0345
Paléoécologie 0426
Paléontologie 0418
Paléozoologie 0985
Palynologie 0427

SCIENCES DE LA SANTÉ ET DE L'ENVIRONNEMENT
Économie domestique 0386
Sciences de l'environnement 0768
Sciences de la santé
- Généralités 0566
- Administration des hipitaux 0769
- Alimentation et nutrition 0570
- Audiologie 0300
- Chimiothérapie 0992
- Dentisterie 0567
- Développement humain 0758
- Enseignement 0350
- Immunologie 0982
- Loisirs 0575
- Médecine du travail et thérapie 0354
- Médecine et chirurgie 0564
- Obstétrique et gynécologie 0380
- Ophtalmologie 0381
- Orthophonie 0460
- Pathologie 0571
- Pharmacie 0572
- Pharmacologie 0419
- Physiothérapie 0382
- Radiologie 0574
- Santé mentale 0347
- Santé publique 0573
- Soins infirmiers 0569
- Toxicologie 0383

SCIENCES PHYSIQUES
Sciences Pures
Chimie
- Genéralités 0485
- Biochimie 487
- Chimie agricole 0749
- Chimie analytique 0486
- Chimie minérale 0488
- Chimie nucléaire 0738
- Chimie organique 0490
- Chimie pharmaceutique 0491
- Physique 0494
- PolymÇres 0495
- Radiation 0754

Mathématiques 0405
Physique
- Généralités 0605
- Acoustique 0986
- Astronomie et astrophysique 0606
- Electronique et électricité 0607
- Fluides et plasma 0759
- Météorologie 0608
- Optique 0752
- Particules (Physique nucléaire) 0798
- Physique atomique 0748
- Physique de l'état solide 0611
- Physique moléculaire 0609
- Physique nucléoire 0610
- Radiation 0756

Statistiques 0463

Sciences Appliqués Et Technologie
Informatique 0984
Ingénierie
- Généralités 0537
- Agricole 0539
- Automobile 0540
- Biomédicale 0541
- Chaleur et ther modynamique 0348
- Conditionnement (Emballage) 0549
- Génie aérospatial 0538
- Génie chimique 0542
- Génie civil 0543
- Génie électronique et électrique 0544
- Génie industriel 0546
- Génie mécanique 0548
- Génie nucléaire 0552
- Ingénierie des systämes 0790
- Mécanique navale 0547
- Métallurgie 0743
- Science des matériaux 0794
- Technique du pétrole 0765
- Technique minière 0551
- Techniques sanitaires et municipales 0554
- Technologie hydraulique 0545

Mécanique appliquée 0346
Géotechnologie 0428
Matières plastiques (Technologie) 0795
Recherche opérationnelle 0796
Textiles et tissus (Technologie) 0794

PSYCHOLOGIE
Généralités 0621
Personnalité 0625
Psychobiologie 0349
Psychologie clinique 0622
Psychologie du comportement 0384
Psychologie du développement 0620
Psychologie expérimentale 0623
Psychologie industrielle 0624
Psychologie physiologique 0989
Psychologie sociale 0451
Psychométrie 0632

DIAGNOSTIC METHODS TO DETECT AGEING IN MOSA VALVE ELEMENTS

BY

XIANGXIAO QIU

A Thesis submitted to the Faculty of Graduate Studies of the University of Manitoba in partial fulfillment of the requirements of the degree of

MASTER OF SCIENCE

Acknowledgements

First of all I would like to express my profound gratitude to Dr. M. R. Raghuveer for his invaluable guidance, advice and inspiration throughout this whole work.

Special thanks to Mr. W. McDermid and Mr. A. Glodjo of Manitoba Hydro for their very valuable advice and help.

Funding from Manitoba Hydro made available by the Manitoba Hydro Research Committee and partial funding from NSERC for this project is gratefully appreciated.

Sincere thanks to Mr. John Kendall, the technician in the McMath High Voltage & Power Transmission Research Laboratory at the University of Manitoba, for his technical help and support in the experiments and his encouragement.

Technical help in Infrared imaging rendered by Mr. Tom Hummerston of Manitoba Hydro is also gratefully acknowledged.

I owe thanks to all friends for their help and encouragement during the course of my study and research.

This thesis is dedicated to my parents and other family members, for their love, encouragement and 'push'. It is also dedicated to all the people who like me and to the people whom I like.

ABSTRACT

Valve elements in Metal Oxide Surge Arresters (MOSA) are subjected to ageing in service due to absorption of energy associated with transients, thermal effect, moisture ingress and pollution. The degradation causes changes in the volt-current characteristics and results in increased magnitude of resistive current flow under normal operation. Due to the negative temperature coefficient of resistance, thermal runaway becomes possible as degradation progresses. Therefore diagnostic methods are necessary to assess the state of MOSA in service.

In this thesis, some diagnostic methods were proposed to detect MOSA valve elements degradation as well as to diagnose the cause of degradation.

The valve elements were laboratory aged; ageing was accomplished by insertion in an oven (thermal ageing), by applying 60*Hz AC* voltage in the presence of moisture, by passage of current impulses of short or long duration (transient ageing) and by hybrid thermal/transient effect.

The diagnostic results were studied and then compared in details. It is shown that some diagnostic methods are capable of detecting ageing but not the cause of degradation; other diagnostic methods are suitable for distinguishing the cause of degradation but not very powerful in detecting the degradation. A comprehensive use of these two types of diagnostic methods yields more reliable result.

Contents

List of Figures

List of Tables

CHAPTER 1

INTRODUCTION

In the last two decades, the use of the Metal Oxide Surge Arresters (MOSA) in power systems as protective devices has grown very rapidly because of their excellent protective characteristics and high energy handling capability. MOSA are now being extensively applied in power systems to protect electrical equipment against over-voltages and to absorb energy resulting from lightning and switching surges as well as from temporary over-voltages.

1.1 History of surge arresters

Historically, various types of surge arresters have been used for power system protection. The use of pellet and expulsion-type arresters diminished when valve-type arresters were introduced and refined. The basic elements of valve-type arresters are the gap unit (employed in some designs and for most silicon carbide arresters) and the valve element. The gap unit is configured and augmented so as to achieve the most desirable balance between (low) sparkover and reseal capability consistent with cost. The valve elements consist of non-linear resistance that exhibit a relatively high resistance at a low voltage (and current) and a much lower resistance at a high (surge) voltage and current. This non-linear property greatly enhances overall arrester performance because it presents the lowest resistance (low surge impedance, in effect) at the important high-surge current condition while its high-resistance property at low surge and normal voltage levels assists the gap unit in resealing after surge discharge to prevent continued flow of follow (power) current [1].

Newly developed highly non-linear metal oxide valve elements, specifically of zinc oxide base, became available in arrester design that rendered series gaps unnecessary because of the sufficiently high non-linearity of valve element resistance [2]. Zinc Oxide (ZnO) varistors were first developed by the Matsushita Electric (Japan) in 1968; the following year they were commercialized under the trade name ZNR. In the first decade after its invention, various additives to improve the electrical properties were discovered and the processing conditions were optimized. In the next decade, the microstructures and the physical properties of the grain boundaries were gradually identified, and applications were rapidly found in the protection of electrical equipment and electronic components such as transistors and ICs against voltage surges [3]. Since a MOSA does not have any series gaps, the disadvantage associated with gaps such as introduction of transients during sparkover by the gaps themselves is avoided. Also the relatively constant voltage characteristic of the valve elements initiates and completes the surge protective cycle in a more ideal manner as compared to valve-type arresters previously available.

1.2 MOSA

MOSA are highly non-ohmic resistors. The resistance of a MOSA element is very high (more than $10^{10}\Omega$cm) below a threshold voltage, whereas it is very low (less than several Ωcm) above the threshold. Hence the MOSA is ideally suited for the purpose of surge protection in power systems.

Empirically the following simple equation is used to represent the non-linear characteristic of MOSA elements.

$$I = \left(\frac{V}{C}\right)^{\alpha} \tag{1.1}$$

where C is a constant. When $\alpha=1$, it is a linear resistor, and when $\alpha=$infinity, it is an ideal varistor. Typical α values for ZnO varistors are between 30 to 100, while α for conventional varistors such as silicon carbide (SiC) varistors do not exceed 10 [3].

A typical non-linear valve element I-V characteristic is shown in Fig. 1.1 (this figure actually shows the relationship between the applied voltage and the current density). The volt-current characteristics of ZnO varistors may be divided into three regions. In region I, below the threshold voltage (typically a voltage at which the current density is $1\mu A/cm^2$), the non-ohmic property is not so prominent and highly dependent on the temperature. In region II between the threshold voltage and a voltage which causes a current density of about $100A/cm^2$, the non-ohmic characteristic is very prominent and almost independent of the temperature. In region III, with current densities above $100A/cm^2$, the non-linearity in the resistance gradually decays. ZnO varistors are characterized by the magnitude of α and the width where the highly non-ohmic property is exhibited. The I-V characteristics below $100mA/cm^2$ are usually measured using a *DC* electric source, whereas those above $1A/cm^2$ are measured using an impulse current source. The data in Fig. 1.1 in region III was obtained by using an impulse current of waveshape 8x20 μs. This waveform is used as a standard impulse current to test lightning arresters. As indicated in Fig. 1.1 the volt-current characteristics measured by impulse current show a voltage higher than those measured using a *DC* source. The difference is usually 10%-20%. This difference is caused by the delay of electrical response in ZnO varistors. The response delay is considered to be caused by electron trapping and hole creation at the grain boundaries.

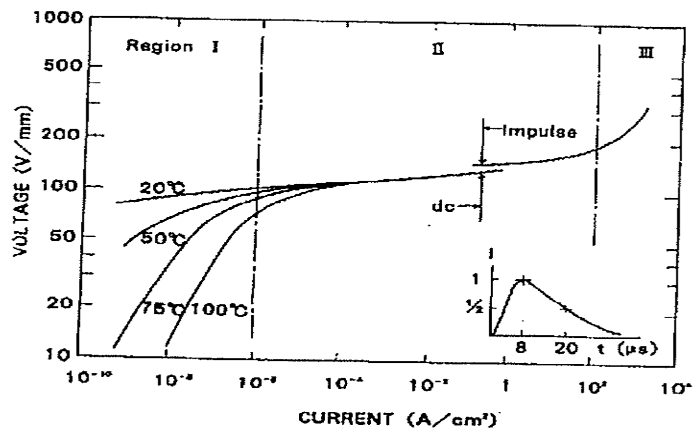

Fig. 1.1 Volt-current characteristics of a typical ZnO varistor [3]

In service, MOSA are subjected to degradation due to various reasons. One cause of ageing is the absorption of energy associated with transients. Secondly, the valve elements are continuously stressed under operating voltage because of the absence of series gaps. This, in combination with the heating effect due to different reasons such as exposure to sun, non-linear voltage distribution [4] and pollution [5, 6, 7, 8, 9] on the external surface, induce thermal ageing. The interaction between the polluted porcelain housing and the inner valve elements column due to capacitive coupling has been found to be responsible for the temperature rise of valve elements. The difference between the internal voltage distribution and the external voltage distribution causes a high radial electric field which can lead to internal discharge if the radial insulation system is not properly designed [10]. Practical experience indicates that moisture ingress is also a major cause for failure of surge arresters including MOSA [11, 12].

Under the above circumstances, it is expected that the MOSA elements maintain their original electrical characteristics. However MOSA elements are known to exhibit an increase in current with time [13], the rate of increase being exacerbated with increasing applied voltage and/or ambient temperature. The consequence of increasing current (therefore resistive current) with time is the eventual attainment of a state of thermal instability that may lead to arrester failure. Therefore it is necessary to detect the degradation of valve elements in MOSA to ensure safe system operation. It is for this reason that the diagnostics are of great value.

1.3 A review of existing diagnostic methods

In practice, measurement of the peak value of the total current through the valve element is probably the easiest in-service diagnostic method. This diagnostic indicator, however is not effective because under MCOV (Maximum continuous operating voltage)[1], the resistive current is usually very small compared to the capacitive current; therefore the total current is not a good indicator unless the valve elements are severely aged.

Another commonly used method by the utilities is to measure the r.m.s. voltage necessary to cause $1mA_{peak}$ resistive current (I_{rp}). This method is used to examine the quality of the arresters before installation or after disconnection from service of the arresters suspected to have aged. The method can not be used when the arresters are in operation.

Measurement of resistive current is a more meaningful in-service diagnostic method for MOSA. Fig. 1.2 shows some proposed methods of measurement of the resistive current through an arrester. Fig. 1.2(a) shows a conventional method using the reference voltage source to generate a capacitive cancelling current component. This method is used widely. Fig. 1.2(b) shows a circuit used for detecting high frequency components in the total cur-

1. MCOV---The maximum designated root-mean-square value of power frequency voltage that may be applied continuously between terminals of arresters [14]. For example, 230kV system uses 140kV MCOV arresters and 345kV system uses 210kV MCOV ones.

rent of MOSA elements. The accuracy of this method is not so high because of the existence of the harmonics in the line voltage. Fig. 1.2(c) shows a circuit in which the arrester terminal voltage is scaled down by a non-linear resistor to derive a reference voltage source to cancel the capacitive current from the total current [15].

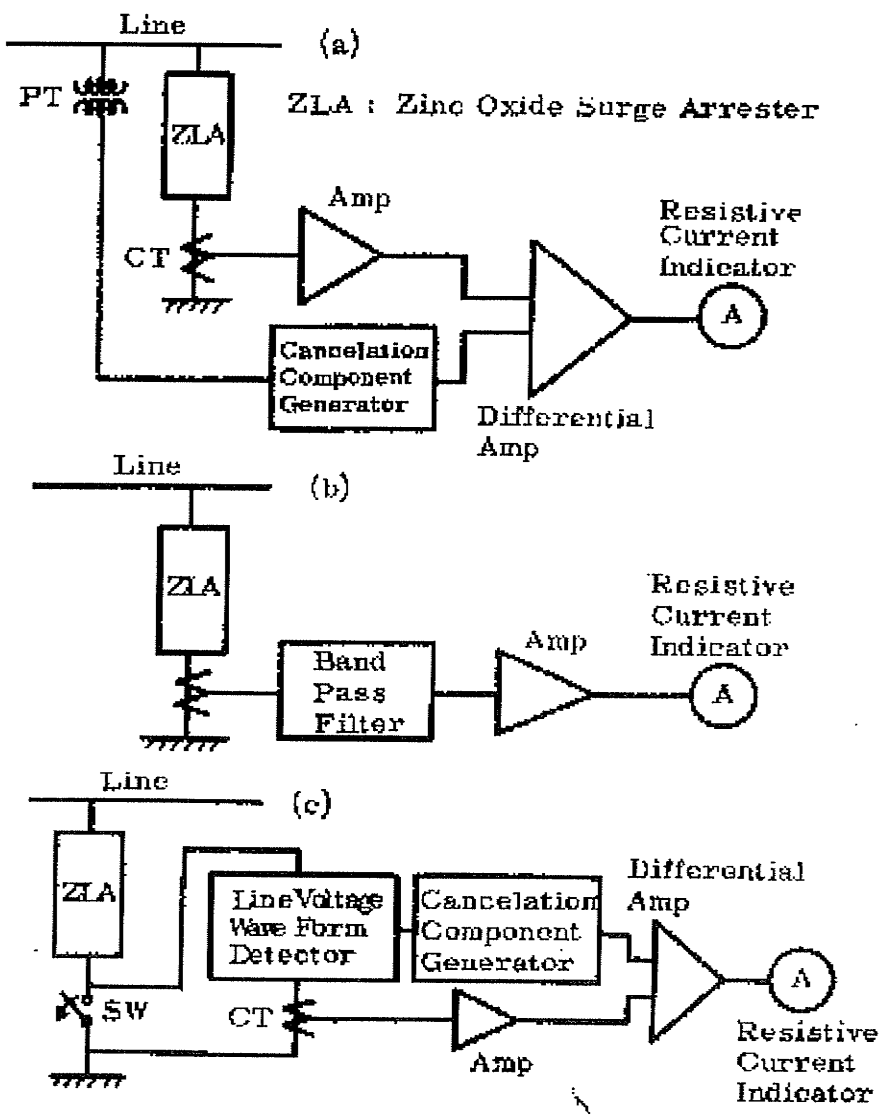

Fig. 1.2 Schematic diagram used to measure resistive component of current [15]

In [16] the author proposed a diagnostic method after extensive experiments on 65 distribution surge arresters (of both gapped silicon carbide type and gapless MOSA type).

The 65 new arresters were supplied by 6 different manufacturers. 3 grams of water were introduced in each arrester and the arresters were energized at their rated voltages for a month. The author discovered that before ageing, 7 of the total 65 arresters emitted electromagnetic radiation in the range of $5 \sim 200MHz$; while after ageing, 64 out of these 65 arresters emitted electromagnetic radiation. The author believes that the electromagnetic radiation before ageing was caused by leaking seals. Comparing to the other parameters such as total leakage current and $60Hz$ sparkover voltage, electromagnetic radiation was the most sensitive to ageing and the signal was easily detectable in the field using a receiver and a directional antenna. He concluded that electromagnetic radiation could be used as a diagnostic tool, but the author did not mentioned the effectiveness of this method for ageing caused by other reasons.

The setup of Fig. 1.3 was used by the author of [17] to detect thermal ageing. A specially designed measuring device allows measurement of the voltage and total current without disconnecting the arrester. A transient recorder was used to record the voltage and total current waveform at a voltage higher than the MCOV (maximum continuous operating voltage). The data were then fed to a computer for calculation of the diagnostic indicator $A_{ref} = \frac{A1}{A1+A2}$ as shown in Fig. 1.4. In Fig. 1.4 the v-i_r curve was obtained for one quarter of a cycle of the applied voltage. The method is capable of detecting a decrease in the parameter A_{ref} if the element is thermally aged only [17].

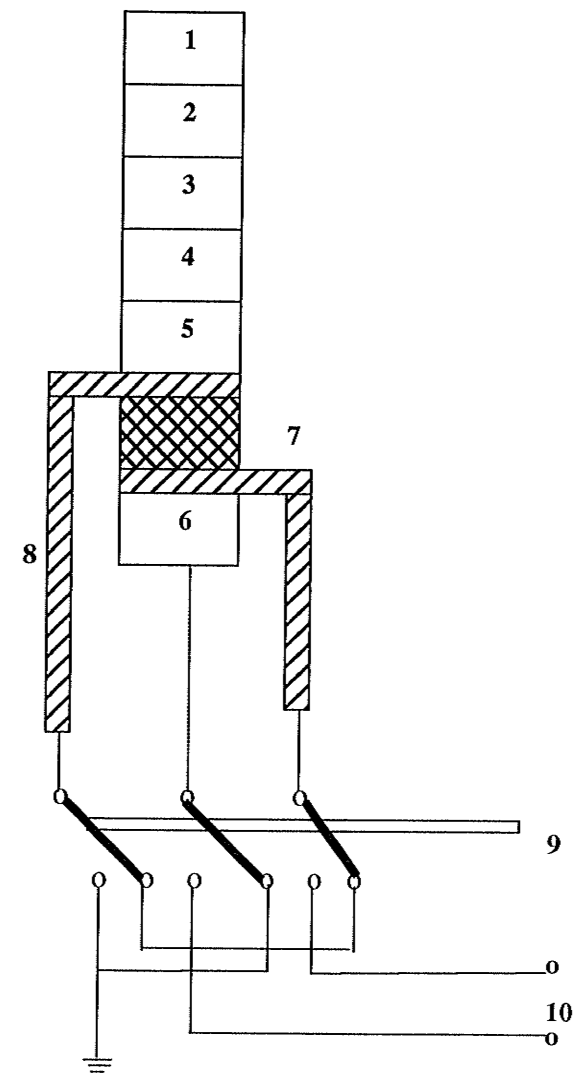

Measurement device:
1-6 valve elements
7- insulating spacer
8- intermediate electrodes
9- selector switch
10-measuring terminal

Fig. 1.3 Measuring scheme used in [17]

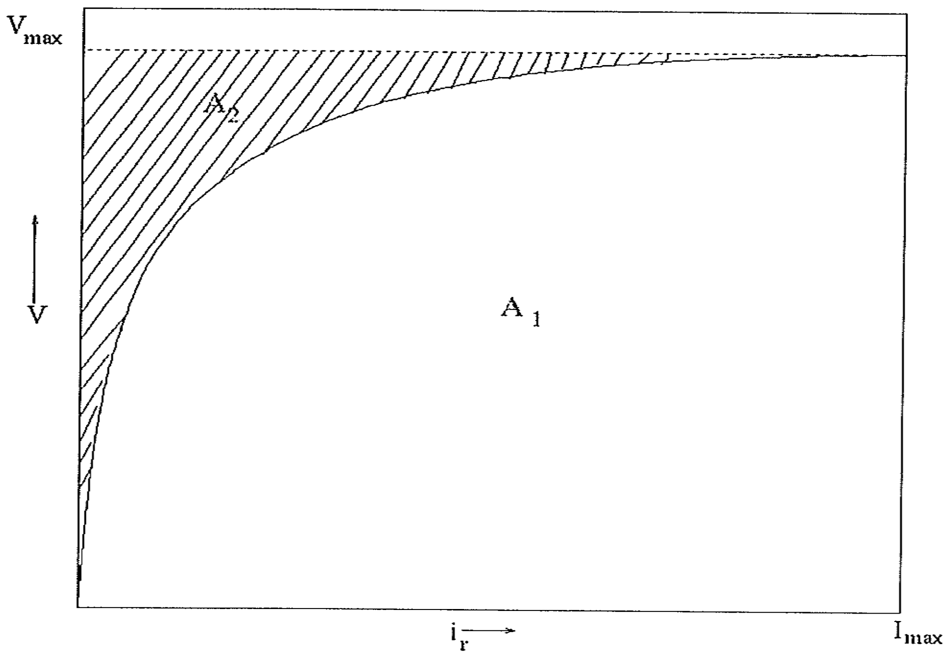

Fig. 1.4 v-i_r characteristics of a ZnO varistor [17], used to calculate A_{ref}

An elaborately designed clamp type CT for detection of arrester current without disconnecting the ground wire has been presented in [18], Fig. 1.5 shows the schematic circuit of the measuring device. A band-pass filter with centre frequency of 150Hz band width of $70Hz$ (developed in Japan where the fundamental frequency is 50Hz) was used to obtain the 3rd harmonic content of resistive current i_r. It was found that the 3rd harmonic content of i_r increases more rapidly with ageing than other harmonic components; hence this parameter was used as an ageing indicator.

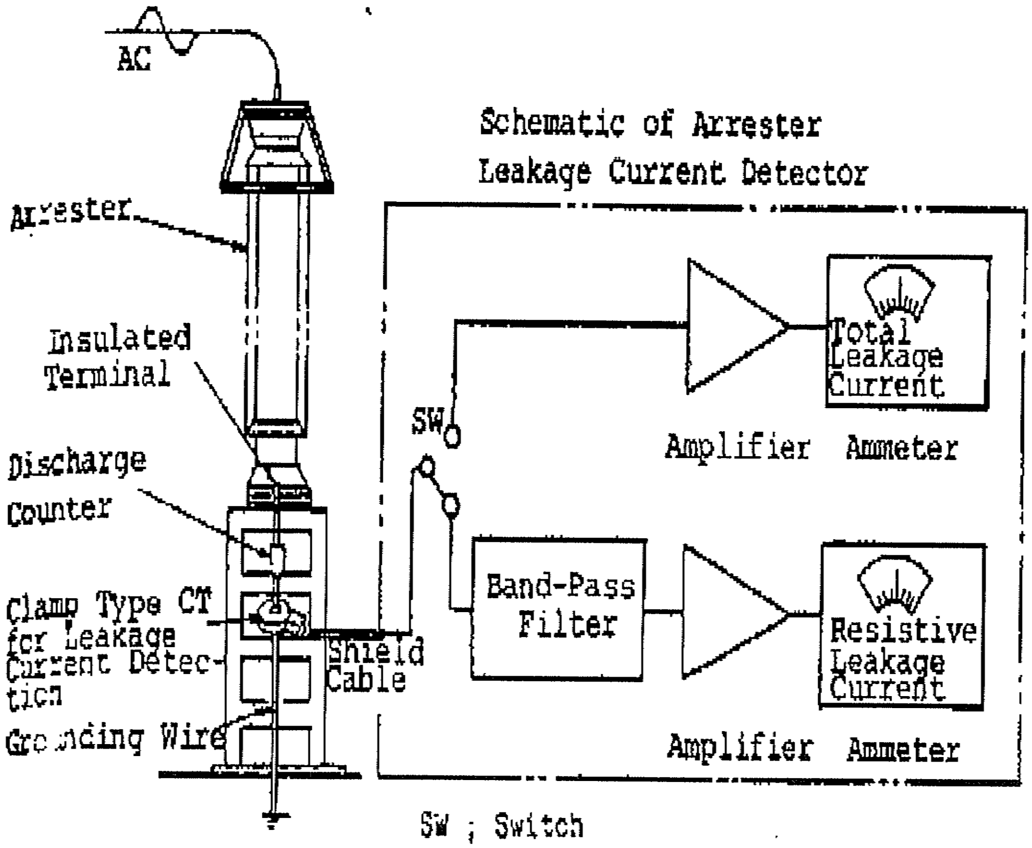

Fig. 1.5 Circuit for measuring resistive current in MOSA [18]

A relatively new method has been presented in [5] to measure the resistive current accurately. This method has low sensitivity to the harmonic content in the system voltage. A field probe was used to calibrate and cancel the capacitive current caused by the harmonics in the voltage. Fig. 1.6 shows the principal design of this leakage current monitoring equipment. This method is reviewed in detail below.

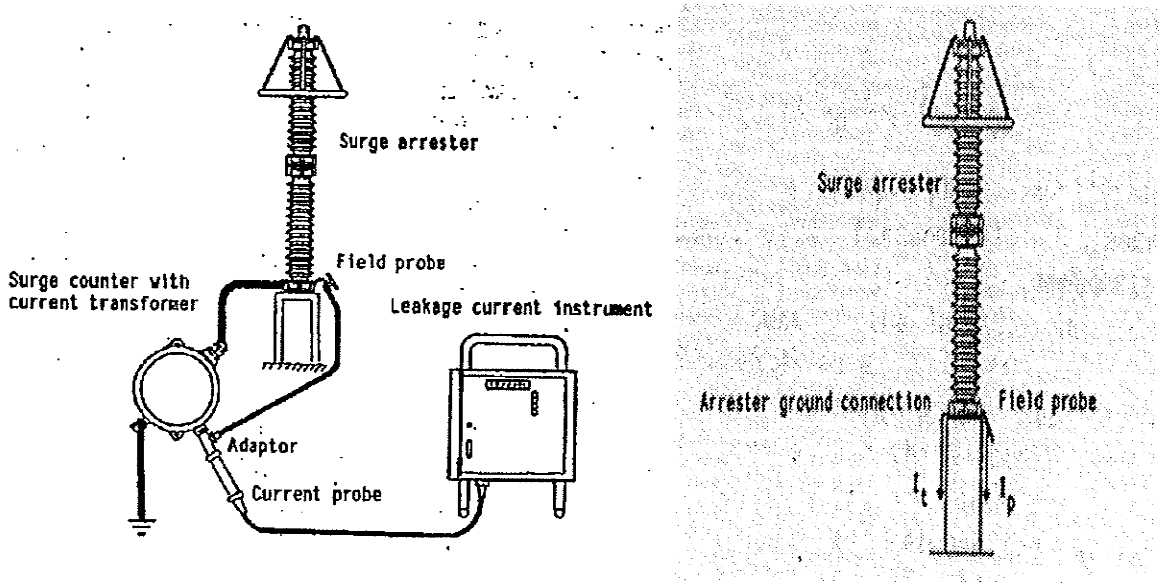

(a) (b)

Fig. 1.6 Principal design of the leakage current monitoring equipment proposed in [5] and main parameters

The author assumes that the 3rd harmonic is the only harmonic present in the system voltage (the method also applies if other harmonics are present). Because the capacitive current caused by the 3rd harmonic voltage is comparable to the total resistive current under operating voltage, it is essential to remove that part of the capacitive current from the diagnostic indicator. The total 3rd harmonic current, i_{3t}, comprised of i_{3r} and i_{3c}, where i_{3c} is the 3rd harmonic capacitive current due to the existence of 3rd harmonic in the system voltage, i_{3r} is caused by application of the applied voltage to the non-linear resistive valve element. These 3 currents are related by

$$i_{3r} = i_{3t} - i_{3c}. \tag{1.2}$$

i_{3t} could be obtained by conducting Fourier analysis on the acquired total current flowing through the arrester. The author uses a field probe to acquire i_{3c}, hence i_{3r} can be obtained by subtraction.

The amplitude of the fundamental frequency component of the field probe current (I_{1p}) and the amplitude of the fundamental component of the total current (I_{1t}) were acquired by application of Fourier analysis on the probe and total current respectively. The factor k was then calculated where

$$k_1 = I_{1t} / I_{1p} \tag{1.3}$$

Since under operating voltage, the resistive current is very small compared to the capacitive current, so

$$k_1 = I_{1t}/I_{1p} \approx I_{1c}/I_{1p} \tag{1.4}$$

Similarly k_3 was defined as

$$k_3 = I_{3c}/I_{3p} \tag{1.5}$$

Therefore $I_{3c} = k_3 I_{3p}$ (1.6)

The author obtained I_{3p} by application of Fourier analysis on the probe current. If k_3 could be found then the component I_{3c} is obtained from Eq. 1.6 and hence I_{3r} can be found using Eq. 1.2 with information of phase angles.

For a three phase arrester there is a phase difference of $2\pi/3$ radian between each fundamental frequency phase voltage while there is no corresponding phase shift for the third harmonic voltage. In a three phase application k_1 is not the same as k_3. The reason is that the measurement of I_{1p} is influenced by the other phases. (In a single phase application $k_1 = k_3$.) Since k_3 can not be found directly, the author finds the ratio of k_3/k_1 and hence k_3 because k_1 is known.

Since k_1 and k_3 are field dependent, the author calculates the field strengths at the location of the field probe and the pedestal of the arrester to find

$$k_1 = \frac{E_{1c}}{E_{1p}} \quad \& \quad k_3 = \frac{E_{3c}}{E_{3p}} \qquad (1.7)\ \&\ (1.8)$$

where E_{1c}, E_{3c}, E_{1p}, E_{3p} are shown in Fig. 1.7.

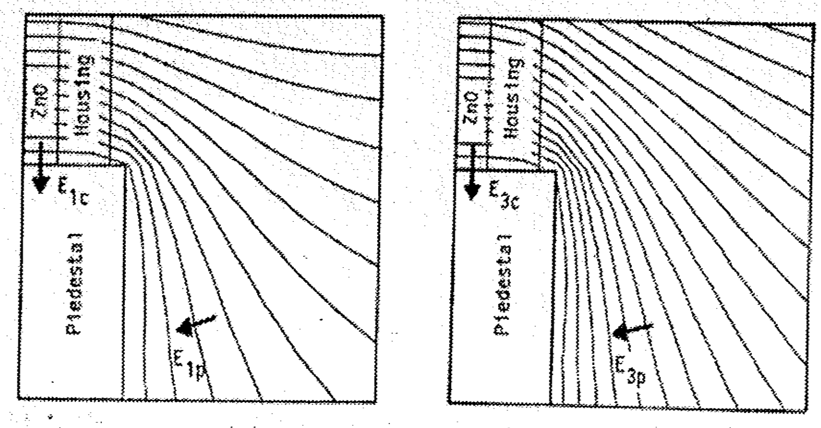

Fig. 1.7 Fundamental frequency and 3rd harmonic fields at arrester base [5]

The ratio of $\frac{k_3}{k_1}$ was therefore established. The author found that this ratio remained relatively constant at all three location under 3 phases with different harmonic content in the system voltage and different arrester geometry. Hence I_{3r} could be determined using Eq. 1.9 with proper phase angles.

$$i_{3r} = i_{3t} - i_{3c} = i_{3t} - k_3 i_{3p} = i_{3t} - \frac{k_3}{k_1} k_1 i_{3p} \qquad (1.9)$$

I_{3r} could be converted to I_r by multiplying a pre-determined converting factor. The author claims that this technique yields a result that has relatively low sensitivity to the harmonics in the system voltage.

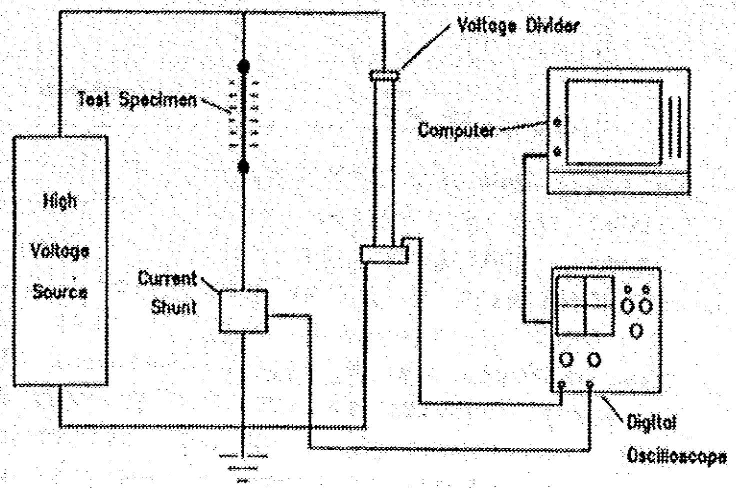

Fig. 1.8 System layout of the measuring device in [19]

Fig. 1.8 shows the layout of a high voltage AC resistive current measuring device of novel design used by the author in [19]. This device uses "computer based digital Watts technique" [19] to calculate the resistive current. V_{rms} was obtained using numerical integration of the digitized voltage data ($V_{rms} = \sqrt{\frac{1}{n}\sum_{k=1}^{n}[v(k)]^2}$). Average Watts $= \frac{1}{n}\sum_{k=1}^{n} v(k)\, i(k)$. $v(k)$ and $i(k)$ represent digitize values of voltage and total current with respect to time. The resistive current was calculated by dividing the average watts by the rms voltage across the valve element.

1.4 Scope of the present work

Since diagnostics are necessary and important for secure operation of power systems, a study of diagnostic methods is therefore of value to utilities.

Ideal diagnostic methods should be capable of detecting ageing, be sensitive to small changes in the v-i_r characteristics and should be able to determine the cause of ageing;

also the methods ought to be easily realizable and preferably have good sensitivity at the operating voltage of MOSA.

The objective of the work reported in this thesis is to compare the effectiveness of several leakage-current based methods in diagnosing degradation of MOSA valve elements due to different causes, namely thermal ageing, moisture ingress and passage of long and short duration surge currents. Also some new diagnostic methods were proposed. The effectiveness of the various methods in distinguishing the cause of ageing is also studied.

Five types of aging have been considered in this project. They are:

1) Thermal ageing: this was accomplished by heating the valve elements in an oven set at a selected high temperature with accurate temperature control.
2) Moisture ingress caused ageing: this was completed by placing the energized element in a sealed chamber into which a controlled amount of tap water was introduced.
3) Ageing caused by absorption of energy related to transients: this was accomplished by passing long and short duration current impulses through the valve elements using an impulse current generator.
4) Thermal ageing followed by transients caused ageing.
5) Transients caused ageing followed by thermal ageing.

The last two types of ageing simulate multi-factor degradation for MOSA in service.

1.5 Electrical representation of MOSA elements

The conduction mechanism of MOSA is still not yet fully understood. Seven possible mechanisms have been proposed [3] and different equivalent circuits have been proposed by different researchers.

The most commonly used simplified equivalent circuit comprises of a non-linear resistance in parallel with a capacitance as shown in Fig. 1.9. The non-linear resistance is a function of the applied voltage across the valve element. The total current flowing through the valve element (i_t) is a combination of the capacitive current i_c and the resistive current i_r which is in phase with the voltage applied to the element. This model has sufficient accuracy and is widely used. Since the diagnostics were all carried out under 60*Hz* voltage and the objective of the project is to compare the effectiveness of the several leakage current based diagnostic methods, the above simplified equivalent circuit was employed throughout this study to represent the MOSA elements.

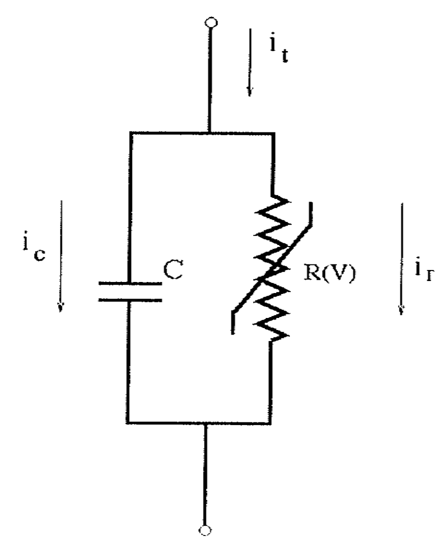

Fig. 1.9 Simplified electrical representation of MOSA elements

CHAPTER 2

EXPERIMENTAL SETUP, PROCEDURE AND DIAGNOSTIC TECHNIQUES

This chapter describes the experimental setup, the details of the experimental procedure employed to artificially age the valve elements and also the diagnostic techniques.

2.1 Data acquisition system

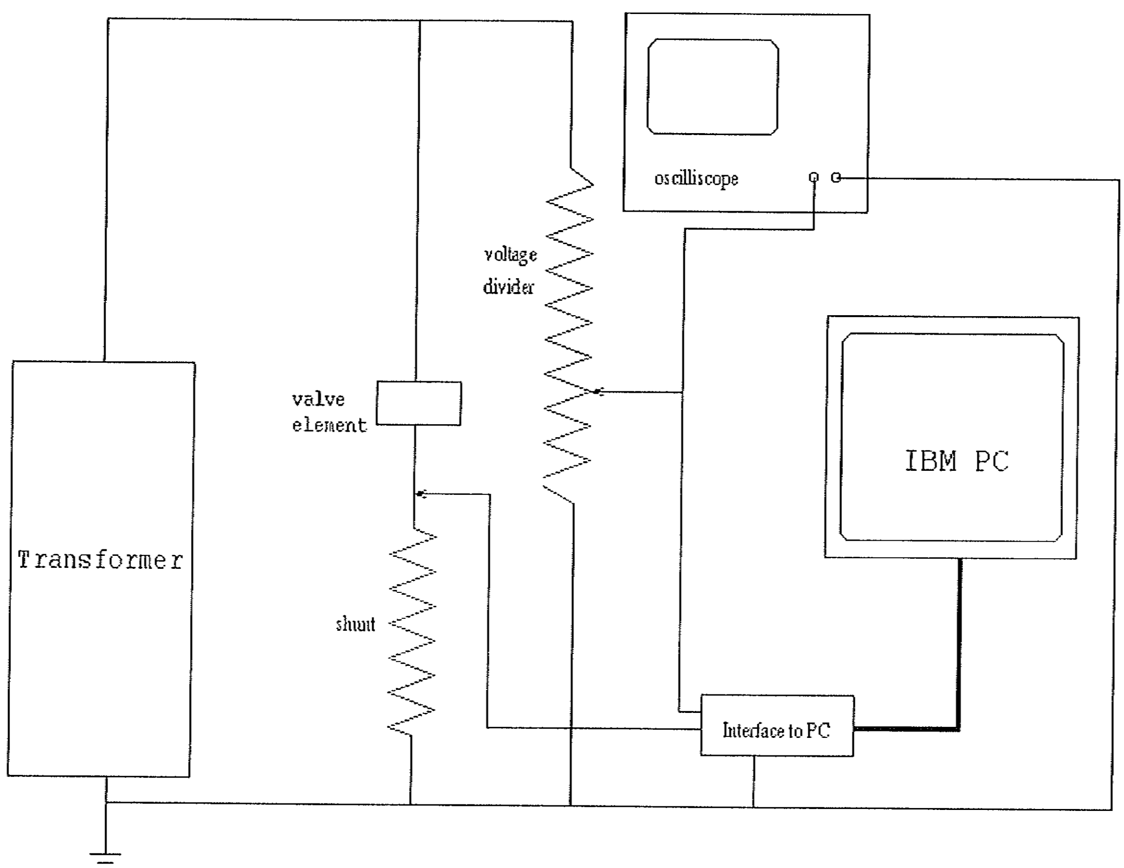

Fig. 2. 1 Computer-aided data acquisition system

The computer aided data acquisition system used in this project is shown in Fig. 2.1. A resistive voltage divider was chosen for measuring the applied voltage across the valve element. This is because the input resistance of the device labelled as "interface to PC" in Fig. 2.1 is not infinity but 650kΩ. Using a capacitive divider for voltage reading introduces error in the measured voltage because the capacitive divider and the 650kΩ input resistance form a local *R-C* circuit. The resistive divider used had a ratio of 5007.127 to 1. The total current through the valve element was measured by measuring the voltage across the shunt resistor. The value of the shunt resistors varies from 101Ω to 1000Ω depending upon the magnitude of the current being measured. The total current and the applied voltage signals were digitized by a set of A/D conversion devices with data acquisition software by ***National Instrument Inc.*** and stored in an IBM PC for diagnostics.

2.2 Experimental setup

2.2.1 Thermal ageing

In this project, thermal ageing was accomplished by exposing the unenergized valve elements to high temperature (160°C) in an environmental chamber. This environmental chamber (-16~360°C) is equipped with an accurate temperature controller (temperature deviation did not exceed ±1°C).

2.2.2 Moisture ingress caused ageing

Moisture ingress caused ageing was investigated using a specially-designed water-tight environmental chamber of dimensions slightly larger than the valve element. A schematic graph of the setup is shown in Fig. 2.2. The applied voltage and total current flowing through the element were continuously monitored by an oscilloscope.

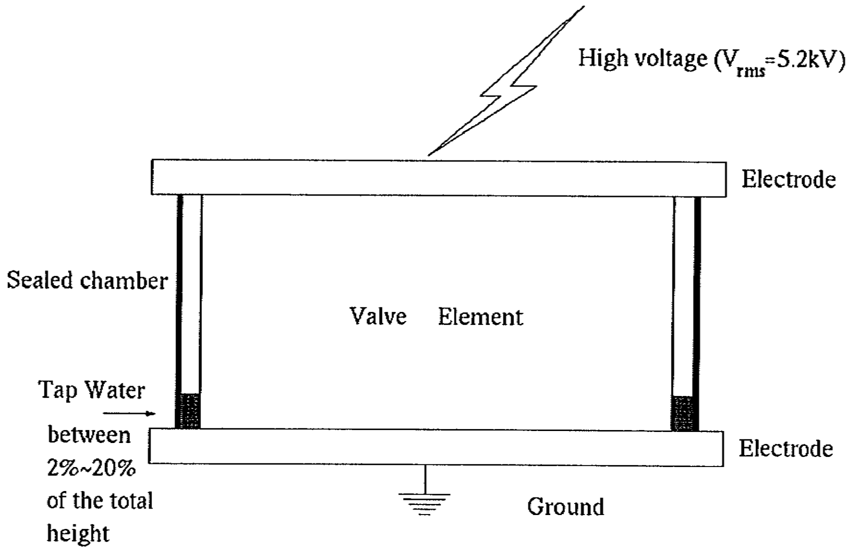

Fig. 2.2 Set-up for moisture ingress caused ageing test

2.2.3 Transients caused ageing

Transients caused ageing was caused by passing long or short duration current impulses of different magnitudes through the valve elements. A self-triggered impulse current generator which comprised of six 0.7μF, 75kV capacitors in parallel was employed to generate current impulses of different waveshapes. This generator produced a short duration waveform of 1.5 x 4 μs without insertion of any external inductance. A long duration waveform, 15 x 29 μs was obtained by insertion of a 6μH external inductance. The impulse current was monitored by a Pearson current monitor, model 1080 in conjunction with a Tektronix TDS 540 oscilloscope.

2.2.4 Thermal ageing followed by transients caused ageing

The element was initially aged thermally in the environmental chamber at 160°C; afterwards the element was subjected to a series of short duration current impulses with a waveform of 1.5 x 4 μs.

2.2.5 Transients caused ageing followed by thermal ageing

A valve element was thermally aged in the environmental chamber at 160°C after being subjected to a series of long duration current impulses (with a waveform of 15 x 29 μs) ageing.

2.2. 6 Infrared imaging

In transient caused ageing tests, an Inframetrics 740 infrared imaging radiometer was used to investigate the temperature distribution in the valve element. The radiometer was connected to a VCR to enable observation of the temperature distribution zone. This information could also be stored on a video tape or a floppy disk for later analysis.

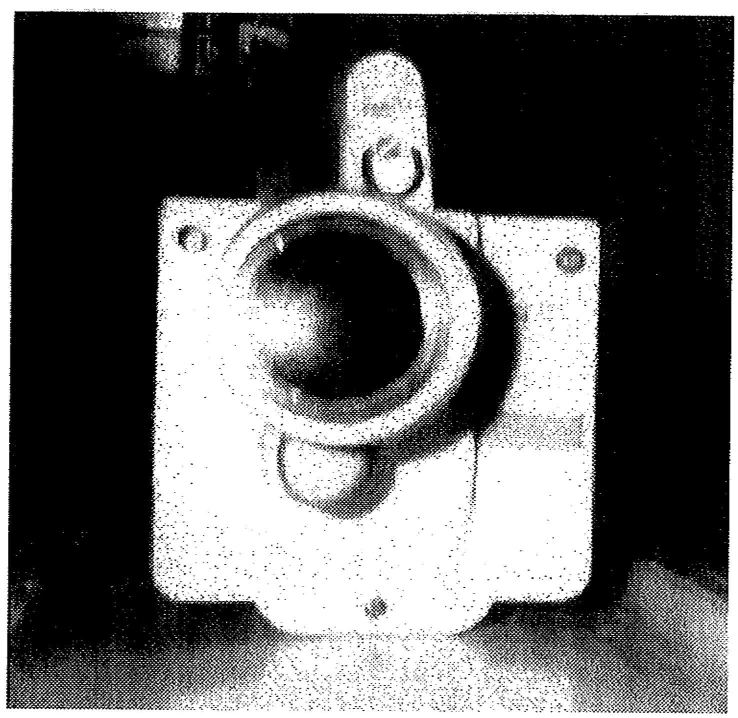

Fig. 2.3 (a) Camera of the Inframetrics 740 infrared imaging radiometer

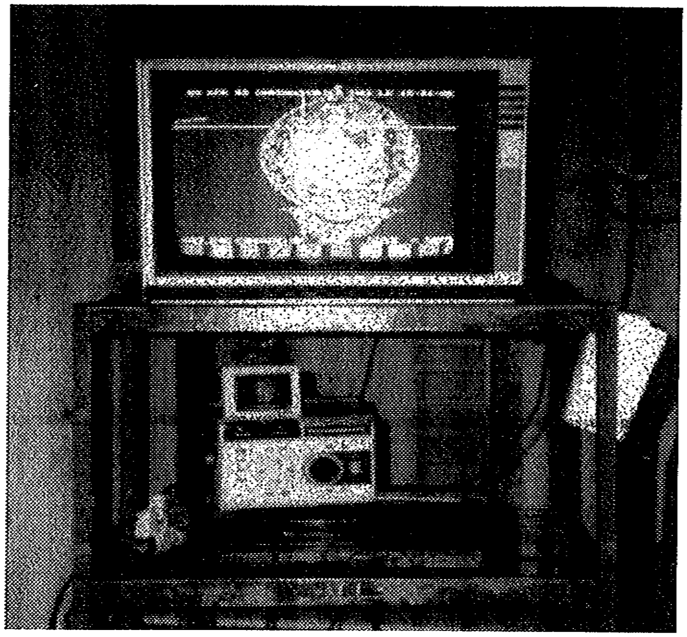

Fig. 2.3 (b)Inframetrics 740 infrared imaging radiometer and the VCR

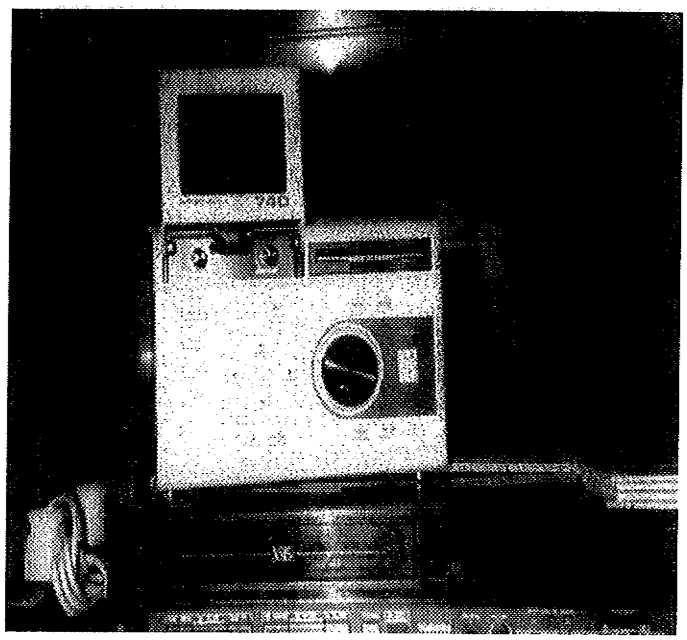

Fig. 2.3(c)A close look of the Inframetrics 740 infrared imaging radiometer and the VCR in conjunction

Fig. 2.3 Setup of the Inframetrics 740 infrared imaging radiometer

2.2.7 MOSA valve elements

Altogether three types of valve elements were used in this project. Type I belongs to a

42kV MCOV distribution type arrester with 10 elements in series. They are 62mm in diameter and 40mm in height. In thermal ageing, transients caused ageing and the two types of hybrid thermal/transient ageing, type I valve elements were used. Type II belongs to a 66kV MCOV substation type arrester with 30 valve elements in series. These elements were also 62mm in diameter but 23mm in height. They were only used to verify some results in the transient caused ageing test. Type III valve elements provided by Manitoba Hydro were 78mm in diameter and 44mm in height. This type of element was used for moisture ingress caused ageing. Its MCOV is approximately 5.2kV as determined by experiment.

Diagnostics were initially carried out on the unaged valve elements. All diagnostics were carried out at five voltage levels. One of the levels corresponds to the MCOV of the valve element (defined as MCOV of the arrester divided by the number of the elements in the arrester); the highest voltage level applied is approximately 40% greater.

2.3 Experimental procedure

2.3.1 Thermal ageing (in the absence of applied voltage)

The unenergized element was heated in the environmental chamber at a selected temperature of 160°C. At first the temperature was set at 140°C according to some literature [20]. The element was heated at 140°C for 20 hours every day and then cooled in ambient air for 4 hours before its volt-amp characteristics was examined. It was found that the aging process under 140°C thermal ageing was very slow; hence the temperature was raised to 160°C in future experiments. Diagnostics were conducted immediately after the element was taken out of the oven. It was ensured that the time used for diagnostic did not exceed 20 seconds.

Two types of thermal ageing were carried out on the same type of valve elements. The first type of thermal ageing was accomplished by heating the element in the oven for 8 hours every day at 160°C followed by 16 hours of cooling in ambient air. The aging scheme simulates the natural heating and cooling cycles an arrester in service is subjected to. This type of ageing is referred to as cyclic thermal ageing in the remaining part of this thesis.

The last type of thermal ageing was accomplished by heating the element without interruption, i.e. 24 hours every day. It is referred to as continuous thermal ageing.

In the above 2 types of thermal ageing, the volt-current characteristics were initially checked everyday for the first 25 days, then checked once every three or four days.

2.3.2 Moisture ingress caused ageing

The element was placed in the sealed chamber shown in Fig. 2.2 (page 19). A measured amount of tap water was introduced in the chamber. Continuous $60Hz$ AC voltage corresponding to V_{ref}[1] [20] was applied to the element in the chamber. In four different tests, 12.1g, 6.6g, 2.2g and 1.1g tap water were introduced into the chamber respectively. In each test, diagnostics were conducted at all five voltage levels[2] at intervals of 30 minutes to 2 hours depending on the time rate of the increase of total leakage current.

1. V_{ref} is the applied AC voltage whose peak value is equal to a DC voltage that results in a current density of $1\mu A/mm^2$ in the valve element.
2. The five voltage levels at which diagnostics were conducted are 70%, 100%, 120%, 130% & 140% of the MCOV respectively.

2.3.3 Transients caused ageing

Two Type I valve elements were subjected to short duration impulse (1.5 x 4 μs) current ageing. The first element was subjected to impulse current tests as follows: 10 shots @10kA, 2 series of 10 shots @ 25kA, 2series of 10 shots @ 30kA, 20 shots @ 40kA, 20 shots @ 50kA, 20 shots @ 65kA and 20 shots @ 70 kA. The second element was subjected to the following series of tests: 20 shots @ 25kA, 20 shots @ 50kA, 20 shots @ 60kA, 40 shots @60 kA, 20 shots @ 60kA, 2 series of 20 shots @ 55kA.

Also two Type I valve elements were aged by long duration impulse (15 x 29 μs) current. The first element was aged as follows: 10 shots @ 6.0kA, 2 series of 30 shots @ 8kA, 25 shots @ 10kA, 4 series of 30 shots @ 9.5kA, 30 shots @ 10kA. The second element was aged as follows: 4 series of 20 shots @ 15~20 kA, 3 series of 30 shots @ 20kA, 10 shots @ 20kA.

Diagnostics were conducted at the conclusion of each series after the element was cooled naturally to ambient temperature.

2.3.4 Thermal ageing followed by transients caused ageing

A type I element was first thermally aged in the environmental chamber at 160°C for 480 hours. Next it was subjected to short duration current impulse ageing as follows: 2 serious of 10 shots @ 30kA, 2 serious of 20 shots @ 30kA, 20 shots @ 40kA, 30 shots @ 50kA, 30 shots @ 60 kA, 18 shots @ 60kA. This type of ageing is referred to as thermal/ transient ageing in the remaining part of the thesis.

Diagnostics were conducted at the conclusion of each series after the element was cooled naturally to ambient temperature.

2.3.5 Transients caused ageing followed by thermal ageing

A type I valve element was first subjected to long duration current impulse ageing as follows: 4 series of 20 shots @ 15~20 kA, 3 series of 30 shots @ 20kA, 10 shots @ 20kA, followed by continuous thermal ageing at 160°C in the environmental chamber for 30 days. The diagnostics were carried out on the elements every 48 hours. This type of ageing is referred to as transient/thermal ageing.

2.3.6 Infrared imaging

The transients caused ageing was monitored by observation of temperature distribution in the valve element using the Inframetrics 740 infrared imaging radiometer. This information was recorded on the tape via the VCR connected to the radiometer. During the ageing tests, the temperature distribution inside the element was continuously monitored and every temperature distribution image that was of interest was stored on a floppy disk for later analysis. Immediately after every series of tests, a top view of the temperature distribution inside the valve element was recorded to study the change in the power handling capability of the valve element.

2.4 Diagnostic techniques

Diagnostic methods were conducted by examination of the following nine indicators.

1) I_{rp} , the peak value of the resistive current $i_r(t)$.

2) I_{r3} , the peak value of the 3rd harmonic content of the resistive current $i_r(t)$.

3) The power dissipated in the valve element under 60 *Hz AC* voltage.

4) The r.m.s. voltage necessary to cause $I_{rp} = 1mA$.

5) The ratio of I_{r3} / I_{rp}.

6) The ratio of two areas (A1/A2) derived from the v-i_r characteristics (see Fig. 2.4), where v is the applied voltage.

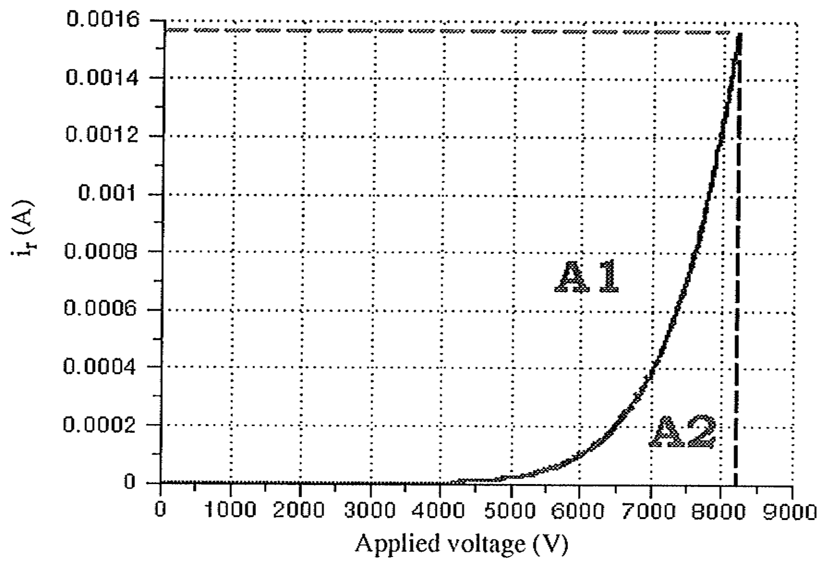

Fig.2.4 Typical $v(t)$-$i_r(t)$ characteristics of MOSA elements

7) The capacitance of the valve element [21].

8) The parameters A and β in the relation

$$i_r(t) = \left(\frac{v(t)}{A}\right)^{\beta} \tag{2.1}$$

relating the instantaneous values of $i_r(t)$ and $v(t)$. This relationship was obtained at specified voltage levels. At each voltage level the relationship is characterized by a value of A and β, which represent the non-linearity in the valve element resistance. The relationship in Eq. 2.1 is not the same as the commonly used empirical relation stated in Eq. 1.1 ($I = \left(\frac{V}{C}\right)^{\alpha}$), which relates peak values of the applied voltages and the resistive currents.

9) In addition to the above indicators, examination of the positive and negative peak values of i_r was included as a diagnostic method to detect impulse current caused ageing after preliminary test results indicated that passage of current impulses resulted in an asymmetry in the waveform of i_r. A similar result has been reported in [22].

All the diagnostic methods are based on the knowledge of resistive current through the valve element $i_r(t)$. This current was obtained by application of Fourier analysis on the total current $i_t(t)$ as well as the applied voltage waveform.

Assume the applied voltage can be represented by

$$v(t) = v_f(t) + v_h(t) = v_1\cos(\omega t) + v_3\cos(3\omega t + \Phi_3) + v_5\cos(5\omega t + \Phi_5) + \dots \tag{2.2}$$

where $v_f(t)$ stands for the fundamental frequency voltage $v_1\cos(\omega t)$ and $v_h(t)$ denotes the total of the harmonic voltages which is comprised of $v_3\cos(3\omega t+\Phi_3)+v_5\cos(5\omega t+\Phi_5)+\dots$, and Φ_3, Φ_5 are the phase angles. Total current $i_t(t)$ is the combination of the resistive current and the capacitive current (see the electrical representation of valve elements shown in Fig. 1.9), hence

$$\begin{aligned} i_t(t) &= i_r(t) + i_c(t) \\ &= i_r(t) + \omega C v_1\cos\left(\omega t - 90^o\right) + 3\omega C v_3\cos\left(3\omega t + \Phi_3 - 90^o\right) \\ &\quad + 5\omega C v_5\cos\left(5\omega t + \Phi_5 - 90^o\right) + \dots \end{aligned} \tag{2.3}$$

where $i_r(t)$ is the resistive current, $i_c(t)$ is the capacitive current, C is the capacitance of the

MOSA valve element.

The capacitance of the valve element C was found by consideration of the fundamental frequency voltage and current component which is 90^o out of phase with the former. By subtraction of all the capacitive current components, caused by the fundamental and harmonic voltages $(\omega Cv_1 cos[\omega t-90^o]+3\omega Cv_3 cos[3\omega t+\Phi_3-90^o]+5\omega Cv_5 cos[5\omega t+\Phi_5-90^o]+...)$, from the total current $i_t(t)$, the resistive current $i_r(t)$ was found. By application of Fourier analysis on the resistive current the harmonic content in i_r could be found. The power dissipated in the element in one cycle could be calculated by numerical integration using $Power=\frac{1}{T}\int_0^T v(t)\, i_r(t)\, dt=\frac{1}{T}\sum_0^{\frac{T}{\Delta t}} v(t)\, i_r(t)\, \Delta t$. ($\Delta t$ being the time interval between 2 successive data points).

The r.m.s. voltage necessary to produce I_{rp} = 1mA was found by interpolating the data of applied voltage (rms value) and the peak resistive current (I_{rp}) obtained under all five voltage levels using a spline function.

The parameters A and β in the relation $i_r(t) = \left(\frac{v(t)}{A}\right)^{\beta}$ were obtained using a curve fitting scheme on the data of $v(t)$ and $i_r(t)$ acquired in one quarter cycle [23].

CHAPTER 3

METHOD TO ACCOUNT FOR THE VOLTAGE HARMONICS IN THE SYSTEM

In this chapter, the method employed to remove the influence caused by voltage harmonics is discussed. Some diagnostic results on a transients aged element are presented to demonstrate the importance of accounting for the influence of harmonics. Since the voltage measurements were taken with the valve element in circuit, the effect of source impedence was eliminated.

3.1 Problem

All of the diagnostic methods studied in this work are based on the measured $60Hz$ current through the valve elements. Because of the non-linear v-i_r characteristics of the MOSA valve elements, even a slight distortion in the applied voltage results in a significant difference in the measured current if the distortion is present at a voltage higher than the turn-on voltage of the element. It was found that the voltage supply in the high voltage laboratory was harmonic contaminated and this caused significant inaccuracy in the results. The harmonic content in the voltage signal (see Table 3.1 on page 30) was different at different times of the day; the most significant being the 3rd and the 5th. If the voltage harmonics are not accounted for, erroneous diagnostics will be obtained.

Table 3.1 Harmonic content in a wall-outlet in the laboratory

Time	Ratio to fundamental of			
	3rd harmonic	5th harmonic	7th harmonic	9th harmonic
Jan. 7, 1995. 16:17	1.14%	1.50%	0.71%	0.33%
March 1, 1995. 18:07	1.82%	1.77%	1.19%	0.19%
April 10, 1995. 17:36	1.29%	1.78%	0.85%	0.30%
August 22, 1995. 17:25	2.13%	1.41%	0.40%	0.30%

Since the v-i_r characteristics of the MOSA valve elements are very non-linear, so unless the intervals between data points are small enough, it is not acceptable to use linear interpolation to correct for the influence. In the experimental setup employed in this work, about 720 data points were collected in every cycle, therefore it is not acceptable to use linear interpolation to account for the influence caused by the harmonics.

3.2 Proposed method

The following method is proposed. Let f be a function defined in a closed interval between a and $a+h$. Assume that the function has n derivatives in this interval, and that all of them are continuous functions. Then

$$f(a+h) = \sum_{k=0}^{n} \frac{f^{(k)}(a)h^k}{k!} + o\left(h^{n+1}\right) \tag{3.1}$$

or

$$f(a+h) = f(a) + f^{(1)}(a)h + \frac{f^{(2)}(a)h^2}{2!} + \ldots + \frac{f^{(n)}(a)h^n}{n!} + o\left(h^{n+1}\right) \tag{3.2}$$

Let $v(t)$ denote the applied voltage, which is comprised of $v_f(t)$, fundamental frequency voltage, and $v_h(t)$, the sum of all the harmonics. The following relationships apply,

$$v = v_f + v_h \tag{3.3}$$

The resistive current, i_r, is a function of the applied voltage, hence

$$i_r = F(v_f + v_h) \tag{3.4}$$

&

$$i_{rf} = F(v_f) \tag{3.5}$$

where i_r is the resistive current (influenced by the voltage harmonics) and i_{rf} is the resistive current if the valve element is only subject to pure fundamental frequency voltage; i_{rf} is the current that gives true ageing information of the valve elements.

Consider:

$$i_r = F(v_f + v_h)$$

$$= F(v_f) + F^{(1)}(v_f)v_h + \frac{F^{(2)}(v_f)v_h^2}{2!} + \ldots + \frac{F^{(n)}(v_f)v_h^n}{n!} + o(v_h^{n+1}) \tag{3.6}$$

Because $v_h << v_f$ (According to IEEE std 519-1992, individual voltage distortion should not exceed 3.0%, total voltage distortion should not exceed 5.0% [24]), hence

$$F^{(n)}(v_f) \approx F^{(n)}(v_f + v_h) \quad n = 1,2,3\ldots$$

Eq. 3.6 may be rewritten as:

$$i_r \approx F(v_f) + F^{(1)}(v_f + v_h)v_h + \frac{F^{(2)}(v_f + v_h)v_h^2}{2!} + \ldots + \frac{F^{(n)}(v_f + v_h)v_h^n}{n!} + o(v_h^{n+1})$$

$$= F(v_f) + F^{(1)}(v)v_h + \frac{F^{(2)}(v)v_h^2}{2!} + \ldots + \frac{F^{(n)}(v)v_h^n}{n!} + o(v_h^{n+1}) \tag{3.7}$$

Hence

$$i_{rf} = F\left(v_f\right) = i_r - F^{(1)}(v)\,v_h - \frac{F^{(2)}(v)\,v_h^2}{2!} - \ldots \tag{3.8}$$

or

$$i_{rf} \approx i_r - F^{(1)}(v)\,v_h \qquad \textit{if } \frac{F^{(n)}(v)\,v_h^n}{n!} \textit{ (n> 1) is relatively small.} \tag{3.9}$$

Eq. 3.9 allows the calculation of i_{rf} from i_r if $\frac{di_r}{dv}$ and $\frac{d^2 i_r}{dv^2}$ etc. are known. In the present work, derivatives of order 2 and higher were not considered since they were relatively small ($\frac{F^{(2)}(v)\,v_h^2}{2!}$ was less than 5% of $F^{(1)}(v)v_h$). $\frac{di_r}{dv}$ was found from

$$\frac{di_r}{dv} = \frac{\left(\frac{di_r}{dt}\right)}{\left(\frac{dv}{dt}\right)} \tag{3.10}$$

$\frac{di_r}{dt}$ and $\frac{dv}{dt}$ were found by performing Fourier analysis on $i_r(t)$ and $v(t)$.

Estimation of errors in the method

The errors arise from the assumptions:

1. $F^{(n)}\left(v_f\right) \approx F^{(n)}\left(v_f + v_h\right)$.

2. $i_{rf} \approx i_r - F^{(1)}(v)\,v_h$.

The second error can be reduced by inclusion of terms of higher order in Eq. 3.9, i.e.

$$i_{rf} = F\left(v_f\right) = i_{rf} - F^{(1)}(v)\,v_h - \frac{F^{(2)}(v)\,v_h^n}{2!} - \ldots.$$

3.3 Verification of the method by simulation

Assume a fundamental voltage of peak value 8200V and 3rd harmonic of 1-2%, i.e.

$$v_f = 8200\sin(\omega t) \qquad \& \quad v_h = 1\sim2\ \%\ [\ 8200\sin(3\omega t + \Phi_3)]$$

$$v = v_f + v_h = 8200\sin(\omega t) + 1\sim2\%\ [\ 8200\sin(3\omega t + \Phi_3)] \tag{3.11}$$

It is assumed that the 3rd harmonic is the only harmonic present. The resistance of the valve element is non-linear and it can be approximated by the relationship

$$i_r = \left(\frac{v}{A}\right)^{\beta}$$

with $A = 25859.57$, $\beta = 5.66$ (3.12)

Hence

$$i_{rf} = \left(\frac{v_f}{A}\right)^{\beta} \tag{3.13}$$

$$\& \quad i_r = \left(\frac{v_f + v_h}{A}\right)^{\beta} \tag{3.14}$$

The suggested method of correction was applied to the waveform of i_r from Eq. 3.14. The derivative $\frac{di_r}{dv}$ was obtained from Eq. 3.12 by direct differentiation as well as by using the method outlined in Eq. 3.10, the difference between the results from both methods is small and negligible. The corrected waveform, i_{rc} , was then compared with i_{rf} from Eq. 3.13. The results are shown in Figs. 3.1 and 3. 2 and Table 3.2.

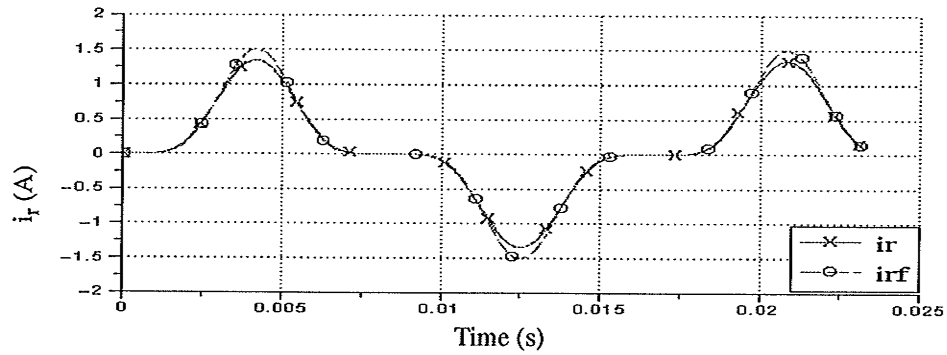

(a)

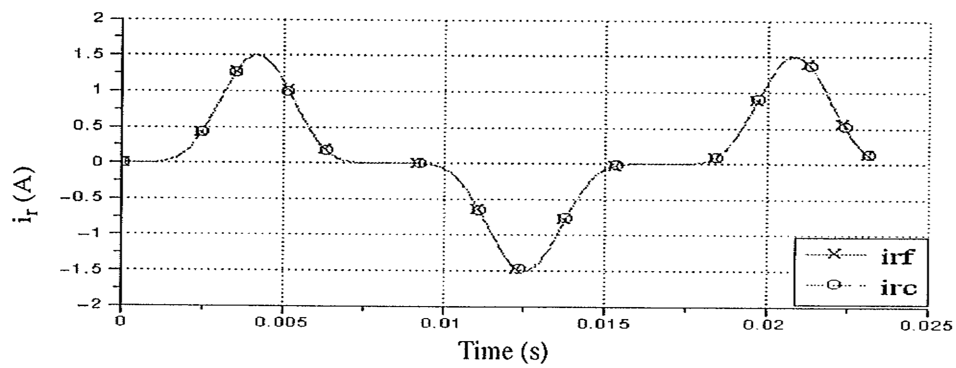

(b)

Fig. 3.1 Resistive current waveforms

(a) Harmonic affected (i_r) and unaffected (i_{rf}) waveform. 3rd harmonic content in voltage = 2%, phase shift $\Phi_3 = 0^o$

(b) Corrected waveform (i_{rc}) and unaffected (i_{rf}) waveform. 3rd harmonic content in voltage = 2%, phase shift $\Phi_3 = 0^o$

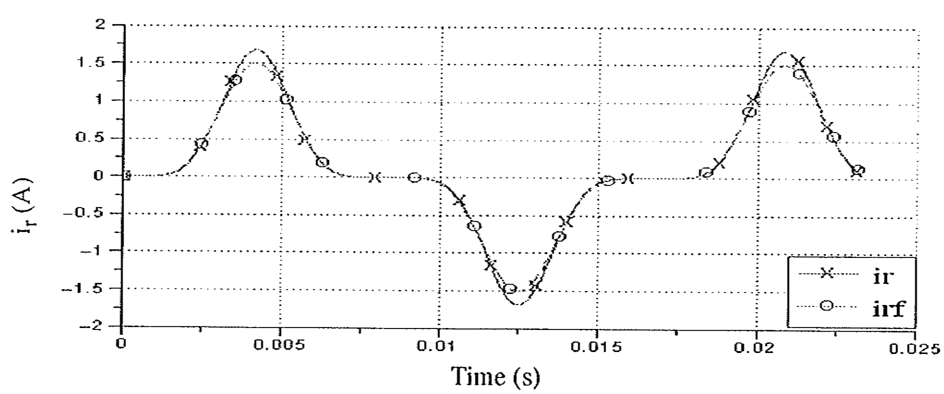

(a)

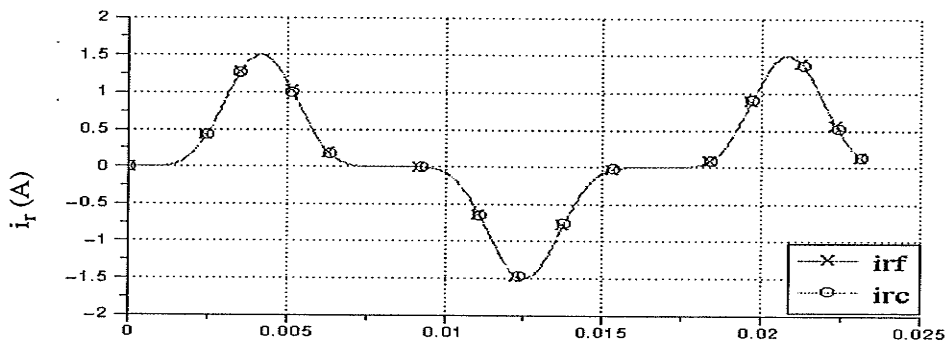

(b)

Fig. 3.2 Resistive current waveforms

(a) Harmonic affected (i_r) and unaffected (i_{rf}) waveform. 3rd harmonic content in voltage = 2%, phase shift $\Phi_3 = 180^{o}$

(b) Corrected waveform (i_{rc}) and unaffected (i_{rf}) waveform. 3rd harmonic content in voltage = 2%, phase shift $\Phi_3 = 180^{o}$

Table 3.2 Absolute percent maximum deviations (a) $\left|\frac{i_r - i_{rf}}{i_{rf}}\right|$ **and (b)** $\left|\frac{i_{rc} - i_{rf}}{i_{rf}}\right|$

phase shift of the 3rd harmonic Φ_3	3rd voltage harmonic content					
	1.0%		1.5%		2.0%	
	(a)	(b)	(a)	(b)	(a)	(b)
0	5.53%	0.13%	8.20%	0.29%%	10.81%	0.50%
π/4	5.43%	0.13%	8.05%	0.29%	10.52%	0.52%
π/2	5.43%	0.15%	8.23%	0.35%	11.10%	0.63%
2π/3	5.61%	0.14%	8.51%	0.32%	11.48%	0.58%
π	5.79%	0.14%	8.79%	0.31%	11.86%	0.55%

From the simulated results, it is obvious that correction is necessary because 1% ~ 2% of third harmonic leads to 5% ~ 12% error if this influence is not corrected; the error may be positive or negative which results in either an over or under-estimation of the degradation of the valve element.

Diagnostic methods were applied to an impulse current aged element at different stages of ageing. The diagnostic indicators are plotted in Figs. 3.3 ~ 3.5 against progress of ageing. In impulse current caused ageing the progress of ageing is monitored by the cumulated energy expended in the valve element. In each plot, the harmonic influenced and corrected results are both shown. These results correspond to the diagnostics conducted under 1.4 times MCOV because at this voltage level, the harmonic influence on the diagnostics is more prominent. Figs. 3.3 ~ 3.5 show the behavior of diagnostic indicators I_{rp}, the power dissipated in the element and I_{r3}/I_{rp}. When the influence of harmonic is not accounted for, Figs. 3.3 and 3.5 show that the variation in the indicator exhibits a different trend; while Fig. 3.4 shows that the power dissipated in the valve element is greater.

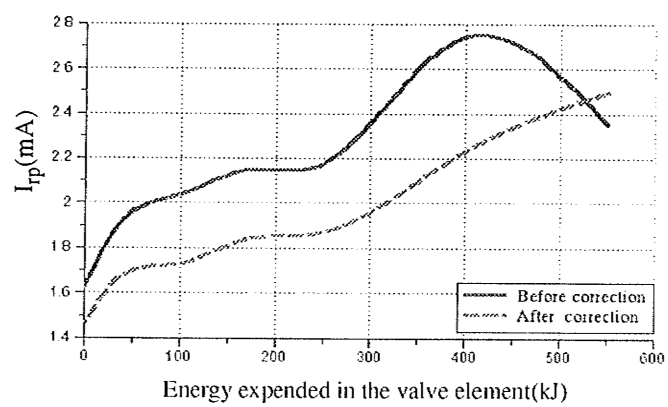

Fig. 3.3 Diagnostic indicator #1, I_{rp}

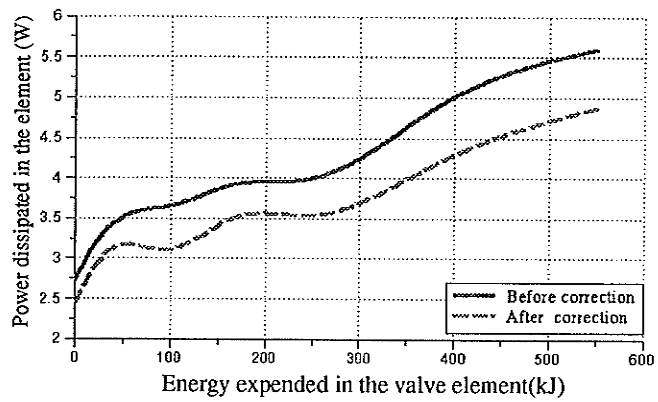

Fig. 3.4 Diagnostic indicator #4, power dissipated in the element under 60*Hz* voltage.

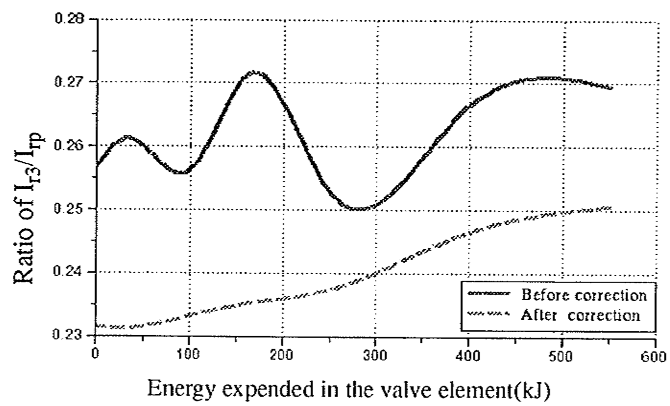

Fig. 3.5 Diagnostic indicator #5, I_{r3} / I_{rp}

Therefore it is important to account for the influence of voltage harmonics in diagnostic results which are used to detect the degradation in valve element of Metal Oxide Surge Arresters. The technique discussed in section 3.2 was applied to all the resistive current data in the rest of this thesis work. In the next chapter, only the harmonics-effect-removed results are presented.

CHAPTER 4

COMPARISON OF DIAGNOSTIC METHODS

In this chapter, all the diagnostic results are presented and the effectiveness of the diagnostic indicators in detecting degradation and detecting the cause of degradation is discussed. Infrared images of temperature distribution in the valve element after being subjected to current impulses are also shown.

4.1 Presentation of the diagnostic data

A. Thermal ageing

Though the procedure for cyclic thermal ageing and continuous thermal ageing is different, it was found that the trend of the results obtained under these two types of thermal ageing was very similar. However continuous thermal ageing caused a greater change in the diagnostic indicators because of the longer ageing time. Therefore in the next section, only the results obtained under continuous thermal ageing are presented.

B. Moisture ageing

When 12.1g water was introduced in the sealed chamber, the initial height of the water in the chamber was approximately one fifth of the valve element's height and thermal runaway occurred very rapidly (See Fig. 4.1(a)). With 6.6g water in chamber, the initial height of water in chamber was about one tenth of the total height of the element. It took a longer time to reach the thermal runaway condition. With 2.2g water in the chamber, the initial height of the water in the chamber was only approximately one twenty-fifth of the element height; it took an even longer time for thermal runaway to occur. In the last experiment with 1.1g water, corresponding to one fiftieth of the element height, the total current rose initially but eventually settled at a stable level (see Fig. 4.1(b)). In the first three cases, after the test was discontinued, very fine water droplets were noticed on the sidewall. These droplets formed a chain between the two electrodes.

In all cases, since the test was interrupted prior to thermal runaway, it was found that the element recovered eventually, i.e. the element displayed its normal volt-current characteristics.

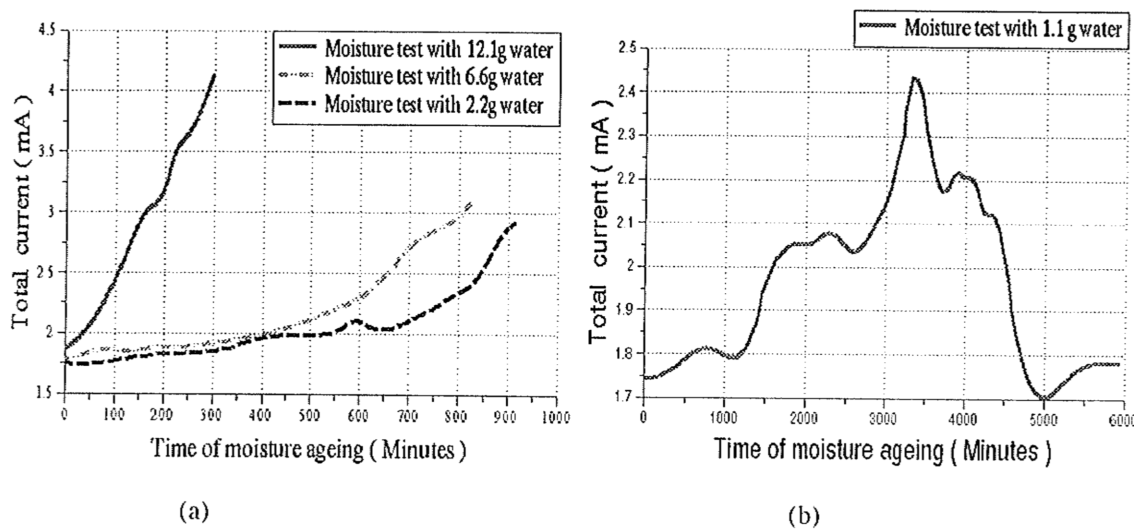

Fig. 4.1 Current variation with time in moisture ageing test

(a) Moisture ageing test with 12.1g, 6.6 g and 2.2g water
(b) Moisture ageing test with 1.1 g water

The results presented in the next section correspond to the case when 6.6g of water was introduced into the chamber.

C. Impulse current caused ageing

In Figs. 4.3~4.13 in the next section, the results presented correspond to ageing caused by short duration current impulses. Similar results were obtained with long duration current impulses except that the progress of deterioration was slower. This is probably due to the different current distribution in the element under this waveshape. The data presented in the next section corresponds to the valve element which was subjected to: 10 shots @ 10kA, 2 series of 10 shots @ 25kA, 2series of 10 shots @ 30kA, 20 shots @ 40kA, 20 shots @ 50kA, 20 shots @ 65kA and 20 shots @ 70kA. After the passage of the last 20 short duration current impulses @ 70kA, 2 more shots of 80kA were applied to the valve element, after which the valve element was shattered by passage of the current impulse. See Fig. 4.2.

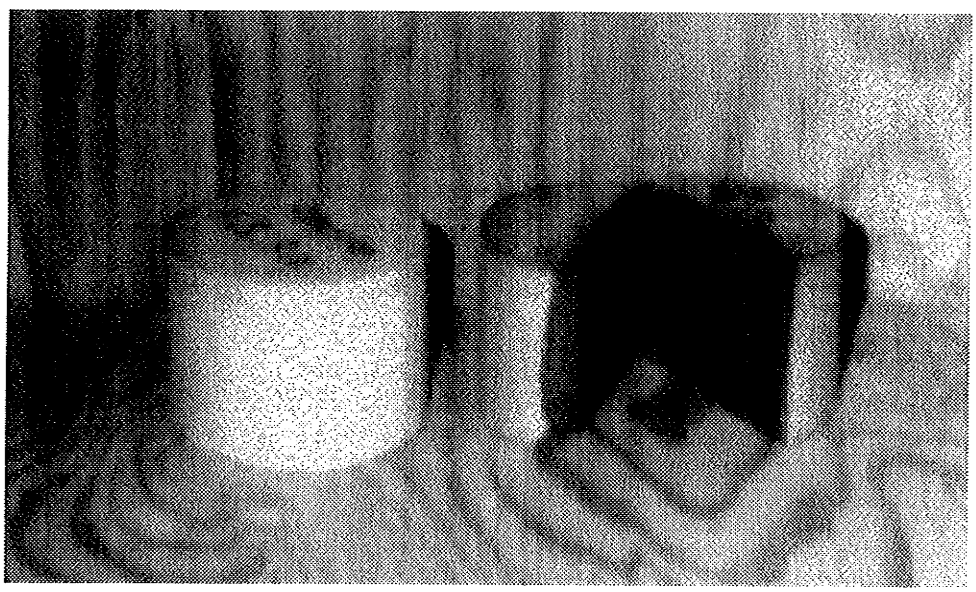

Fig. 4.2 The shattered valve element (right) and a new valve element (left)

4.2 Comparison of the diagnostic methods

In this section, all the diagnostic results will be presented. The values of the diagnostic indicators acquired on the unaged valve elements (before laboratory-controlled ageing started) are considered as base values. The values of the diagnostic indicators acquired on the degraded valve elements are expressed in p.u. with respect to the above base. The changes in the diagnostic indicators are plotted against the progress of ageing. Under thermal, moisture and transient/thermal ageing, the changes in diagnostic indicators are plotted against the time of ageing. Under transients and thermal/transient ageing, the indicators are plotted versus the cumulative energy expended in the valve element. In each case two curves are presented: one corresponds to tests conducted under the MCOV of the valve element and the other curve corresponds to the those conducted under 1.4 times MCOV.

In Fig. 4.3 (a) ~(e) the behaviour of diagnostic indicator #1, I_{rp} (the peak value of the resistive current) is presented. It is seen that there is an increase in I_{rp} in all cases. The indicator obtained under the application of MCOV shows more sensitivity to the degradation except in the case of thermally aged valve element and the transient/thermal aged element. The behaviour of this diagnostic indicator is more or less the same for every type of ageing, it is therefore difficult to distinguish the cause of the ageing using this indicator.

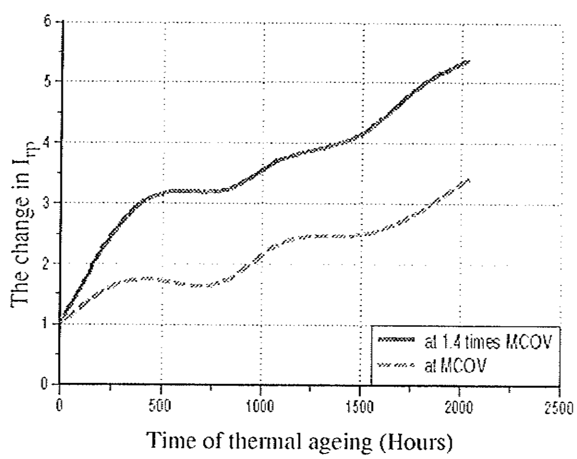

(a)

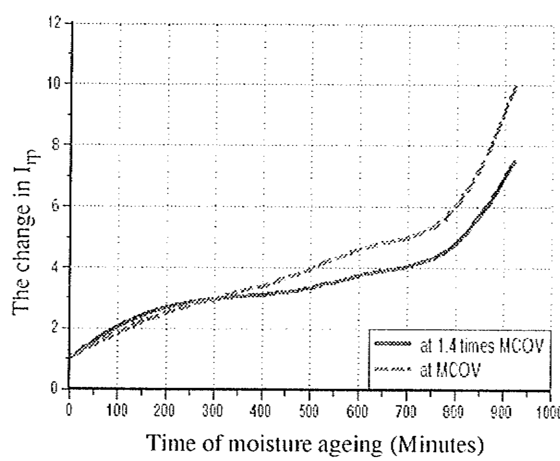

(b)

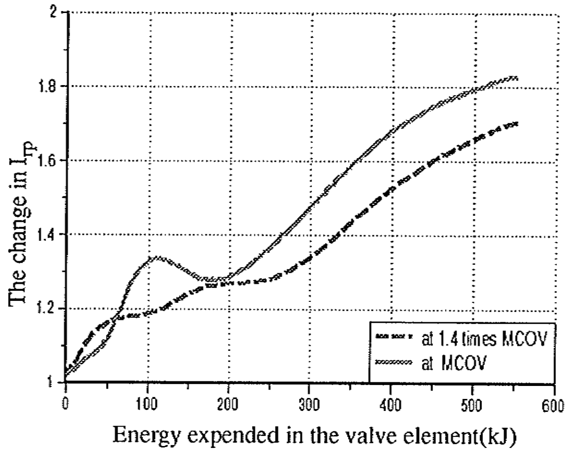

(c)

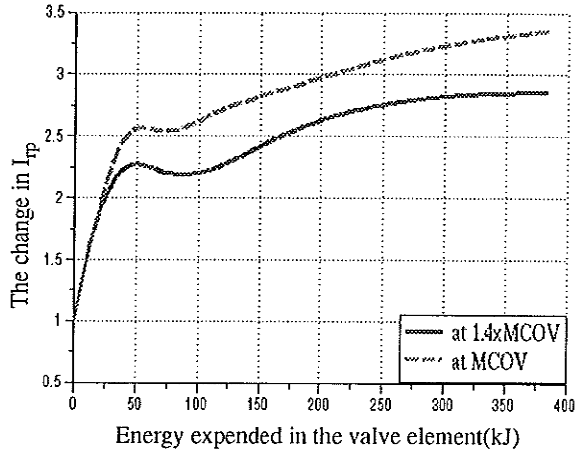

(d)

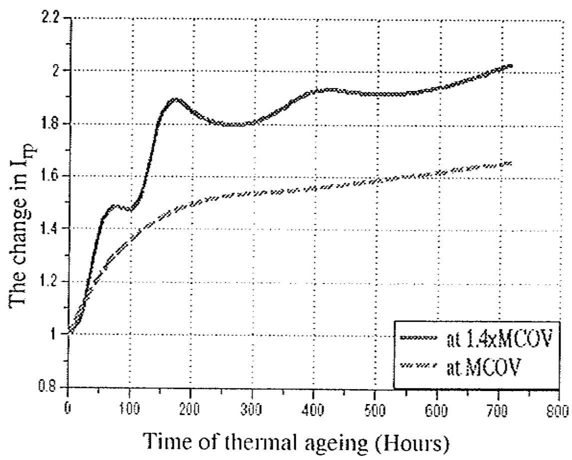

(e)

Fig. 4.3 Behaviour of diagnostic indicator #1, the peak value of the resistive current (I_{rp})
(a) Thermal ageing
(b) Moisture ingress caused ageing
(c) Transient ageing
(d) Thermal/transient ageing
(e) Transient/thermal ageing

Fig. 4.4(a) ~ (e) shows almost the same trend as that shown in Fig. 4.3. The peak values of the resistive third harmonic current (I_{r3}) increase in all cases. Also tests conducted under MCOV exhibit better sensitivity than those conducted under 1.4 times MCOV except under thermal ageing and transient/thermal ageing. The trend under each type of ageing is once again more or less the same which makes this diagnostic indicator incapable of distinguishing the cause of ageing.

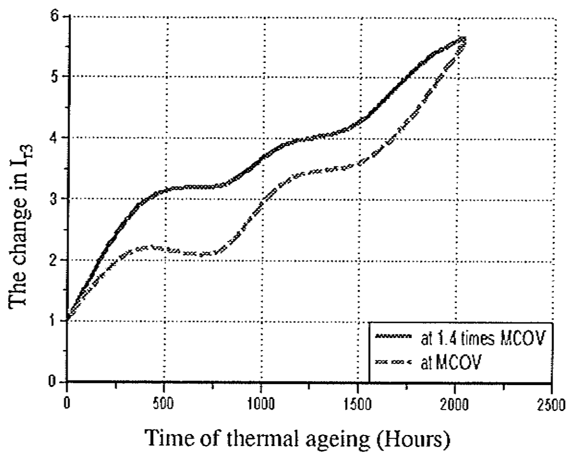

(a)

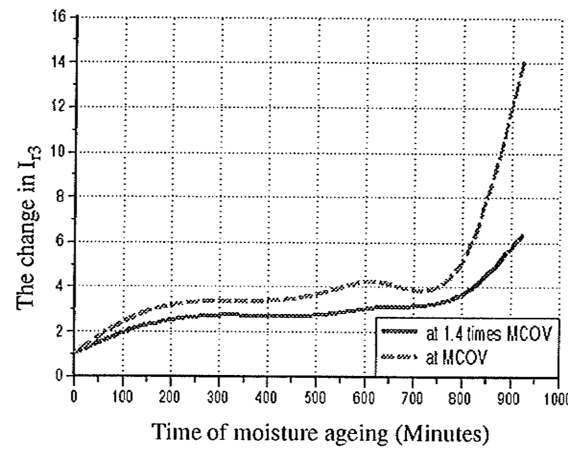

(b)

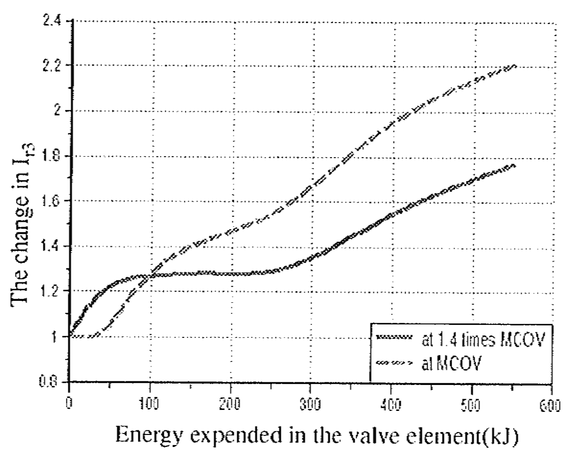

(c)

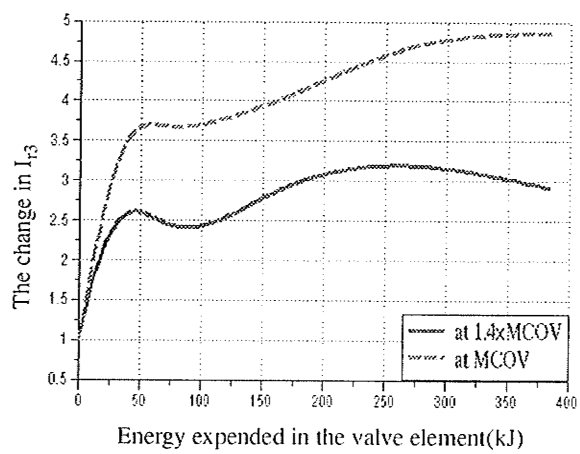

(d)

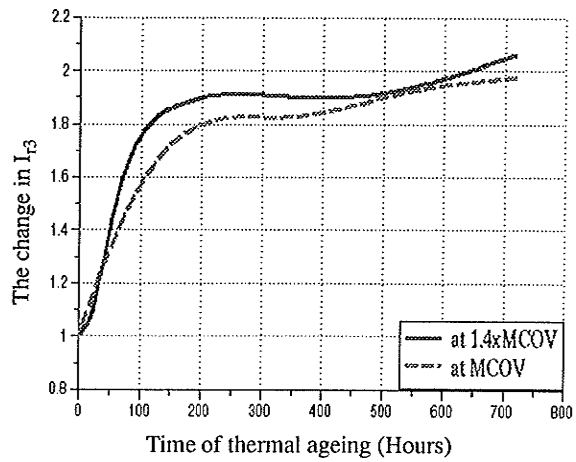

(e)

Fig. 4.4 Behaviour of diagnostic indicator #2, the peak value of the 3rd harmonic content in i_r (I_{r3})
(a) Thermal ageing
(b) Moisture ingress caused ageing
(c) Transient ageing
(d) Thermal/transient ageing
(e) Transient/thermal ageing

In Fig. 4.4(b) the increase in I_{r3} between 0 ~ 200 minutes and between 700 ~ 900 minutes is mainly due to the fact that the valve element is heated by the increasing current caused by the presence of moisture as well as the fine water droplets on the sidewall. During the 200~700 minute period, the change in I_{r3} is very small.

Fig. 4.5 (a) ~ (e) shows the trend of diagnostic indicator #3, the power dissipated in the valve element. As a consequence of the increasing resistive current, this indicator also increases with the progress of ageing. The deteriorated v-i_r characteristics result in an increasing resistive current, hence an increasing power dissipated in the valve element, this increasing power dissipation in turn accelerates the progress of deterioration.

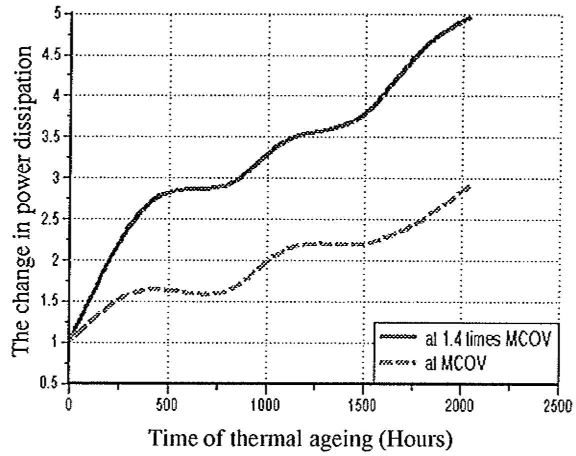
The change in power dissipation
Time of thermal ageing (Hours)
at 1.4 times MCOV
at MCOV

(a)

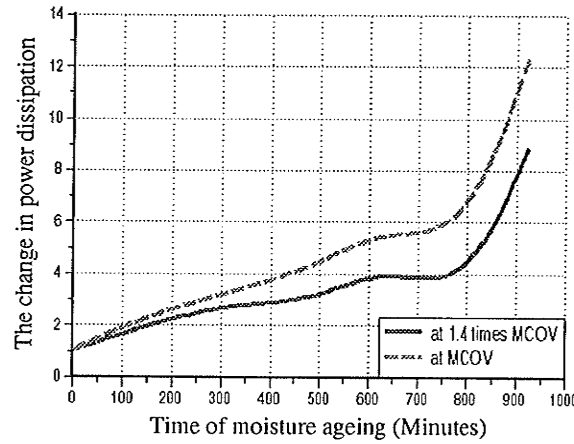
The change in power dissipation
Time of moisture ageing (Minutes)
at 1.4 times MCOV
at MCOV

(b)

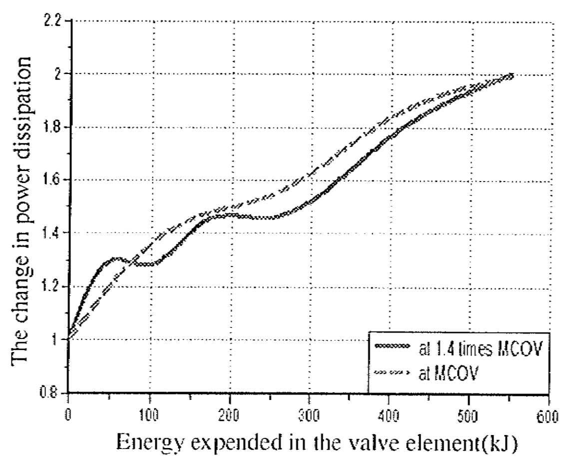
The change in power dissipation
Energy expended in the valve element(kJ)
at 1.4 times MCOV
at MCOV

(c)

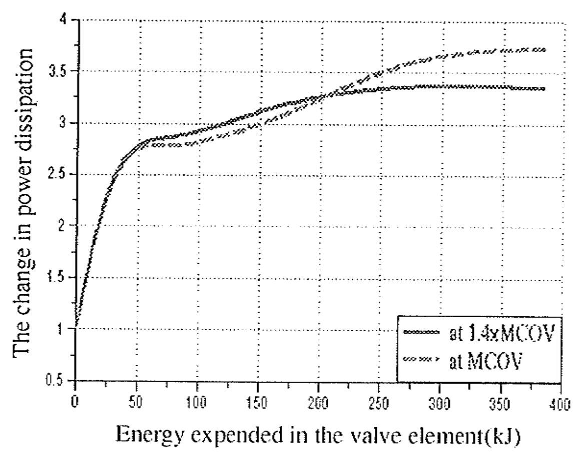
The change in power dissipation
Energy expended in the valve element(kJ)
at 1.4xMCOV
at MCOV

(d)

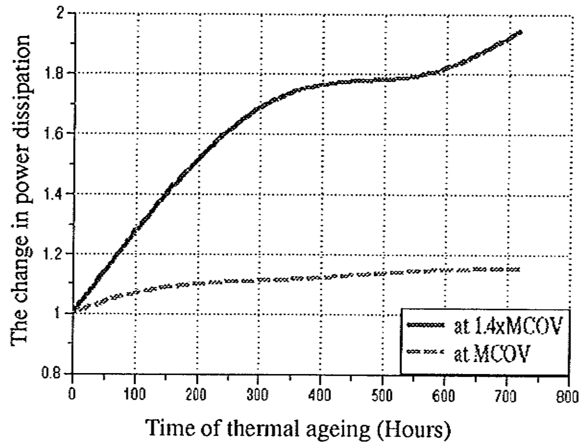

(e)

Fig. 4.5 Behaviour of diagnostic indicator #3, power dissipated in the valve element
(a) Thermal ageing
(b) Moisture ingress caused ageing
(c) Transient ageing
(d) Thermal/transient ageing
(e) Transient/thermal ageing

In Fig. 4.6 (a) ~ (e) the behaviour of diagnostic indicator #4 is shown. Since the resistive current increases as ageing progresses, the voltage to cause $I_{rp} = 1mA$ decreases. Again a similar trend in this diagnostic indicator is observed for each type of ageing. This indicator is therefore only capable of detecting ageing; it is not suitable for detecting the cause of ageing.

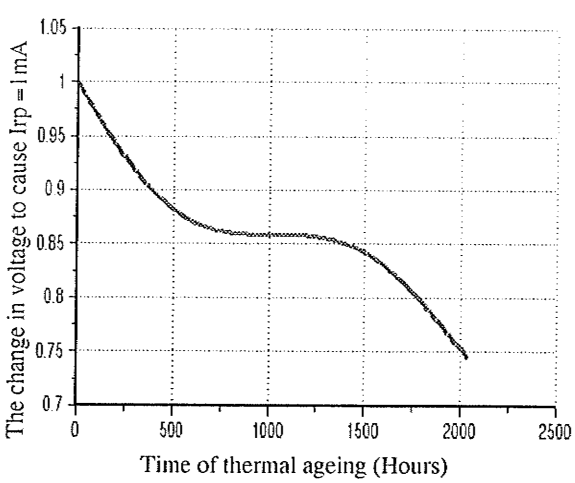

(a)

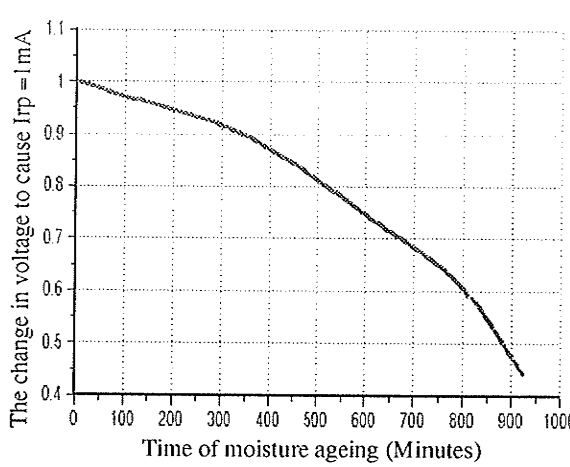

(b)

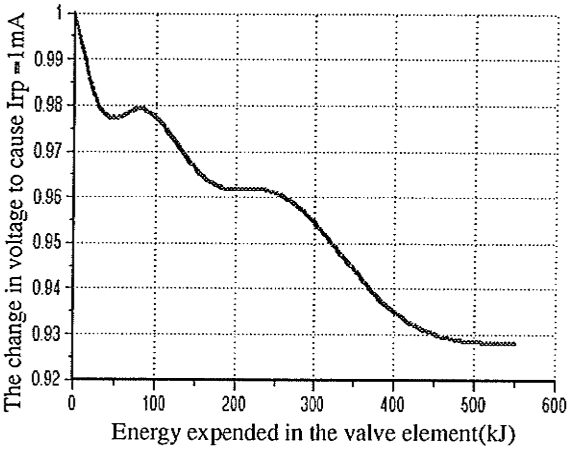

(c)

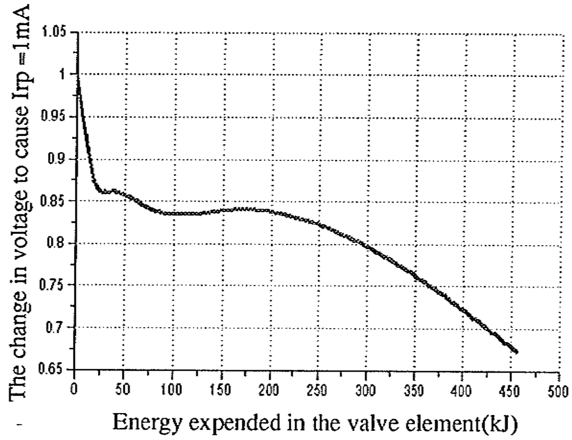

(d)

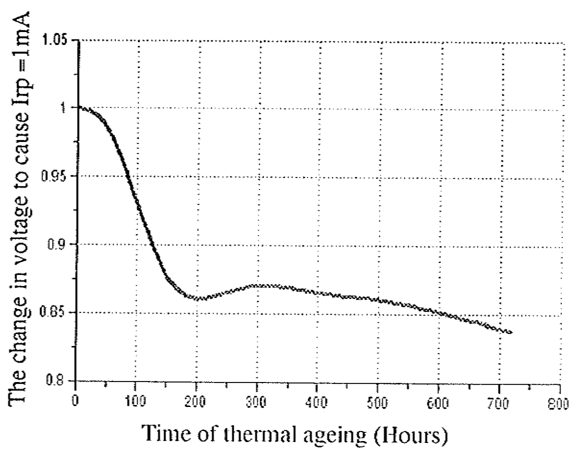

(e)

Fig. 4.6 Behaviour of diagnostic indicator #4, voltage to cause I_{rp}=1mA
(a) Thermal ageing
(b) Moisture ingress caused ageing
(c) Transient ageing
(d) Thermal/transient ageing
(e) Transient/thermal ageing

In Fig. 4.7 (a) ~ (e) the behaviour of diagnostic indicator #5, I_{r3}/I_{rp} , is presented. As the valve element deteriorates, the third harmonic content in the resistive current increases the fastest among all harmonics and the increase in i_{r3} is also more rapid than that in the total resistive current [18]. The value of this indicator therefore increases as may be observed from the Fig. 4.7 (a), (c), (d) and (e). A different trend is observed under moisture ingress caused ageing. Here the increase in the resistive current is mainly caused by the presence of moisture and the fine water droplets on the sidewall. The increase of I_{rp} is greater than the increase of I_{r3}; therefore this indicator decreases with ageing. At the end of the ageing test, the indicator increases. This is probably caused by the heating effect due to the passage of increasing total current.

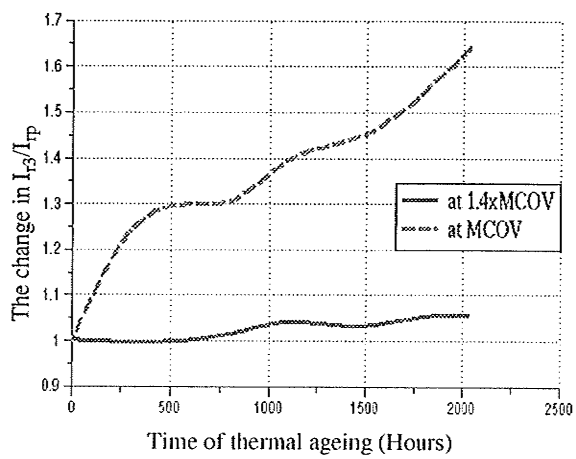

(a)

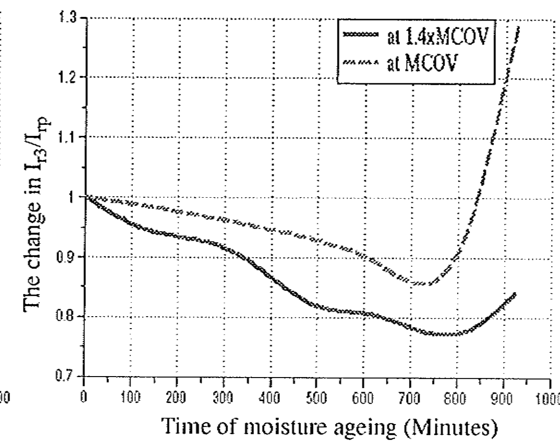

(b)

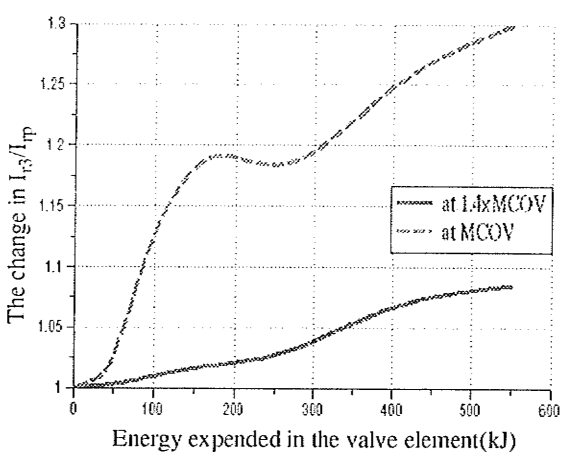

(c)

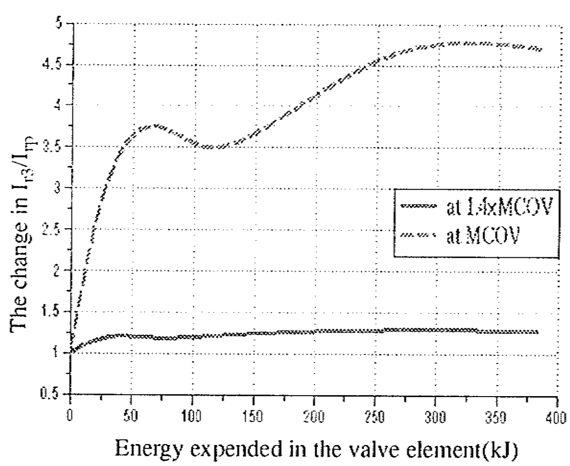

(d)

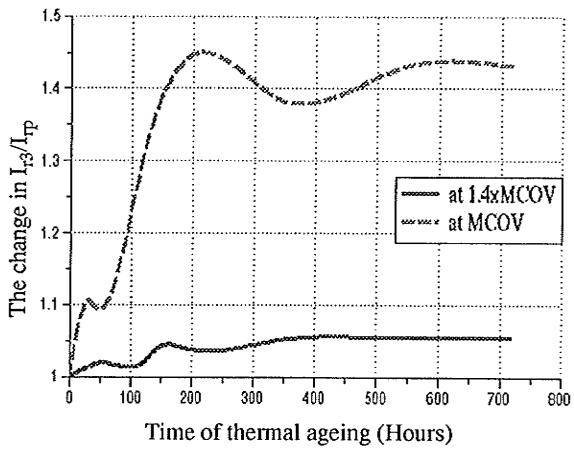

(e)

Fig. 4.7 Behaviour of diagnostic indicator #5, I_{r3} / I_{rp}

(a) Thermal ageing
(b) Moisture ingress caused ageing
(c) Transient ageing
(d) Thermal/transient ageing
(e) Transient/thermal ageing

Since under moisture ingress caused ageing, this indicator exhibits a different trend from the other types of ageing, diagnostic indicator #5 can be used for differentiating between moisture ingress caused ageing and other types of ageing.

Fig. 4.8 (a) ~ (e) shows results obtained with diagnostic method #6, A1/A2. Thermal ageing resulted in an increase in this indicator at the higher applied voltage, which is in agreement with the conclusion in [17]. The indicator generally decreases with ageing under moisture ingress caused ageing. For impulse current caused ageing, the behaviour is different; there exists a decreasing but oscillating trend of this indicator. In the case of the hybrid thermal/transient ageing, the trend is, quite different. The change in this indicator shows an increase at first and then a decrease. Transient/thermal ageing caused an increase in the indicator which is somewhat similar to that of thermal ageing. Because of the unique trend shown in Figs. 4.8(a), (d) and 4.8(e), this may be useful in detecting the cause of ageing if the element has been aged thermally (both thermal ageing and transient/ thermal ageing) or has been aged due to the combined effect of thermal and transient ageing (thermal/transient ageing).

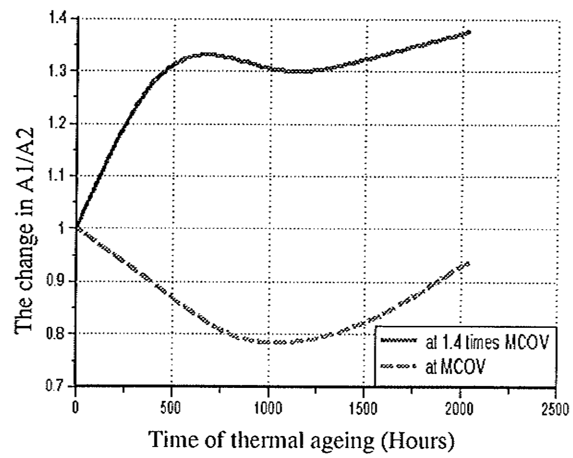

(a)

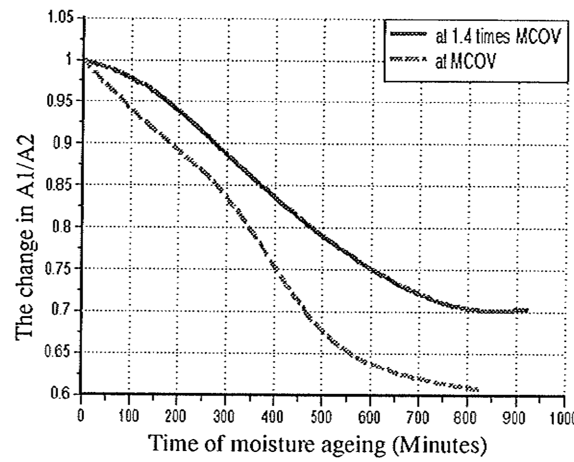

(b)

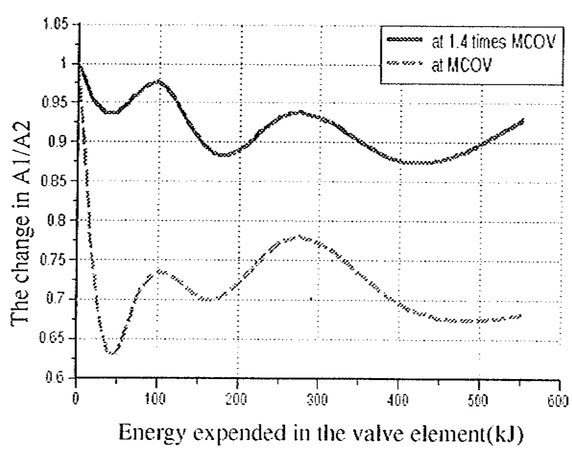

(c)

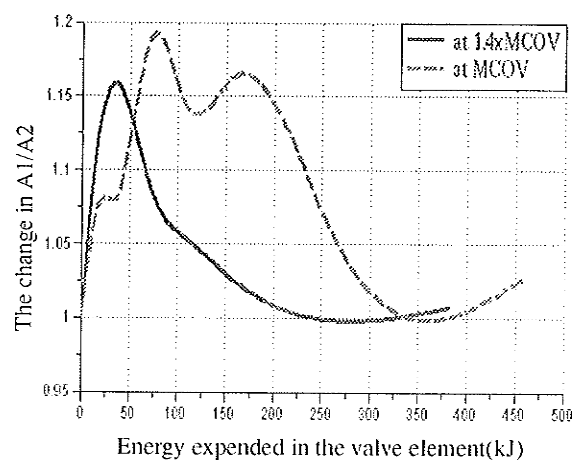

(d)

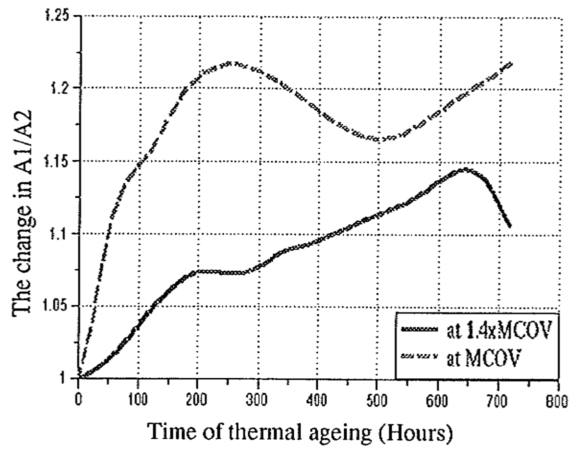

(e)

Fig. 4.8 Behaviour of diagnostic indicator #6, A1 / A2
(a) Thermal ageing
(b) Moisture ingress caused ageing
(c) Transient ageing
(d) Thermal/transient ageing
(e) Transient/thermal ageing

Fig. 4.9 (a) ~ (e) shows the changes in valve element capacitance as ageing progresses. With thermal and moisture ingress caused ageing, the capacitance increases and the change is quite pronounced. Under impulse current caused ageing, at MCOV and at the higher voltage, the capacitance decreases initially and then increases, the change in capacitance is very small. Fig. 4.9(d) shows that the combined effect of thermal ageing and transients caused ageing (thermal/transient ageing) results in a trend which is very similar to that under pure transients caused ageing. For transient/thermal ageing, the trend of this diagnostic indicator is increasing, which is somewhat similar to the behaviour exhibited under pure thermal ageing. Therefore this method is capable of differentiating between transients caused ageing and other non-transients caused ageing.

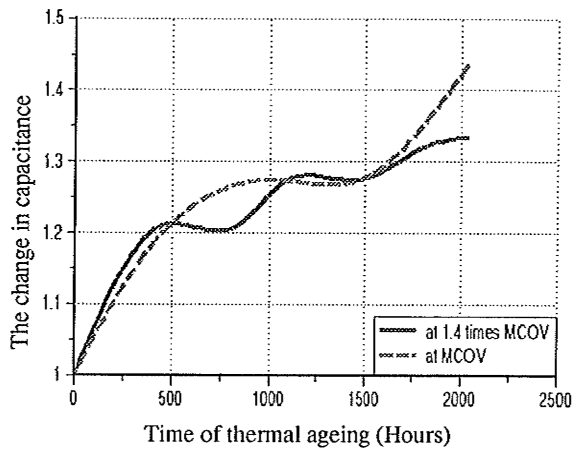
The change in capacitance
Time of thermal ageing (Hours)
at 1.4 times MCOV
at MCOV

(a)

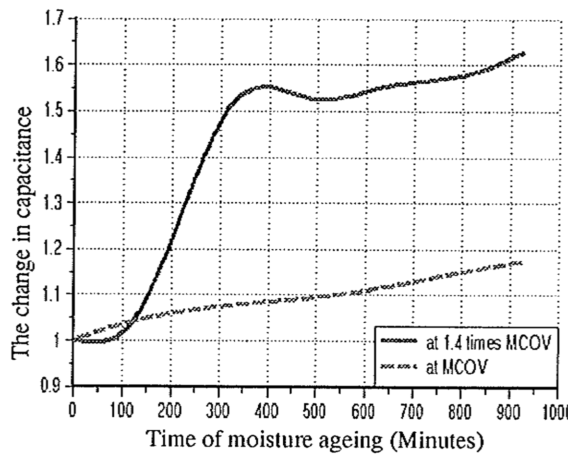
The change in capacitance
Time of moisture ageing (Minutes)
at 1.4 times MCOV
at MCOV

(b)

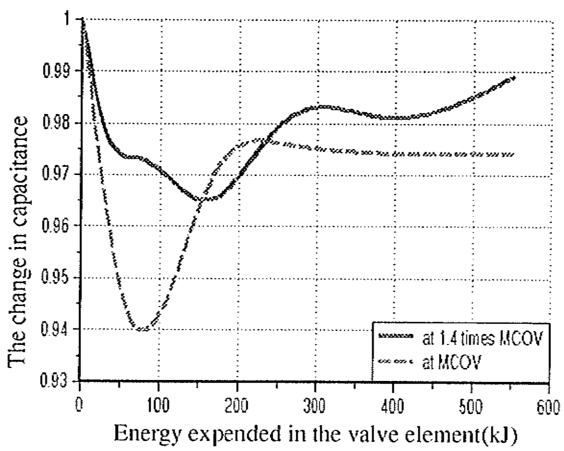
The change in capacitance
Energy expended in the valve element(kJ)
at 1.4 times MCOV
at MCOV

(c)

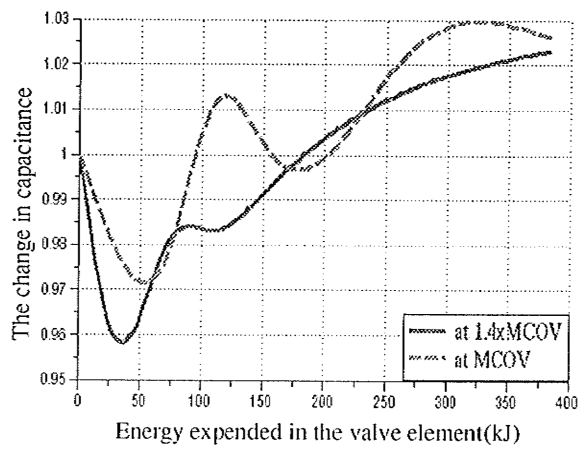
The change in capacitance
Energy expended in the valve element(kJ)
at 1.4xMCOV
at MCOV

(d)

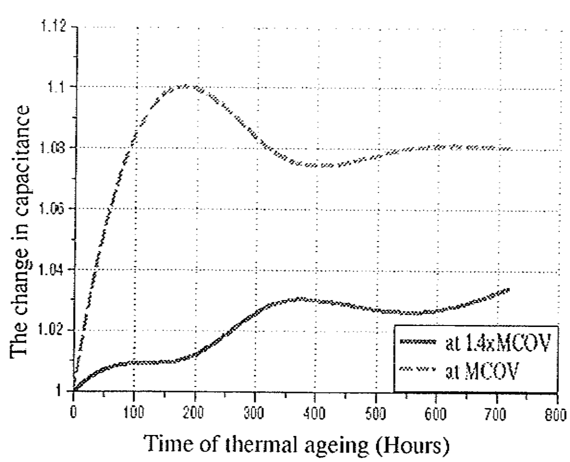
The change in capacitance
Time of thermal ageing (Hours)
at 1.4xMCOV
at MCOV

(e)

Fig. 4.9 Behaviour of diagnostic indicator #7, the capacitance of the valve element
(a) Thermal ageing
(b) Moisture ingress caused ageing
(c) Transient ageing
(d) Thermal/transient ageing
(e) Transient/thermal ageing

Fig. 4.10 (a) ~ (e) shows the effectiveness of diagnostic indicator #8, the parameter β in Eq. 2.1, which, together with the parameter A, characterize the non-linearity in the valve element resistance. Fig. 4.10(a) shows that the parameter β increases as thermal ageing progresses. In Fig. 4.10(b) (moisture ingress caused ageing), β shows no definite trend because the resistive current i_r was influenced by the surface current due to the presence of moisture. Under transients caused ageing (see Fig. 4.10(c)) β decreases steadily when diagnostics were conducted under 1.4 times MCOV while under MCOV the change in β is not monotonous. This is probably due to the fact that under 1.4 times MCOV, the resistive current is larger and the curve-fit obtained indicator, β, is more reliable. The thermal/transient ageing results in a general decrease in β, which is somewhat similar to that shown in Fig. 4.10(c) for transients ageing; but β shows an oscillatory behaviour and therefore no general conclusion can be drawn. While under transient/thermal ageing, β increases with ageing and is similar to the behaviour under pure thermal ageing. β may be used to differentiate thermal ageing and transient/thermal ageing from the rest since its behaviour is unique for this kind of ageing.

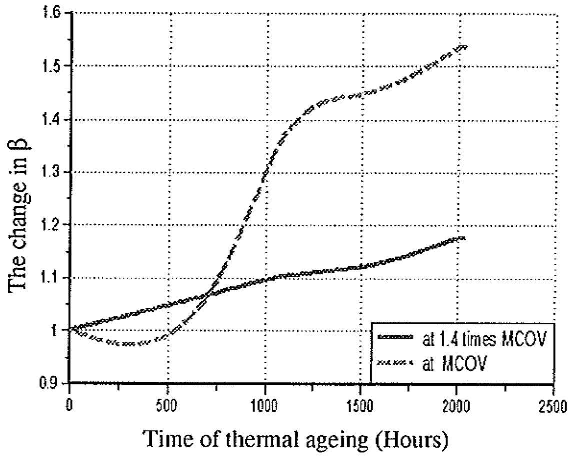
The change in β
Time of thermal ageing (Hours)
at 1.4 times MCOV
at MCOV
0 500 1000 1500 2000 2500
0.9 1 1.1 1.2 1.3 1.4 1.5 1.6

(a)

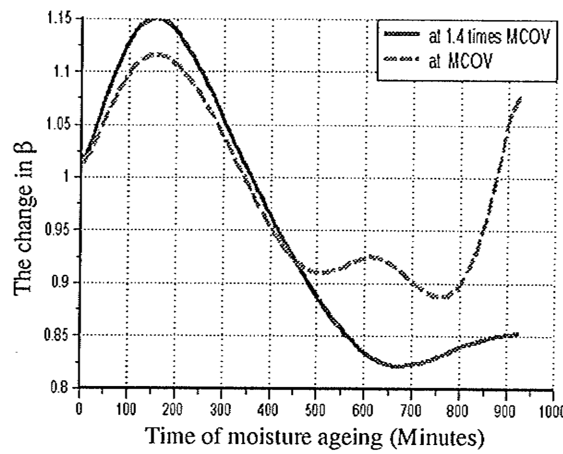
The change in β
Time of moisture ageing (Minutes)
at 1.4 times MCOV
at MCOV
0 100 200 300 400 500 600 700 800 900 1000
0.8 0.85 0.9 0.95 1 1.05 1.1 1.15

(b)

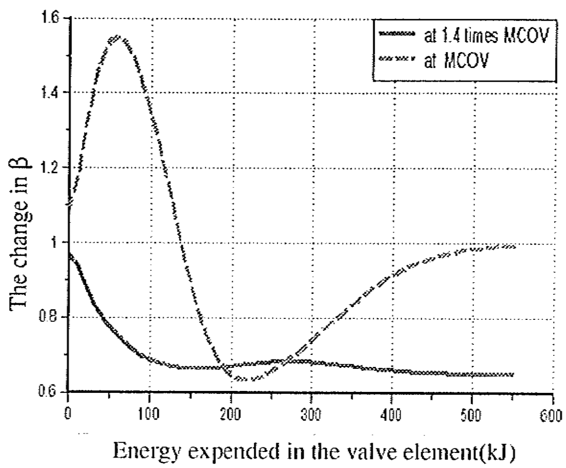
The change in β
Energy expended in the valve element(kJ)
at 1.4 times MCOV
at MCOV
0 100 200 300 400 500 600
0.6 0.8 1 1.2 1.4 1.6

(c)

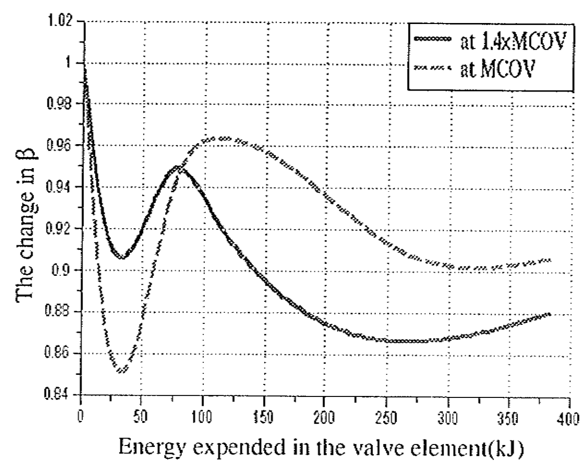
The change in β
Energy expended in the valve element(kJ)
at 1.4xMCOV
at MCOV
0 50 100 150 200 250 300 350 400
0.84 0.86 0.88 0.9 0.92 0.94 0.96 0.98 1 1.02

(d)

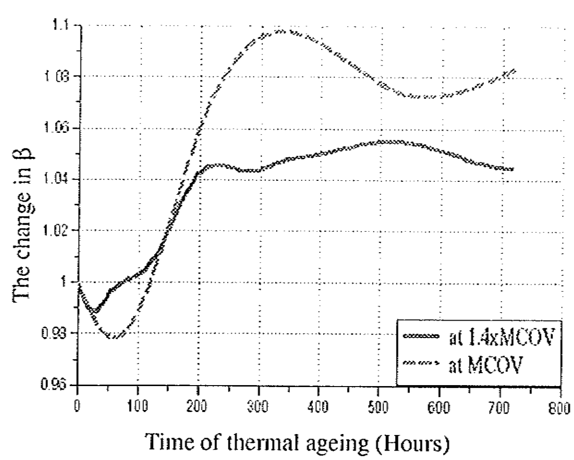
The change in β
Time of thermal ageing (Hours)
at 1.4xMCOV
at MCOV
0 100 200 300 400 500 600 700 800
0.96 0.98 1 1.02 1.04 1.06 1.08 1.1

(e)

Fig. 4.10 Behaviour of diagnostic indicator #8, parameter β in Eq. 2.1
(a) Thermal ageing
(b) Moisture ingress caused ageing
(c) Transient ageing
(d) Thermal/transient ageing
(e) Transient/thermal ageing

Fig. 4.11 (a) ~ (e) shows the effectiveness of the other parameter, A, in Eq. 2.1. This parameter displays a steady decrease with ageing as may be seen in Fig. 4.11(a). Once again the results from the moisture ageing test, Fig. 4.11(b), shows no definite trend because of the moisture caused surface current. Under impulse current caused ageing the parameter A increases as ageing progresses when it is obtained at a voltage higher than the MCOV (see Fig. 4.11(c)); the reason for this behaviour has been pointed out in the above paragraph. Under thermal/transient ageing, no monotonous change in A is noticed; again in transient/thermal ageing, the behaviour of this indicator is decreasing and similar to that of the pure thermal ageing.

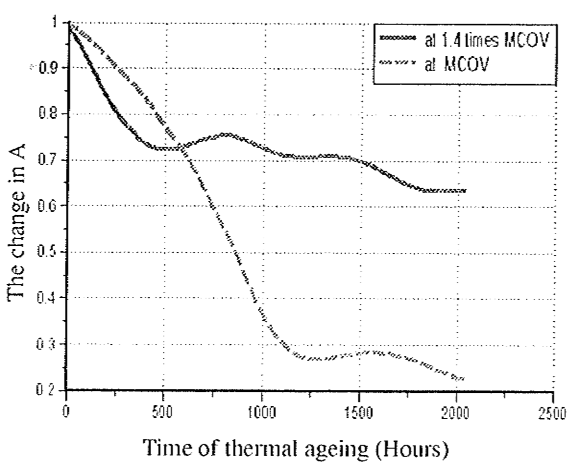

(a)

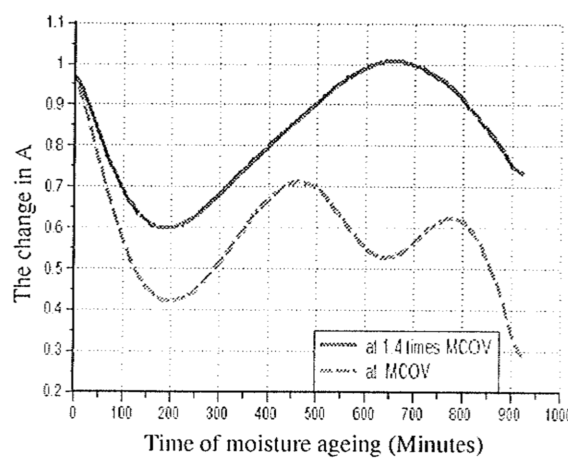

(b)

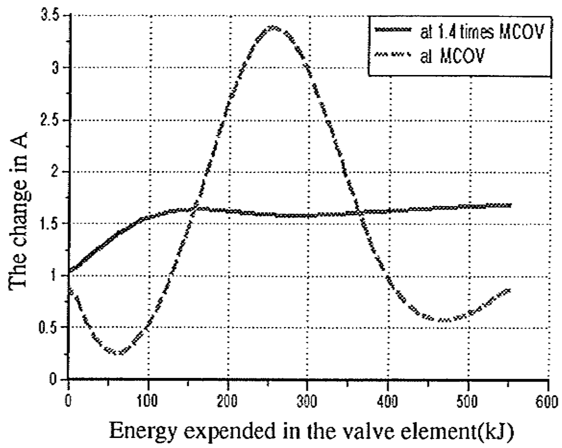

(c)

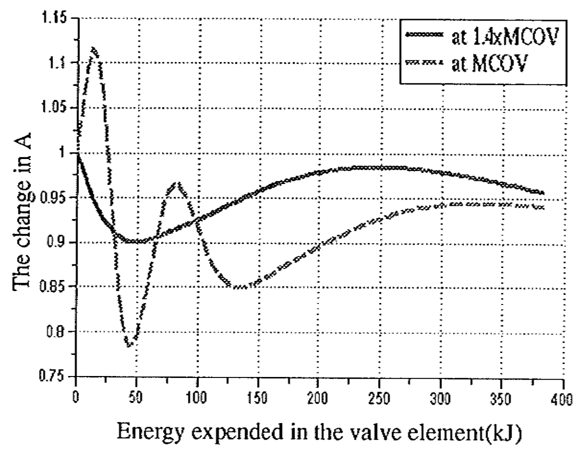

(d)

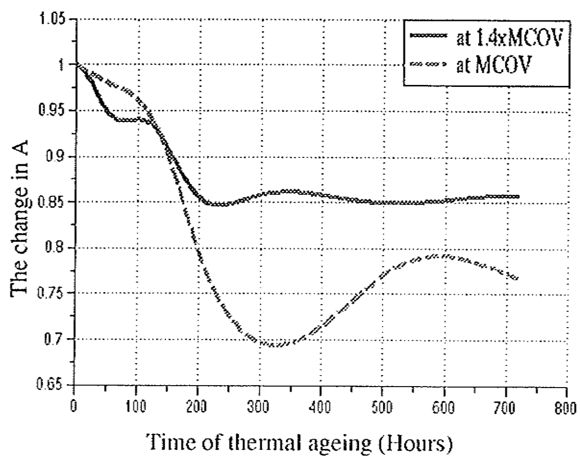

(e)

Fig. 4.11 Behaviour of diagnostic indicator #8, parameter A in Eq. 2.1
(a) Thermal ageing
(b) Moisture ingress caused ageing
(c) Transient ageing
(d) Thermal/transient ageing
(e) Transient/thermal ageing

The behaviour of the 2 diagnostic indicators in #8, i.e. parameters A and β, show that it is possible to differentiate thermal ageing and transient/thermal ageing from the other types of ageing considered.

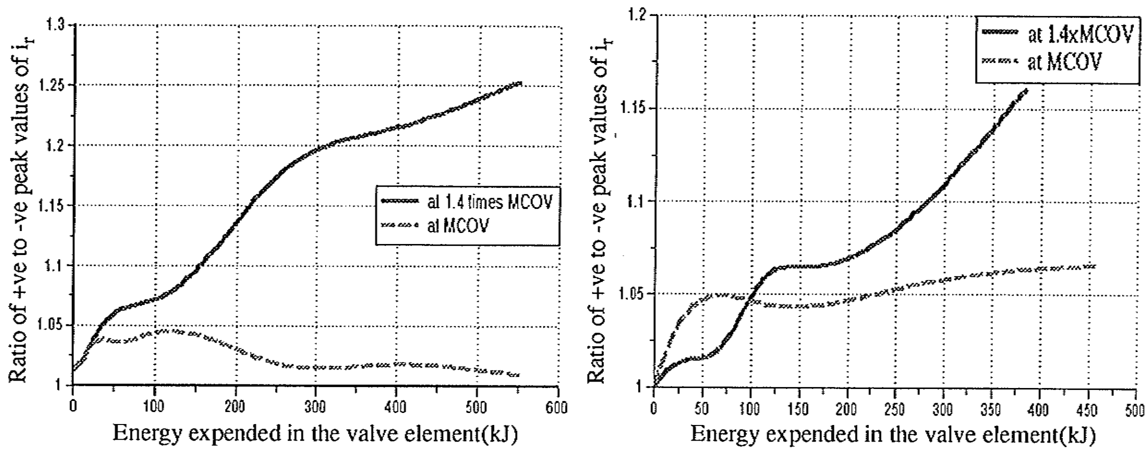

(a) (b)

Fig. 4.12 Behaviour of diagnostic indicator #9, asymmetry in the waveshape of i_r
(a) Transient ageing
(b) Thermal/transient ageing

After the very first series of impulse tests it was noticed that the waveshape of i_r became asymmetrical. The asymmetry worsened with further impulsing. Fig. 4.12 shows this result. From the above figure, it is seen that the asymmetry increases as ageing progresses, especially at a voltage higher than the MCOV. In Fig. 4.12(a) there is a slight drop of this indicator acquired under MCOV as ageing progresses, the reason being that under MCOV the resistive current is too small compared with the capacitive current and also the precision of the computer-aided data acquisition system and the precision of the numerical method itself might have some influence. In transient/thermal ageing, asymmetry appeared after transients caused ageing, but this asymmetry did not worsen with further thermal ageing. In thermal ageing and moisture ingress caused ageing, no asymmetry in i_r waveform is observed, so this diagnostic method is useful for determining whether the degradation is caused by the passage of surge current or whether the element has been subjected to transient ageing.

In order to check if the direction of passage of impulse current has any effect on the asymmetry, tests were performed on another element (a type II element). Impulse currents were passed in one direction for the first five series (4 serious of 30 shots @ 40kA, one serious of 20 shots @ 55kA); for the remaining 2 series of tests (2 serious of 20 shots @ 55kA), impulse currents were passed in the opposite direction. Figures 4.13 shows the results. The asymmetry disappears after application of the impulses in the reverse direction as can be seen in Fig. 4.13(a). However as Fig. 4.13(b) shows, in spite of this, the ageing is not reversible.

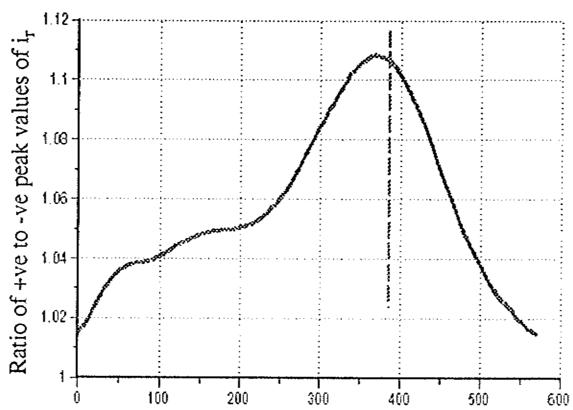

(a)

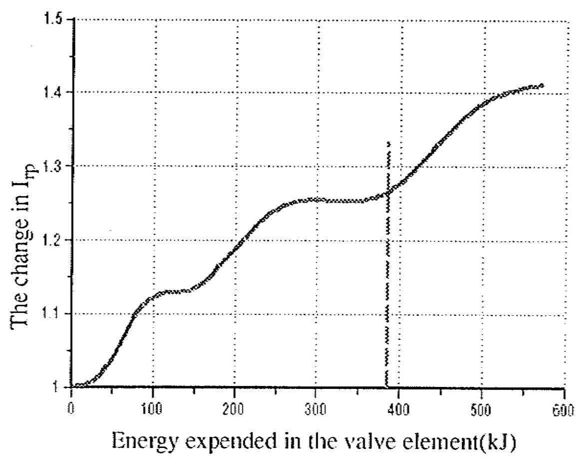

(b)

Fig. 4.13 The effects of the reversal of impulse current.
(a) Effect of reversal of impulse current on asymmetry in waveform of i_r
(b) Effect of reversal of impulse current on degradation of the element
Vertical dotted line indicates that impulse currents passed in reverse direction beyond this stage

It is noticed that though diagnostic methods #5 ~ #9 show detectable difference amongst the five types of ageing considered, they are not equally effective in detecting ageing. For example, diagnostic indicator #7, valve element capacitance could be used as a diagnostic tool to differentiate transients caused ageing and thermal/transient ageing from other types of ageing, but if the degradation is caused by passage of surge current (See the "V" curve in Fig. 4.9 (c), (d)), the change in the capacitance does not give explicit information about how serious the degradation is. Similar remarks apply to other indicators in diagnostic methods #5 ~ #9. So a comprehensive use of the diagnostic methods #1 ~ #4 (capable of detecting degradation) and the diagnostic method #5 ~ #9 (capable of determining the cause of degradation) is more reliable. To conclude this section, Table 4.1 shows the effectiveness of the discussed diagnostic methods.

Table 4.1 The effectiveness of the discussed diagnostic methods

Diagnostic indicators	#1. I_{rp}	#2. I_{r3}	#3. Power dissipation	#4. rms voltage to cause Irp=1mA	#5. I_{r3}/I_{rp}	#6. A1/A2	#7. Element capacitance	#8. β and A	#9. Asymmetry in i_r
Able to detect ageing?	Y	Y	Y	Y	NA	NA	NA	NA	NA
Able to distinguish thermal ageing?	N	N	N	N	N	Y	N	Y	N
Able to distinguish moisture ingress caused ageing?	N	N	N	N	Y	N	N	N	N
Able to distinguish transients caused ageing?	N	N	N	N	N	N	Y	N	Y
Able to distinguish thermal/transient ageing?	N	N	N	N	N	N	Y	N	Y
Able to distinguish transient/thermal ageing?	N	N	N	N	N	Y	N	Y	Y

Notes: Y----Yes; N---No; NA---Not able to detect all types of ageing

4.3 Temperature distribution in the valve element under impulse current

The temperature distribution in the valve element under transients caused ageing is investigated in this project using an Inframetrics 740 infrared imaging radiometer.

Fig. 4.14. shows the temperature distribution inside the valve element obtained immediately after the conclusion of the first four series of short impulse tests. The figure shows that

1) The temperature distribution inside the valve element is non-uniform. This might be caused by inhomogeneity in the valve element [25].

2) As the element ages the temperature distribution gets worse which implies that the element is very non-uniformly aged.

As ageing progressed, higher temperature rises were recorded even though impulsing was carried out at the same energy level. This indicates the declining power handling capability of the valve element.

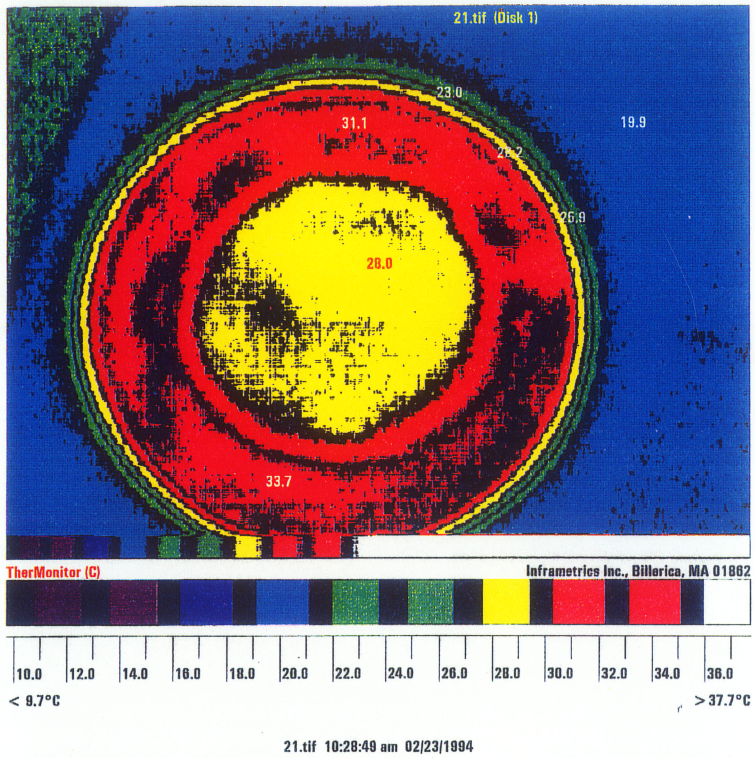
21.tif (Disk 1)
23.0
31.1
19.9
28.0
33.7
TherMonitor (C)
Inframetrics Inc., Billerica, MA 01862
10.0 12.0 14.0 16.0 18.0 20.0 22.0 24.0 26.0 28.0 30.0 32.0 34.0 36.0
< 9.7°C
> 37.7°C
21.tif 10:28:49 am 02/23/1994

(a)

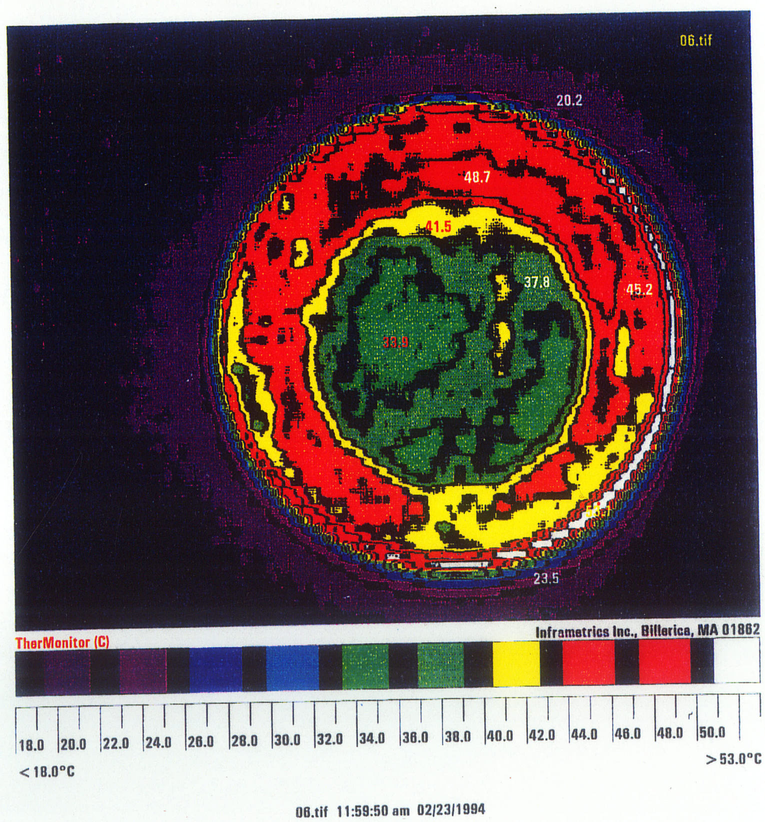
06.tif
20.2
48.7
41.5
37.8
45.2
23.5
TherMonitor (C)
Inframetrics Inc., Billerica, MA 01862
18.0 20.0 22.0 24.0 26.0 28.0 30.0 32.0 34.0 36.0 38.0 40.0 42.0 44.0 46.0 48.0 50.0
< 18.0°C
> 53.0°C
06.tif 11:59:50 am 02/23/1994

(b)

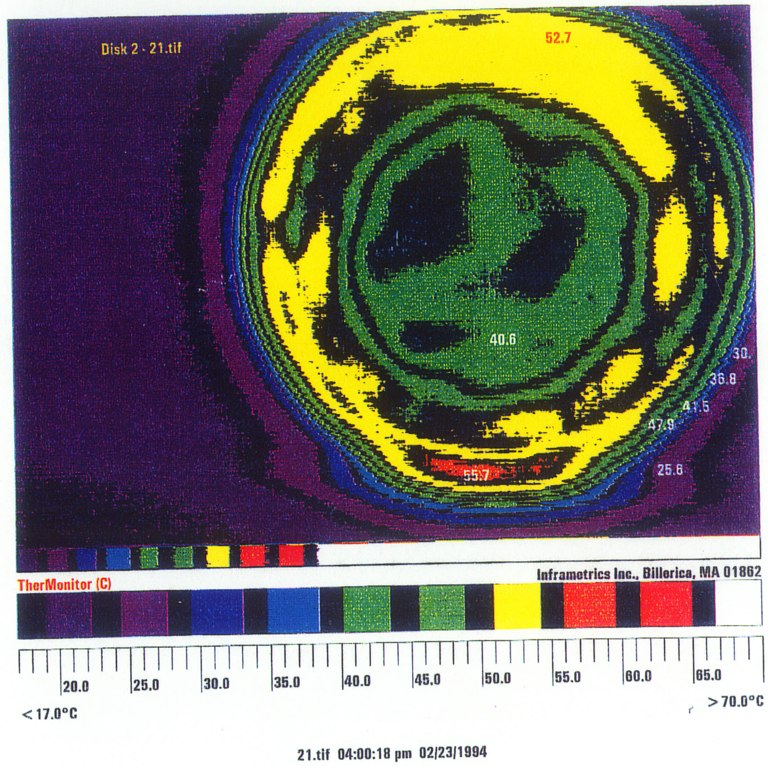

(c)

Fig. 4.14 Temperature distribution in the valve element under impulse current
(a) After 30.6kJ energy was expended in the element.
(b) After 190.3kJ energy was expended in the element
(c) After 360.4kJ energy was expended in the element

The temperature distribution in the valve element under long duration impulse current is almost the same as that in the short duration impulse current, so it is not presented here.

CHAPTER 5

CONCLUSIONS

5.1 Conclusions

In the work presented in this thesis, diagnostic methods for detecting degradation and differentiating between the cause of degradation in MOSA valve elements are studied.

Chapter 1 briefly introduces the history and the basic properties of MOSA as well as the existing diagnostic methods. In Chapter 2, the experimental setup and the procedure employed for different types of laboratory controlled ageing methods are described in detail, followed by the outline of the diagnostic methods used. A discussion is presented in Chapter 3 on the method employed to account for the influence caused by the voltage harmonics. Experimental results for all the proposed diagnostic methods are presented in Chapter 4 with a discussion of their effectiveness in detecting ageing and distinguishing the causes of ageing. Also the temperature distribution in the valve element under impulse current ageing was monitored using an Inframetrics 740 infrared imaging radiometer and some selected images are shown.

The following conclusions may be drawn:

1) A method is proposed to account for the influence caused by the harmonics in the system on the diagnostic results. This is very important especially when the diagnostics are carried out at voltage levels higher than the MCOV.

2) Diagnostic indicators #1 ~ #4 (pp. 25-26) all show a definite trend as ageing progresses, hence these diagnostic methods are all capable of detecting ageing; however the trend of these indicators is similar for all types of ageing considered, which

makes them unsuitable for diagnosing the cause of the ageing.

3) The indicators in diagnostic methods #5 ~ #9 (pp. 26 - 27) show detectable differences amongst all types of ageing considered, which may be useful for differentiating between the cause of ageing.

4) Though diagnostic methods #5 ~ #9 show promise of distinguishing the cause of ageing, they are not equally effective in detecting ageing in the valve elements. Explicit degradation information could be obtained if they are used together with diagnostic methods #1 ~ #4.

5) The temperature distribution in the valve element is non-uniform and gets worse as ageing progresses due to the passage of current impulses. This implies the ageing inside the valve element is non-uniform and the non-uniformity worsens with further ageing.

5.2 Suggestions for future work

The presented work is only a preliminary study on the diagnostic methods for MOSA, continued and detailed research on this topic could be of practical value. Below are some suggestions for future work.

1. All the diagnostic methods are conducted on a single valve element in this project. Some experiments with real arresters would be very interesting. One suggestion is to age some valve elements using the 5 proposed laboratory ageing methods, at different stages of ageing, insert the aged element into a real arrester with other elements in the arrester unaged and conduct the diagnostics.

2. In this thesis work, all the degradation on valve elements are caused by laboratory

controlled ageing methods. It would be of great interest to have these diagnostic methods conducted on naturally aged arresters in site to observe the behaviour of diagnostic indicators.

3. The diagnostic methods do detect ageing but do not give explicit criteria that indicate the end of the life for the aged valve elements. A more comprehensive study of the stability, the electrical and thermal properties of the arresters under different operation conditions and the behaviour of the ageing indicators could be helpful to determine the criteria and make the diagnostics more powerful.

4. Multi-factor ageing schemes that simulate real arrester degradation should be studied in more detail.

References

[1] IEEE recommended practice for electric power distribution for industrial plants. (ANSI/IEE Std 141-1986), American National Standards Institute.

[2] E.C. SakShaug, J.S. Kresge and S.A. Miske Jr., "A new concept in station arrester Design," IEEE Trans. on Power Apparatus and Systems, Vol. 96, No. 2, 1977, pp. 647-656.

[3] Kazuo. Eda, "Zinc Oxide Varistors", IEEE Electrical Insulation Magazine, Vol. 5, No. 6, Nov./Dec., 1989, pp. 28-41.

[4] Andrew Sweetana, Ned Kunkle, Narain Hingorani, Vasu Tahiliani, "Design, development and testing of 1200kV & 550kV gap-less surge arresters," IEEE Trans. on Power Apparatus and Systems, Vol. 101, No. 7, July 1982, pp. 2319-2327.

[5] J. Lundquist, L. Stenstrom, A. Schei, B. Hansen, "New method for measurement of resistive leakage current of metal oxide surge arresters in service," IEEE Trans. Power delivery, Vol. 5, No. 4, Nov. 1990, pp. 1811-1819.

[6] A. Bargigia, G. Mazza, G. Le Roy, A. Rousseau, L. Sparrow, "Behaviour of Metal Oxide Surge Arresters under different environment conditions," CIGRE 33-14, 1988.

[7] V.Chaudhry, R.S. Gorur, M. Dyer, R.S. Thallam, "Electrical performance of polymer housed Zinc Oxide arresters under contaminated conditions," IEEE Trans

on Power Delivery, Vol. 6 No. 2 April 1991, pp. 696-705.

[8] S. Vitet, L. Stenstrom, J. Lundquist, "Thermal stress on ZnO surge arresters in polluted conditions, Part I, Laboratory test methods," IEEE Trans on Power Delivery, Vol. 7, No. 4, October, 1992, pp. 2012-2022.

[9] S. Vitet, A. Schei, L. Stenstrom, J. Lundquist, "Thermal stress on ZnO surge arresters in polluted conditions, Part II, Field test results," IEEE Trans on Power Delivery, Vol. 7, No. 4, October, 1992, pp. 2023-2036.

[10] K.Feser, W. kohler, D.Qiu, K.Chrzan, "Behaviour of Zinc Oxide Surge Arresters under pollution", IEEE Trans. on Power Delivery, Vol. 6, No. 2, April, 1991, pp. 688-695.

[11] "Study of lightning current magnitude through distribution arresters", EPRI EL1140 final reports, Sept. 1979.

[12] E.C. Sakshaug, J.J Burke, J.S. Kresge, "Metal oxide arresters on distribution systems fundamental considerations," IEEE Trans. on Power Delivery, Vol. 4 No. 4 October 1989, pp. 2076 -2089.

[13] S. Tominaga, Y. Shibuya, Y. Fujiwara, M. Imataki, T.Nitta, "Stability and long term degradation of Metal Oxide Surge Arresters," IEEE Trans. on Power Apparatus and Systems, Vol. 99, No. 4, July/Aug. 1980, pp. 1548-1556.

[14] IEEE guides for the application of Metal-Oxide Surge Arresters for alternating

current systems, (IEEE std C62.22-1991), American National Standards Institute.

[15] A. Mizukoshi, J.Ozawa, S.Shirawara, K.Nakano, "Influence of uniformity on energy absorption capabilities of zinc Oxide elements as applied in arresters", IEEE Trans. on Power Apparatus and Systems, Vol. 102, No. 5, 1983, pp. 1384-1390.

[16] J. Howard Shaw, Nils V. Holmgren, "Characteristics which can be used to detect defective distribution surge arresters," IEEE Trans. on Power Apparatus and Systems, Vol. 104, No. 1, Jan. 1985, pp. 137-141.

[17] H. Waitschat, H. C. Karner, "Service check of Zinc Oxide arresters," in Proceedings of the 5th ISH, pp. 1-4.

[18] S. Shirakawa, F. Endo, H. Kitajima, S. Kobayashi, K. Kurita, "Maintenance of surge arrester by a portable arrester leakage current detector," IEEE Trans. on Power Delivery, vol. 3, No. 3, July 1988, pp. 998-1003.

[19] Larry T. Coffeen, James E. Mcbride, "High voltage ac resistive current measurement using a computer based digital watts technique," IEEE Trans. on Power Delivery, Vol. 6, No. 2, April 1991, pp. 550-556.

[20] Peter Kirkby, C. C. Erven, O. Nigol, "Long-term stability and energy discharge capacity of metal oxide valve elements," IEEE Trans. on Power Delivery, Vol. 3, No. 4, Oct. 1988, pp. 1656-1665.

[21] Kazuo Eda, Atsushi Iga and Micchio Matsuoka, "Degradation mechanism of non-Ohmic Zinc oxide ceramics," Journal of applied physics, Vol. 51, May 1980, pp. 2678-2684.

[22] Y. Fujiwara, Y. Shibuya, M. Imataki and T. Nitta, "Evaluation of surge degradation of metal oxide surge arrester," IEEE Trans. on Power Apparatus and Systems, Vol. 101, No. 4, 1982, pp. 978-985.

[23] Cuthbert Daniel, Fred S. Wood, John W. Gorman, "Fitting equations to data, Computer analysis of multifactor data for scientists & engineers," Wiley Interscience.

[24] IEEE recommended practices and requirements for harmonic control in electrical power systems, (IEEE std 519-1992), American National Standards Institute.

[25] K.Eda, "Destruction mechanism of ZnO varistors due to high currents," Journal of applied Physics, Vol. 56, Nov. 1984, pp. 2948-2955.

Appendix A Some specifications for the Data acquisition system

1. 5B40 wide bandwidth millivolt and volt input module (Main part for the component labelled as "Interface to PC" in Fig.2.1).

Input range: -10 V ~ 10 V

Output range: -5 V ~ 5 V

Accuracy: $\pm$0.05%span$\pm$0.05(Vz)

Input resistance: 650kΩ

Stability vs. Ambient Temperature

Input offset: $\pm 20\mu V/^{o}C$

Output offset: $\pm 40\mu V/^{o}C$

Noise

Input: 0.1/10Hz: 2μV rms RTI

Output: 20mV, peak-peak

Environmental

Temperature range (rated performance): -25°C to +85°C

Temperature range (Operating): -40°C to +85°C

2. NI-DAQ data acquisition Software

Input: 12 bit integer results from A/D conversion

Recommended data acquisition rates: 100,000 ~ 200,000 samples/sec

Appendix B Programs

1. Program for data acquisition

```
/* The program to acquire experimental data */
#define pi 3.1415926
static double u1[5000],ilk[5000],peak[10];
static int glt[2], chlt[2],node[15];
int hdl,hdl1,hdl2,hdl3,hdl4;
main(){
    int i,j;
    int samples,rec,rec1,rec2,pos,temp,frequency;
    int uv[8000],h_ps,ps2;
    double delt,rate, an,dan,imax,umax,phase,dr,rmsv,rmsi;
    double T,dt,Rm,temp1;
    double u[5000],v[5000],tem[6000],ilk1[5000];


    cls();
    samples=6000;
    dr=5007.127;
    Rm=1000.;          /*initialization*/
    AI_Config (1, 2, 10, 0);          /*initialize the board*/
    chlt[0]=0;
    gltlt[1]=1;
    glt[0]=2;
    glt[1]=2;  /*specify the channels & gains*/
    rate=86400.;
    frequency=60;

    /* Aquire data, scale & store in buffers */

    SCAN_Op (1, 2, chlt, glt, uv, samples, 86400.0, 0);
    FmtOut("Data acquired, Please shut down the voltage ! ");
    DAQ_Scale (1, 1, samples, uv, tem);
    for (i=0;i<samples/2;i++){
```

```
  u[i]=tem[2*i]*dr;
  v[i]=tem[2*i+1]/Rm;
 }

 temp = rate / ( 2 * frequency );
 umax=0.;
 for (i=0; i<temp; i++) {
   if ( u[i] >umax ) {
   rec = i;
   umax = u[i];
 }
 if ( v[i] >imax ) {
   rec1 = i ;
   imax = ilk[i];
 }
 FmtOut("rec=%d\n",rec);
 phase= ( ( rec1 - rec )) / 360. * pi ;
 for ( i= 0 ; i < samples/2 - rec ; i++ ) {
   u1[i]=u[i+rec] ;
   ilk[i]=v[i+rec];
   if ( u1[i] > umax ) {
     umax = u1[i] ;
     rec2 = i ;
   }
   if (ilk[i] > imax ) {
   imax = ilk[i] ;
   rec1 = i ;
   }
 }

/* Specify the points may be contained in 1/4 cycle*/
temp1=3*rate/(20*frequency);
for (i=0 ; i<temp1 ; i++){     /* how many points in 1/4 cycle */
if ( u1[i] >= 0. ) pos++;
}
node[0]=0;
```

```
node[1] = pos-1 ;
FmtOut("node[1] =%d\n",node[1]);
peak[0] = u1[0] ;
h_ps=3*pos; /*peak[1] = - 10. ;*/
for (i=pos ; i<pos+temp1 ; i++){
  if (u1[i] < peak[1] ) {
    node[2] = i;
    peak[1] = u1[i] ;
  }
}
FmtOut("node[2] =%d\n",node[2]);
for (i = node[2]+1 ; i < node[2]+temp1 ; i++) {
  if ( u1[i] < 0. ) ps2++;
}
node[3] = node[2] + ps2 -1 ;
FmtOut("node[3] =%d\n",node[3]);
/*bj= 10. ; */
for (i =node[3]+1 ; i< node[3] + temp1 ; i++ ){
if ( u1[i] > peak[2] ) {
  node[4] = i;
  peak[2] = u1[i];
  }
}
FmtOut("node[4] =%d\n",node[4]);
pos=0;
for (i=node[4]+1 ; i<node[4]+temp1 ; i++){
  if ( u1[i] >= 0. ) pos++;
}
node[5] = node[4]+pos-1 ;
FmtOut("node[5]= %d \n",node[5]);
for (i=node[5]+1 ; i<node[5]+temp1 ; i++){
  if (u1[i] < peak[3] ) {
  node[6] = i;
  peak[3] = u1[i] ;
  }
}
```

```
FmtOut("node[6] =%d\n",node[6]);
ps2=0 ;
for (i = node[6]+1 ; i < node[6]+temp1 ; i++) {
  if ( u1[i] <= 0. ) ps2++ ;
}
node[7] = node[6] + ps2 -1 ;
FmtOut("node[7]= %d \n",node[7]);
for (i =node[7]+1 ; i< node[7] + temp1 ; i++ ){
  if ( u1[i] > peak[4] ) {
  node[8] = i;
  peak[4] = u1[i];
  }
}
FmtOut("node[8]= %d \n",node[8]);
pos=0;
for (i=node[8]+1 ; i<node[8]+temp1 ; i++){
  if ( u1[i] >= 0. ) pos++;
}
node[9] = node[8]+pos-1 ;
FmtOut("node[9]= %d \n",node[9]);
for (i=node[9]+1 ; i<node[9]+temp1 ; i++){
if (u1[i] < peak[5] ) {
  node[10] = i;
  peak[5] = u1[i] ;
  }
}
FmtOut("node[10]= %d \n",node[10]);
ps2=0 ;
for (i = node[10]+1 ; i < node[10]+temp1 ; i++) {
  if ( u1[i] <= 0. ) ps2++ ;
}
node[11] = node[10] + ps2 -1 ;
FmtOut("node[11]= %d \n",node[11]);
for (i =node[11]+1 ; i< node[11] + temp1 ; i++ ){
if ( u1[i] > peak[6] ) {
  node[12] = i;
```

```
  peak[6] = u1[i];
  }
}
FmtOut("node[12]= %d \n",node[12]);
/* calculates the RMS values*/
dt=2./rate;
T=(node[12]-node[0])/3.*dt;
rmsv=0.; rmsi=0.;
for (i=0;i<node[12];i++){
  rmsv =rmsv+ u1[i]*u1[i]*dt/(3.*T);
  rmsi =rmsi+ ilk[i]*ilk[i]*dt/(3.*T);
}
rmsv = sqrt (rmsv); rmsi = sqrt (rmsi);
/* write original data to 2 disk files */
hdl =OpenFile("9iob51",2,0,1);
hdl1=OpenFile("9uob51",2,0,1);
for (i=0;i<samples/2-1-rec;i++){
  FmtFile(hdl1,"%s<%f[w15],",u1[i]);
  FmtFile(hdl,"%s<%f[w15],",ilk[i]);
    if ((i%5)==4)
    {
      WriteFile (hdl,"\n",1);
      WriteFile (hdl1,"\n",1);
    }
}
CloseFile (hdl);
CloseFile (hdl1);

YGraphPopup (u1, 2100, 4);
YGraphPopup (ilk, 2100, 4);
cls();
FmtOut ( "rmsv = %f\n",rmsv);
FmtOut ( "rmsi = %f\n",rmsi);
FmtOut ( "maximum of the voltage = %f\n",umax);
FmtOut ( "maximum of the current = %f\n",imax);
FmtOut ( "phase between peaks = %f\n",phase);
```

```
   FmtOut("The end. ");
}
```

2. Program for diagnostics

```
/* The main program for diagnostics */
/*** Last modified April 2nd 1995. ***/
#include "ovenchk.h"
#define pi 3.1415926
#define true 1
#define false 0

static int node[10], nodeir[5],rec, rec3;
static double u1[3000],ilk[3000],ch[50],area1,area2,Imax,Ir[2500];
double max,cap,da[10],slope[2000],u2[2500],ilkc[2000] ;
static double bi[4];
double av[50], av1[50]  ;
double ar[50], ar1[50] ;
double fv[50], fv1[50] ;
double fr[50], fr1[50] ;
int hdl,hdl1,hdl2,hdl3,hdl4,hdl5,hdl7,hdl8;
double ratio,ratio2,aratio,Irmax,v1,Ir1[2000],pr,dt,c1,ct;
double rmsv,rmsi,por,vi_slope,loop_area,uir,nf, nom , w , capmax ;

double smooth( in ,  stp , enp )
double in[]   ;
int stp, enp ;
 {
  int i ;
  double out[3000];

  Clear1D(out, 3000);
  out[stp] = in[stp] ; out[enp] = in[enp] ;
  /***smooth ***/
  for ( i = stp+1 ; i < enp ; i ++ ){
     out[i] = 0.5 * in[i] + 0.25 * ( in[i-1] + in[i+1] ) ;
```

```
    }
   /**** Put it back ****/
   for ( i = stp+1 ; i < enp ; i ++ ){
      in[i] = out[i] ;
    }
  }


double Fourier( array , stan, stp , enp , dan , res ,  shift, order , fac )
double array[], stan , dan , res[] ,  shift[] , fac ;
int stp , enp , order ;
{
  double ann , rec[50] ;
  int i , j , n  ;
  Clear1D ( res , 50 ) ; Clear1D( rec , 50 ) ; Clear1D ( shift , 50 ) ;

  ann = stan ;
  for ( i = stp ; i <= enp ; i ++ ){
     if ( ( i == stp ) || ( i == enp ) ){
        for  ( j = 1 ; j <= order ; j ++ ){
           res[j] += 0.5*array[i]*sin(j*ann)*dan ;
           rec[j] += 0.5*array[i]*cos(j*ann)*dan ;
           j++ ;
        }
     }
     else
      {
        for  ( j = 1 ; j <= order ; j ++ ){
           res[j] += array[i]*sin(j*ann)*dan ;
           rec[j] += array[i]*cos(j*ann)*dan ;
           j++ ;
        }
      }
     ann += dan ;
   }
 for ( j = 1 ;  j <= order ; j++ ){
     shift[j] = atan(rec[j]/res[j]);
```

```
      res[j] =res[j]/( cos(shift[j])*pi*fac ) ;
      j++ ;
     }
}

void findnode(st,first)
int st , first;
 {
  int half_cycle,pos,pos1, i ;
  half_cycle = 185*2 ;  pos = 0 ; pos1 = 0 ;

  for ( i = st ; i <st+half_cycle ; i++) {
    if ( u1[i] >= 0. ) pos++;
   }
  if (st==0 ) node[first] = pos-1 ;      /**** first node ****/
   else node[first] = pos + st -1 ;
  for ( i = node[first]+1 ; i < node[first]+1+half_cycle ; i ++ ){
    if ( u1[i] <=0. ) pos1++ ;
   }
  node[first+1] = node[first]+pos1 ;
 }

/**** stan can be removed ****/
double Calcap( capi , a , f , stp , enp , C , order , dan )
double capi[] , a[] , f[] , C ,  dan ;
int stp , enp , order ;

{
 int i , j ;
 double ann ;

 ann = 0. ;
 for ( i = stp ; i <= enp ; i ++ ){
   capi[i] = 0. ;
   for ( j = 1 ; j <= order  ; j ++ ){
      capi[i] += w*j*C*a[j]*sin(pi/2.+j*ann+f[j]) ;
```

```
        j++ ;
      }
    ann += dan ;
    }
  }

/**** stan  can be removed ****/
double Calslope(res,a,f,ia,iif,stan,dan,stp,enp,order,vorder, num)
double res[] , a[] , f[] , ia[] , iif[] , dan , stan ;
int stp , enp , order, vorder , num ;
{
  int i , j , k , rec , rec3 , ep , sp ;
  double up , down , ann , slop1, slop2 ;

  ann = stan ;
  for ( i = stp ; i <= enp ; i++ ){
    up = 0. ;  down = 0. ;
    for ( j = 1 ; j <= order ; j ++ ){
      if ( j <= vorder )
          down+= j*a[j]*cos(j*ann+f[j]) ;
      up += j*ia[j]*cos(j*ann+iif[j]) ;
      j++ ;
    }
    if ( down != 0. ) ;
      res[i] = up / down ;
    if ( res[i] <= 0. ){
      if ( i!= 0 ) res[i] = res[i-1]*fabs(u1[i]/u1[i-1]) ;
    }
    ann += dan ;
  }
  for ( k = 0 ; k<=1 ; k++ ){
    sp = nodeir[num+k]-9 ; ep = nodeir[num+k]+9 ;
    slop1 = 0. ; slop2 = 1. ; rec = 0 ; rec3 = 0 ;
    for ( i = sp ; i <= ep ; i++ ){
      if ( slope[i] > slop1 ) { slop1 = slope[i] ; rec = i ; }
      if ( slope[i] < slop2 ) { slop2 = slope[i] ; rec3 = i ; }
```

```
    }
   slope[rec] = (slope[rec-1]+slope[rec+1])/2. ;
   slope[rec3] = ( slope[rec3-1] + slope[rec3+1])/2. ;
   for ( j = 1 ; j <= 5 ; j++ ){
     smooth(slope, sp,ep) ;
    }
  }
}

double Calratio( a , arr , order , imax1, irmax2 )
double a[] , arr[] ,  imax1 , irmax2 ;
int order ;
{
  int i , j;

  ratio2=fabs(a[3]/imax1) ;
  c1 = fabs(a[1])/irmax2 ;
  Clear1D (arr, 21);
  ratio = 0.; ct = 0. ;
  for ( i = 3 ; i <= 21 ; i++ ){
     ratio += fabs(a[i]/imax1);
     arr[i] =fabs(a[i]/a[1]) ;
     ct += fabs(a[i]/irmax2) ;
     i++ ;
  }
}

double Calrms( stp , enp )
int stp , enp ;
{
  int i ;
  double  Tp ;

  Tp = ( enp - stp ) * dt ;
  rmsv = 0. ; rmsi = 0. ; uir = 0. ;
  for (i = stp ; i <= enp ; i++ )
```

```
   {
    rmsv +=  u1[i]*u1[i] ;
    rmsi +=  ilk[i]*ilk[i] ;
    uir +=  u1[i]*Ir[i] ;
   }
  rmsv = sqrt (rmsv*dt/Tp);
  rmsi = sqrt (rmsi*dt/Tp);
  uir = uir*dt/Tp;
}

double Calloop( stp , enp  )
int stp , enp ;
{
 int i ;

 loop_area = 0. ;
 /* V-Itotal  */
 for ( i = stp  ; i < enp  ; i++ ){
    if ( ilk[i] < 0.)
         loop_area += fabs(u1[i+1]-u1[i])*fabs(ilk[i]);
    else if ( ilk[i] > 0.)
        loop_area += (u1[i+1]-u1[i])*ilk[i];
  }
}

double Calaratio(stp , enp ,  uran)
int enp , stp ;
double  uran ;
{
 int i ;

 area1=0.; area2=1E-12;
 for ( i = stp  ; i <= enp  ; i++ ){
    if  ( u1[i]<= uran  ){
       area1  += fabs((Ir[i]-Ir[i-1])*u1[i]);
       area2 += fabs((u1[i]-u1[i-1])*Ir[i]);
```

```
      }
    }
  aratio  = area1 / area2 ;
}

double Calvislop( stp , enp , uran )
int enp , stp ;
double uran;
{
 int i , rea  ;
 double tm ;

 tm=500. ;   rea = 0;
 for ( i = stp ; i <= enp ; i ++ ){
     if ( fabs(u1[i]-uran)< tm ) { tm=fabs(u1[i]-uran) ; rea=i; }
   }
 if ( tm == 0. ){
     vi_slope = uran / ilk[rea]* 1E-6 ;
   }
  else {
     if ( u1[rea] < uran ){
         vi_slope = uran / ( ilk[rea] + (uran-u1[rea])/u1[rea]*ilk[rea] );
      }
     else vi_slope = uran/ ( ilk[rea] - (u1[rea]-uran)/u1[rea]*ilk[rea] );
   }
  vi_slope = vi_slope * 1E-6 ;
}

double Calnn( stp , enp  )
int enp , stp  ;
{
 double x1,x2,x3,x4, bj ;
 int j ,i, record  ;

 x1 = 0.; x2 = 0. ; x3 = 0. ; x4 = 0. ; j = 0; bj = 5. ; record = 0 ;
 for ( i = stp  ; i <= enp ; i++ ){
```

```
    if ( fabs(Ir[i]-0.001)<bj ){
      bj = fabs( Ir[i]-0.001 ) ; record = i ;
     }
     if (( u1[i] > 4200. )&& ( Ir[i] >0. )){
      x1 += log (u1[i])*log (u1[i]);
      x2 += log (u1[i]);
      x3 += log (u1[i])*log (Ir[i]);
      x4 += log (Ir[i]) ;
      j += 1 ;
      }
  }
 nom = ( x3-x1*x4/x2 ) / ( x2 -x1*j/x2 ) ; /** r1-- nom **/
 nf = ( x3 - x2*nom) / x1 ;  /** r2--nf **/
 nom = exp (-nom/nf);
 return(record) ;
}

double Calv1( record )
int record ;
{
 if ( Ir[record] == 0.001 )  v1 = u1[record] ;
 else if ( Ir[record] > 0.001 )
   v1 = u1[record]-(Ir[record]-0.001)/(Ir[record]-Ir[record-1])*(u1[record]-u1[record-1]);
 else
   v1 = u1[record]+(0.001-Ir[record])/(Ir[record+1]-Ir[record])*(u1[record+1]-u1[record]);
}

void appendfile(filehdl, d1 , r1 , r2 , r3 , r4 , r5, fac )
int filehdl , d1 , fac ;
double r1 , r2 , r3 , r4 , r5 ;
{
 FmtFile(filehdl,"%s<%d[w8],", d1 ) ;
 FmtFile(filehdl,"%s<%f[w9],", r1 ) ;
 FmtFile(filehdl,"%s<%f[w10],", r2 ) ;
 FmtFile(filehdl,"%s<%f[w10],", r3 ) ;
 FmtFile(filehdl,"%s<%f[w10],", r4 ) ;
```

```
 FmtFile(filehdl,"%s<%f[w10],", r5 ) ;
 WriteFile (filehdl,"\n",1) ;
 if ( fac==1 )  WriteFile (filehdl,"\n",1) ;
}

void appendfile1(filehdl, d1 , r1 , r2 , r3 , r4, fac )
int filehdl , d1 , fac ;
double r1 , r2 , r3 , r4   ;
{
 FmtFile(filehdl,"%s<%d[w8],", d1 ) ;
 FmtFile(filehdl,"%s<%f[w9],", r1 ) ;
 FmtFile(filehdl,"%s<%f[w10],", r2 ) ;
 FmtFile(filehdl,"%s<%f[w10],", r3 ) ;
 FmtFile(filehdl,"%s<%f[e],", r4 ) ;
 WriteFile (filehdl,"\n",1) ;
 if ( fac == 1 ) WriteFile (filehdl,"\n",1) ;
}

double rite( time ,array , par1, par2 , num , limit ,posp,negp,capac,fac,rms )
int time , num , fac ;
double array[] , par1, par2 , limit, posp , negp ,capac,rms;
{
 int rec3 ;

 rms = rms/1.41421;
 Calratio(array , ch , 21 , par1  , par2 ); /* par1--Imax, par2--Irmax */
 Calrms(node[num], node[num+2] ) ;
 Calloop( node[num] , nodeir[num+2] ) ;
 Calaratio(node[num]+1 , nodeir[num+1] , limit ) ;
 Calvislop(node[num] , nodeir[num+1] ,  limit ) ;
 rec3 = Calnn( node[num]+30 , nodeir[num+1] ) ;
 Calv1(rec3 ) ;

 appendfile(hdl2, time , rms , rmsi , par1  , par2 , fabs(array[3]), fac ) ;
 appendfile(hdl3, time , rms , ratio2 , ratio  , -posp/negp , posp/par1  , fac ) ;
 appendfile(hdl4, time , rms , aratio , loop_area , area2 , v1  , fac ) ;
```

```
  appendfile1(hdl5, time , rms , vi_slope , uir , capac ,  fac ) ;
  appendfile(hdl7, time , rms , nf , nom , c1 , ct , fac ) ;
  appendfile(hdl8, time , rms , ch[3] , ch[5] , ch[7] , ch[9] , fac ) ;
}

double correct( rearr , arr, f ,h, rea ,  stp , enp ,  dan,C )
int stp , enp, h;
double rearr[] , arr[] , rea[] , f[] ,  dan , C;
{
 int i , j ;
 double ann, uhar ;

 ann = 0. ;
 for ( i =stp ; i < enp ; i ++ ) {
   uhar = 0. ;
   if (fabs(Ir[i]) >0.25*capmax ){
     for ( j = 3 ; j <= h ; j ++ ) {
       uhar += arr[j]*sin(j*ann+f[j]) ;
         j++ ;
     }
     rearr[i] = Ir[i] - uhar*slope[i] ;
    }
   else  rearr[i] = Ir[i] ;
   rea[i] = Ir[i] - rearr[i] ;
   ann += dan ;
   Ir[i] =rearr[i]  ; /** Ir corrected **/
   ilk[i] = arr[1]*sin(ann+f[1]+pi/2.)*w*C+Ir[i] ;
   u1[i] = arr[1]*sin(ann+f[1]) ;  /*** Voltage corrected ***/
  }
}

void Beeep()
{
beep () ;
delay (0.1) ;
beep () ;
```

```
delay (0.1) ;
beep () ;
}

void Dsplay( pnl1 , pnl2 )
int pnl1 , pnl2 ;
{
 DisplayPanel (pnl1);
 DisplayPanel (pnl2);
}

void Plott( p1 , p2 , p1c, p2c,input , enp )
int p1 , p2 , p1c , p2c , enp ;
double input[] ;
{
 PlotY ( p1 , p1c , slope , node[2] , 4 , 1 , 10 , 20 , 5 ) ;
 PlotY ( p2 , p2c , input , enp, 4 , 1 , 10 , 20 , 5 ) ;
}

void Write2disc(a1,a2,a3,a4)
double a1[],a2[],a3[],a4[] ;
{
 int i , handle ;
 handle = OpenFile ("t85b", 2, 0, 1);
 for (i=0; i<node[4]; i++ ) {
 FmtFile(handle,"%s<%f[w10],",i*dt);
 FmtFile(handle,"%s<%f[w10],",a1[i]/1000.);
 FmtFile(handle,"%s<%f[w10],",a2[i]*1000.);
 FmtFile(handle,"%s<%f[w10],",a3[i]*1000.);
 FmtFile(handle,"%s<%f[w10],",a4[i]*1000.);
 WriteFile (handle,"\n",1);}
 CloseFile (handle);
}

void ritefile ()
{
```

```
int handle;
char *bf,bf2[30],*bf3,*name,*other,bf4[30],*bf5,bf6[30],*bf7,bf8[30],*bf9;
char bf10[30],*bf11,bf12[30],*bf13,bf14[30],*bf15,bf16[30],*bf17,bf18[30];
char *st1,st2[30],*st3,st4[30],*st5,st6[30],*vol,volt[30];
char *cm1,*cm3,cm2[30],cm4[30],*cm5,*cm6,cm7[30],*cm8,cm9[30];
char *dm1,*dm3,*dm5,dm2[30],dm4[30],dm6[30],*ef1,*ef3,ef2[30],ef4[30],*ef5,ef6[30];

Fmt(bf2,"%s<%f",ar[3]);
Fmt(bf4,"%s<%f[p4]",ratio);
Fmt(bf12,"%s<%f",cap);
Fmt(bf14,"%s<%f",ct);
Fmt(bf8,"%s<%f",c1);
Fmt(bf6,"%s<%f",aratio);
Fmt(bf10,"%s<%f",Imax);
Fmt(bf16,"%s<%f",loop_area);
Fmt(st2,"%s<%f",vi_slope);
Fmt(st4,"%s<%f",rmsv);
Fmt(st6,"%s<%f",rmsi);
Fmt(volt,"%s<%f",max);
Fmt(ef6,"%s<%f",por);
Fmt(dm2,"%s<%f",Irmax);
Fmt(dm4,"%s<%f",ratio2);
Fmt(dm6,"%s<%f",uir);
Fmt(bf18,"%s<%f",v1);
Fmt(bf8,"%s<%f",nf);
Fmt(ef2,"%s<%f",nom);
Fmt(ef4,"%s<%f",area2);

cm5="The time of ageing is 0680 series! ";
name="The method of ageing is oven  ageing.";
other="Element number is 13.26" ;
handle=OpenFile("r58c.out",2,0,1);
bf="3) The magnitude of 3rd harmonic resistive current is :";
bf3="4) The ratio of the sum of the harmonics to the total current is :";
bf5="6) The ratio of areas is :";
bf7="8) The ratio of 1st/Ir is :";
```

```
bf9="7) The maximum value of total leakage current is :";
bf11="5) The calculated capacitance is :";
bf13="9) The ratio of total harmonic to Ir is :";
bf15="11) The loop area is :";
bf17="17) The voltage to cause 1 mA instant resistive current is : ";
st1="12) The slope of the pre-set point in V-I curve is :";
st3="1) The rms value of voltage ";
st5="2) The rms value of current ";
vol="13) The magnitude of the applied voltage  is ";
/*cm8="17) The maximum of the resistive current is :"; */
dm1="14) The maximum of the resistive current is :";
dm3="15) The ratio of the 3rd resistive Har to the max of resistive is :";
dm5="16) The integration of U*Ir is :";
ef5="10) The ratio of rmsir to total rms current is : ";
bf7="18) The non-linear factor of V-Ir is : ";
ef1="19) The nom of V-Ir is : ";
ef3="20) The area in V-Ir is : ";

WriteFile(handle,name,36);
WriteFile (handle,"\n",1);
WriteFile (handle,"\n",1);
WriteFile(handle,cm5,33);
WriteFile (handle,"\n",1);
WriteFile (handle,"\n",1);
WriteFile(handle,other,23);
WriteFile (handle,"\n",1);
WriteFile (handle,"\n",1);
WriteFile(handle,st3,28);
WriteFile(handle,st4,15);
WriteFile (handle,"\n",1);
WriteFile (handle,"\n",1);
WriteFile(handle,st5,28);
WriteFile(handle,st6,15);
WriteFile (handle,"\n",1);
WriteFile (handle,"\n",1);
WriteFile(handle,bf,54);
```

```
WriteFile(handle,bf2,14);
WriteFile (handle,"\n",1);
WriteFile (handle,"\n",1);
WriteFile(handle,bf3,66);
WriteFile(handle,bf4,16);
WriteFile (handle,"\n",1);
WriteFile (handle,"\n",1);
WriteFile(handle,bf11,33);
WriteFile(handle,bf12,16);
WriteFile (handle,"\n",1);
WriteFile (handle,"\n",1);
WriteFile(handle,bf5,25);
WriteFile(handle,bf6,14);
WriteFile (handle,"\n",1);
WriteFile (handle,"\n",1);
WriteFile(handle,bf9,49);
WriteFile(handle,bf10,14);
WriteFile (handle,"\n",1);
WriteFile (handle,"\n",1);
WriteFile(handle,bf7,27);
WriteFile(handle,bf8,14);
WriteFile (handle,"\n",1);
WriteFile (handle,"\n",1);
WriteFile(handle,bf13,41);
WriteFile(handle,bf14,14);
WriteFile (handle,"\n",1);
WriteFile (handle,"\n",1);
WriteFile(handle,ef5,49);
WriteFile(handle,ef6,14);
WriteFile (handle,"\n",1);
WriteFile (handle,"\n",1);
WriteFile(handle,bf15,21);
WriteFile(handle,bf16,14);
WriteFile (handle,"\n",1);
WriteFile (handle,"\n",1);
WriteFile(handle,st1,52);
```

```
WriteFile(handle,st2,14);
WriteFile (handle,"\n",1);
WriteFile (handle,"\n",1);
WriteFile(handle,vol,45);
WriteFile(handle,volt,15);
WriteFile (handle,"\n",1);
WriteFile (handle,"\n",1);
WriteFile(handle,dm1,45);
WriteFile(handle,dm2,15);
WriteFile (handle,"\n",1);
WriteFile (handle,"\n",1);
WriteFile(handle,dm3,67);
WriteFile(handle,dm4,15);
WriteFile (handle,"\n",1);
WriteFile (handle,"\n",1);
WriteFile(handle,dm5,32);
WriteFile(handle,dm6,15);
WriteFile (handle,"\n",1);
WriteFile (handle,"\n",1);
WriteFile(handle,bf17,61);
WriteFile(handle,bf18,15);
WriteFile (handle,"\n",1);
WriteFile (handle,"\n",1);
WriteFile(handle,bf7,39);
WriteFile(handle,bf8,15);
WriteFile (handle,"\n",1);
WriteFile (handle,"\n",1);
WriteFile(handle,ef1,23);
WriteFile(handle,ef2,15);
WriteFile (handle,"\n",1);
WriteFile (handle,"\n",1);
WriteFile(handle,ef3,26);
WriteFile(handle,ef4,15);
WriteFile (handle,"\n",1);
WriteFile (handle,"\n",1);
CloseFile (handle);
```

```
}

main(){
int i,j,sp,ep,n,hn,days,poos,rea0,jn,hn1,hn2 ;
int samples,frequency,ps2,temp1,cmax,cmin;
int hdl6, hv, umax , umin , ilmax, ilmin , newhn1 , newhn2 ;
char str[55], str1[55] , str2[55] , str3[55] ;
double ch1[70], uran ;
double rate, an,dan,ii,ui, cap2;
double rmsv1,bj,Irmaxn, peak1 ;
double rmsir, pp1 , pp2 , np2 , np1 , uhar;
double i2[2500],capi[2000], slope2[1000];
double oldslope[30], tslope,upre,ipre , imin , min,capmin ;
int Panel1, Panel2,Panel3,Panel4, hd,id,menu_bar,cond;

cls();
Imax=0.; samples=5000; max = 0.; ps2 = 0;
rate=86400.; frequency=60; w=2*pi*frequency; /*initialization*/
hn =39 ; dt = 2. / rate ;

/**** Retrieve the data in the disk ****/
hdl =OpenFile("85ieh58",1,2,1);
hdl1=OpenFile("85ueh58",1,2,1);
        days = 680;
        uran = 5750. *1.4 ;

ScanFile ( hdl1, "%s>%*f[x]" , samples/2 , u1);
ScanFile ( hdl , "%s>%*f[x]" , samples/2 , ilk);
CloseFile (hdl);
CloseFile (hdl1);

/*** Change the voltage to a sine fumnction ***/
/*** Find the nodes first ***/

poos =0 ;
/* Specify the points may be contained in 1/4 cycle*/
```

```
temp1=3*rate/(20*frequency);
for (i=0 ; i<temp1 ; i++){     /* how many points in 1/4 cycle */
 if ( u1[i] >= 0. ) poos++;}
node[0]=0; node[1] = poos-1 ;
peak1 = 0. ;
for (i=poos ; i<poos+temp1 ; i++){
 if (u1[i] < peak1 ) { node[2] = i; peak1 = u1[i] ; } }
/**FmtOut("node[2] =%d\n",node[2]);**/
for (i = node[2]+1 ; i < node[2]+temp1 ; i++) {
 if ( u1[i] <= 0. ) ps2++; }
node[3] = node[2] + ps2  ;
/**FmtOut("node[3] =%d\n",node[3]);**/

/**** Change ****/
sp = node[3] ;
for ( i = 0 ; i <= 2000 ; i ++ )
  {  u2[i] = u1[i+sp+1] ; i2[i] = ilk[i+sp+1] ;
  }

Clear1D (u1, 2200);      Clear1D (ilk, 2200);
Copy1D (u2, 2000, u1);   Copy1D (i2, 2000, ilk);
Clear1D (u2, 2200);      Clear1D (i2, 2200);

/*Smooth the collected data*/
smooth( u1 , 0 , 1600 ) ;
smooth( ilk , 0 , 1600) ;

/**** Find the MAXIMUM ****/
MaxMin1D (u1, 1600, &max, &umax, &min, &umin);
MaxMin1D (ilk, 1600, &Imax, &ilmax, &imin, &ilmin);

/*** Find the info about the voltage signal ***/
node[0]=0;
findnode(0, 1 ) ; node[2] += 1;
findnode(node[2]+1,3) ; node[4] += 1;
for ( i = 1 ; i <= 4; i ++ ){
```

```
    da[i] = pi / (node[i] - node[i-1]) ;
    FmtOut(" da[%d] = %f\n", i,da[i] );
  }
  for ( i=1 ; i<=4 ; i ++ ) {
    FmtOut("node[%d] =%d\n",i,node[i]);
   }

  Clear1D (av, 40); Clear1D (av1, 40);
  Clear1D (fv, 40); Clear1D (fv1, 40); Clear1D (fr, 40); Clear1D (fr1, 40) ;
  Clear1D (ar, 40); Clear1D (ar1, 40);
  Clear1D (bi, 4);

  /**** Fourier integration on the voltage signal ****/
  Fourier( u1 , 0. , node[0], node[2], 2.*pi/(node[2]-node[0]), av , fv , hn , 1. ) ;
  Fourier( u1 , 0. , node[2], node[4], 2.*pi/(node[4]-node[2]), av1 , fv1 , hn , 1. ) ;

  for ( i = 3 ; i <= 19 ; i++ ) {
    FmtOut("av[%d]=%f ",i,av[i] ) ;
    FmtOut("av1[%d]=%f\n ",i,av1[i] ) ;
    i++ ;
   }

  FmtOut(" Please enter the highest harmonic order to calculate capacitive current " );
  ScanIn ("%l>%i",&hv);

  if ( hv == 0 )             /*** If no input, default value = 11 ***/
    hv = 11;

  /**** Calculate the capacitive current caused by the fundermental component
      of voltage ****/

  for ( n = 0 ; n <= 2 ; n ++ ) {
    an = 0. ;   dan = 2.*pi/(node[n+2]-node[n]);
    for ( i = node[n] ; i <= node[n+2] ; i ++ ) {
      if ( ( i == node[n] ) || ( i == node[n+2] ) ) {
        bi[n] += 0.5*ilk[i]*cos(an)*dan ;
```

```
        }
      else {
        bi[n] += ilk[i]*cos(an)*dan ;
        }
      an += dan ;
    }
  bi[n] =bi[n]/( pi ) ;
  n++ ;
 }

FmtOut("bi[%d]=%f ", 0 , bi[0] ) ;
FmtOut("bi[%d]=%f\n ",2, bi[2] ) ;

/*** Calculate the capacitance ***/
cap =  bi[0] / (w*av[1]);
FmtOut("capacitance=%f\n",cap) ;
cap2 = bi[2] / (w*av1[1]);
FmtOut("capacitance=%f\n",cap2) ;
FmtOut("capacitance=%f\n",(cap+cap2)/2) ;

/**** Calculate the capacitive current ****/
Calcap(capi,av,fv,node[0],node[2],cap,hv,2.*pi/(node[2]-node[0]) ) ;
Calcap(capi,av1,fv1,node[2],node[4],cap2,hv,2.*pi/(node[4]-node[2]) ) ;
MaxMin1D (capi, node[4], &capmax, &cmax, &capmin, &cmin);

/***** Substract capacitive component from the total leakage current ****/
Sub1D (ilk, capi, node[4], Ir);
MaxMin1D (Ir, node[2], &pp1, &nodeir[1], &np1, &nodeir[2]); /*** Max & Min Ir in the 1st cycle ***/
Clear1D ( Ir1, 2000 );
for ( i = node[2]+1 ; i <= node[4] ; i ++ ) {
   Ir1[i] = Ir[i] ;
 }
MaxMin1D (Ir1, node[4], &pp2, &nodeir[3], &np2, &nodeir[4]); /*** Max & Min Ir in the 2nd cycle ***/
Clear1D( Ir1 , 2000 ) ;

for ( i = 1 ; i <= 4 ; i ++ ) {
```

```
  FmtOut("nodeir[%d]=%d\n",i,nodeir[i]) ;
 }

/*** Fourier analyze the resistive current ***/
/**** Use a factor of 2 , on half cycle ****/
Fourier( Ir , 0. , node[0], node[2], 2.*pi/(node[2]-node[0]), ar , fr , hn , 1. ) ;
Fourier( Ir , 0. , node[2], node[4], 2.*pi/(node[4]-node[2]), ar1 , fr1 , hn, 1. ) ;
for ( i = 1 ; i <= 21 ; i++ ) {
  FmtOut("ar[%d]=%f ar1[%d]=%f\n ",i,ar[i],i,ar1[i]) ;
  i++ ;
 }
FmtOut(" Please enter the highest harmonic order to calculate slope in 1st cycle " );
ScanIn ("%l>%i",&newhn1);
FmtOut(" Please enter the highest harmonic order to calculate slope in 2nd cycle " );
ScanIn ("%l>%i",&newhn2);

Irmax=(pp1+pp2)/2. ; Irmaxn = -(np1+np2)/2. ;
pr = Irmax / Irmaxn ;  por = Irmax/Imax ;

hdl2 = OpenFile ("eccur", 2, 1, 1);
hdl3 = OpenFile ("ecratio", 2, 1, 1);
hdl4 = OpenFile ("ecaratio ", 2, 1, 1);
hdl5 = OpenFile ("ecslopinv ", 2, 1, 1);
hdl7 = OpenFile ("ecnncc ", 2, 1, 1);
hdl8 = OpenFile ("ec3579 ", 2, 1, 1);

/*MessagePopup ("You need to enter the highest harmonic order");*/
SetBackgroundColor (3);
/*PromptPopup ("Pls input the highest harmonic # for 1st cycle", str, 50);
PromptPopup ("Pls input the highest harmonic # for 2nd cycle", str1, 50);
RemovePopup (1);
Scan ( str , "%s>%i" , &hn1 ) ;
Scan ( str1 , "%s>%i" , &hn2 ) ; */
hn1 =9; hn2 =9 ;
if ( newhn1 == 0 )  newhn1 = hn ;
if ( newhn2 == 0 )  newhn2 = hn ;
```

```
/**** Calculate the slope ****/
if ( hn1 == 0 ) hn1 = 7 ;  if ( hn2 == 0 ) hn2 = 7 ;
Calslope(slope,av,fv,ar,fr,0. , 2.*pi/(node[2]-node[0]), node[0],node[2],hn,hn1 , 1);
Calslope(slope,av1,fv1,ar1,fr1,0. , 2.*pi/(node[4]-node[2]), node[2],node[4],hn,hn2, 3);

sp = node[2] ; ep = node[4]-node[2];
for ( i= 1 ; i <= ep ; i ++ ) {
   slope2[i] = slope[i+sp] ;
  }

menu_bar = LoadMenuBar ("ovenchk.uir", Bar);
if ( menu_bar < 0 ) {
  FmtOut("Unable to load the required menu from the designated resoure file\n");
  return ;
  }

Panel1 = LoadPanel ("ovenchk.uir", P1) ;
Panel2 = LoadPanel ("ovenchk.uir", P2) ;
Panel3 = LoadPanel ("ovenchk.uir", P3) ;
Panel4 = LoadPanel ("ovenchk.uir", P4) ;

if ( ( Panel1 < 0 )||( Panel2 < 0 ) ) {
  FmtOut("Unable to load the required panel from the designated resource file\n");
  return ;
  }

/*MessagePopup (" Double click to select the hn from the list");
MessagePopup (" Choose return after selecting ! "); */

Dsplay( Panel1 , Panel2 ) ;
Plott(Panel1 , Panel2 , P1_1slope , P2_2slope , slope2 , ep ) ;

cond = 1 ;
while ( cond ) {
  GetUserEvent (1, &hd, &id);
```

```
if (hd==menu_bar) {
  switch(id)
   {
    case Bar_view_parameter :
     breakpoint() ;
     break ;
    case Bar_view_Ic  :
     YGraphPopup (capi, node[4], 4);
     break ;
    case Bar_view_Ir :
     YGraphPopup (Ir, node[4], 4);
     break ;
    case Bar_view_Irc :
     break ;
    case Bar_select_Newhn :
     PromptPopup ("Select new value for the current harmonic order", str, 50);
     Scan ( str , "%s>%i" ,  &newhn1  ) ;
     newhn2 = newhn1 ;
     break ;
    case Bar_select_newhv :
     PromptPopup ("Select new value for the voltage harmonic order", str, 50);
     Scan ( str , "%s>%i" ,  &hn1  ) ;
     hn2 = hn1 ;
     break ;
    case Bar_again :
     DisplayPanel (Panel3);
     Calslope(slope,av,fv,ar,fr,0. , 2.*pi/(node[2]-node[0]), node[0],
            node[2],newhn1,hn1 , 1);
     Calslope(slope,av1,fv1,ar1,fr1,0. , 2.*pi/(node[4]-node[2]), node[2],
            node[4],newhn2,hn2, 3);
     sp = node[2] ; ep = node[4]-node[2];
     for ( i= 1 ; i <= ep ; i ++ ) {
       slope2[i] = slope[i+sp] ;
      }
     HidePanel (Panel3);
     DeletePlots ( Panel1, P1_1slope );
```

```
DeletePlots ( Panel2, P2_2slope ) ;
Dsplay( Panel1 , Panel2 ) ;
Plott(Panel1 , Panel2 , P1_1slope , P2_2slope , slope2 , ep ) ;
break ;
case Bar_write_1st :
  Beeep() ;
  rite( days,ar,Imax, pp1 , 0 , uran , pp1 , np1 , cap , 0, av[1] ) ;
  Beeep() ;
  break ;
case Bar_write_2nd :
  Beeep() ;
  rite( days,ar1,Imax, pp2 , 2 , uran , pp2 , np2 , cap2, 1 , av1[1] );
  Beeep() ;
  break ;
case Bar_write_all :
  /* Beeep() ;  */
  rite( days,ar,Imax, pp1 , 0 , uran , pp1 , np1 , cap , 0, av[1] ) ;
  rite( days,ar1,Imax, pp2 , 2 , uran , pp2 , np2 , cap2, 1, av1[1] ) ;
  /* Beeep() ; */
  cond = 0 ;
  UnloadPanel (Panel1) ;
  UnloadPanel (Panel2) ;
  UnloadPanel (Panel3) ;
  UnloadPanel (Panel4) ;
  UnloadMenuBar () ;
  break ;
case Bar_write_2disc :
  Beeep() ;
  Write2disc(u1,ilk,capi,Ir) ;
  Beeep() ;
  break ;
case Bar_correct :
  /* Beeep() ; */
  correct( i2,av ,fv , hv , Ir1 , node[0] , node[2] , 2.*pi/( node[2] -node[0]),cap );
  correct( i2,av1,fv1, hv , Ir1 , node[2] , node[4] , 2.*pi/( node[4] -node[2]),cap2 );
  Fourier( Ir , 0. , node[0], node[2], 2.*pi/(node[2]-node[0]), ar , fr , hn , 1. ) ;
```

```
        Fourier( Ir , 0. , node[2], node[4], 2.*pi/(node[4]-node[2]), ar1 , fr1 , hn, 1. ) ;
        MaxMin1D (u1, 1600, &max, &umax, &min, &umin);
        MaxMin1D (ilk, 1600, &Imax, &ilmax, &imin, &ilmin);
        MaxMin1D (Ir, node[2], &pp1, &nodeir[1], &np1, &nodeir[2]);
          /*** Max & Min Ir in the 1st cycle ***/
        Clear1D ( Ir1, 2000 );
        for ( i = node[2]+1 ; i <= node[4] ; i ++ ) {
          Ir1[i] = Ir[i] ;
          }
        MaxMin1D (Ir1, node[4], &pp2, &nodeir[3], &np2, &nodeir[4]);
          /*** Max & Min Ir in the 2nd cycle ***/
        Clear1D( Ir1 , 2000 ) ;
        YGraphPopup (i2, node[4], 4);
        break ;
      case Bar_return :
       cond = 0 ;
       UnloadPanel (Panel1) ;
       UnloadPanel (Panel2) ;
       UnloadPanel (Panel3) ;
       UnloadPanel (Panel4) ;
       UnloadMenuBar () ;
       break ;
      }
   }
else if (hd== Panel1) {
  switch(id)
    {
     case P1_1select :
      DisplayPanel (Panel4);
      delay (.5);
      HidePanel (Panel4);
      GetCtrlVal (Panel1, P1_1select, str);
      Scan ( str , "%s>%i" , &hn1 ) ;
      Dsplay( Panel1 , Panel2 ) ;
      break ;
     case P1_selecthn1 :
```

```
        DisplayPanel (Panel4);
        delay (.5);
        HidePanel (Panel4);
        GetCtrlVal (Panel1, P1_selecthn1, str);
        Scan ( str , "%s>%i" , &newhn1 ) ;
        Dsplay( Panel1 , Panel2 ) ;
        break ;
      case  P1_go :
        DisplayPanel (Panel3);
        Calslope(slope,av,fv,ar,fr,0. , 2.*pi/(node[2]-node[0]), node[0],
                node[2],newhn1,hn1 , 1);
        HidePanel (Panel3);
        DeletePlots ( Panel1, P1_1slope );
        DeletePlots ( Panel2, P2_2slope ) ;
        Dsplay( Panel1 , Panel2 ) ;
        Plott(Panel1 , Panel2 , P1_1slope , P2_2slope , slope2 , ep ) ;
        break ;
    }
  }
else if (hd== Panel2) {
  switch(id)
    {
      case P2_2select :
        DisplayPanel (Panel4);
        delay (.5);
        HidePanel (Panel4);
        GetCtrlVal (Panel2, P2_2select, str1);
        Scan ( str1 , "%s>%i" , &hn2 ) ;
        Dsplay( Panel1 , Panel2 ) ;
        break ;
      case P2_selecthn2 :
        DisplayPanel (Panel4);
        delay (.5);
        HidePanel (Panel4);
        GetCtrlVal (Panel2, P2_selecthn2, str1);
        Scan ( str1 , "%s>%i" , &newhn2 ) ;
```

```
        Dsplay( Panel1 , Panel2 ) ;
        break ;
      case  P2_go :
        DisplayPanel (Panel3);
        Calslope(slope,av1,fv1,ar1,fr1,0. , 2.*pi/(node[4]-node[2]), node[2],
              node[4],newhn2,hn2, 3);
        sp = node[2] ; ep = node[4]-node[2];
        for ( i= 1 ; i <= ep ; i ++ ) {
          slope2[i] = slope[i+sp] ;
         }
        HidePanel (Panel3);
        DeletePlots ( Panel1, P1_1slope );
        DeletePlots ( Panel2, P2_2slope ) ;
        Dsplay( Panel1 , Panel2 ) ;
        Plott(Panel1 , Panel2 , P1_1slope , P2_2slope , slope2 , ep ) ;
        break ;
     }
   }
 }

/*Calratio(ar , ch , 21 , Imax , Irmax);
Calrms(node[0], node[1] ) ;
FmtOut( " rmsv = %f rmsi=%f \n " ,rmsv, rmsi);
Calloop( node[0] , nodeir[1] ) ;
Calaratio(node[0]+1 , nodeir[1] , uran ) ;
Calvislop(node[0] , nodeir[1] , uran ) ;
rec3 = Calnn( node[0]+30 , nodeir[1] ) ;
Calv1(rec3 ) ;

appendfile(hdl2, days , rmsv , rmsi , Imax , Irmax , fabs(ar[3]), 0 ) ;
appendfile(hdl3, days , rmsv , ratio2 , ratio , -pp1/np1 , pp1/Imax , 0 ) ;
appendfile(hdl4, days , rmsv , aratio , loop_area , area2 , v1 , 0 ) ;
appendfile1(hdl5, days , rmsv , vi_slope , uir , cap , 0 ) ;
appendfile(hdl7, days , rmsv , nf , nom , c1 , ct , 0 ) ;
appendfile(hdl8, days , rmsv , ch[3] , ch[5] , ch[7] , ch[9] , 0 ) ; */
```

```
CloseFile ( hdl2 ) ;
CloseFile ( hdl3 ) ;
CloseFile ( hdl4 ) ;
CloseFile ( hdl5 ) ;
CloseFile ( hdl7 ) ;
CloseFile ( hdl8 ) ;

YGraphPopup (u1, node[4], 4);
YGraphPopup (ilk, node[4], 4);
YGraphPopup (capi, node[4], 4);
YGraphPopup (Ir, node[4], 4);
YGraphPopup (slope, node[4], 4);
YGraphPopup (Ir1, node[4], 4);
YGraphPopup (i2, node[4], 4);
XYGraphPopup (Ir, u1, node[4], 4, 4);
XYGraphPopup (ilk, u1, node[4], 4, 4);

ritefile() ;
/*Some results through standard in&out*/
/*FmtOut("\nMagnitude of applied voltage =%f\n",max);
FmtOut("rmsv=%f\n", rmsv);
FmtOut("rmsi=%f\n", rmsi);
FmtOut("ratio=%f\n", ratio);
FmtOut("loop_area=%f\n", loop_area);
FmtOut("aratio=%f\n", aratio);
FmtOut("Irmax=%f\n",Irmax) ;
FmtOut("ratio2=%f\n",ratio2); */

}
```